

Evidence for an Enzymatic Activity of Exuperantia Necessary for *bicoid* mRNA Localization

Dissertation

der Mathematisch-Naturwissenschaftlichen Fakultät

der Eberhard Karls Universität Tübingen

zur Erlangung des Grades eines

Doktors der Naturwissenschaften

(Dr. rer. nat.)

vorgelegt von

Ines Wolff

aus Berlin

Tübingen

2012

Tag der mündlichen Qualifikation:

19.09.2012

Dekan:

Prof. Dr. Wolfgang Rosenstiel

1. Berichterstatter:

Prof. Dr. Christiane Nüsslein-Volhard

2. Berichterstatter:

Prof. Dr. Rolf Reuter

Summary

The anterior localization of *bicoid* mRNA in the *Drosophila* oocyte is a prerequisite for the establishment of the anterior-posterior axis later in the embryo. Few factors are known to be essential for this process. Aside from *swallow*, *staufer* and the *ESCRTII*, all of which are important for late steps in *bicoid* mRNA localization, the only early acting factor is *exuperantia*. Previous work has shown that Exuperantia needs to be present in the nurse cells to promote anterior localization of *bicoid* mRNA after transport into the oocyte. In *exu*-mutant flies *bicoid* mRNA is transported into the oocyte but cannot localize specifically. So far, the molecular function of Exuperantia is not understood and it is unclear how Exuperantia modifies *bicoid* mRNA in the nurse cells. Previously, two phosphorylation sites in the C-terminal part had been identified, but they are dispensable for Exuperantia's role in *bicoid* mRNA localization. In addition, an alignment of Exuperantia's N-terminus with exonucleases was published in 1997, but this finding was not followed up.

Within this thesis a SAM-like domain in the central part of Exuperantia was identified, and there is evidence that this domain might be RNA-binding. Furthermore, the homology to exonucleases was confirmed and a DEDD exonuclease domain (SCOP family c.55.3.5) was characterized in the N-terminus of Exuperantia. Biochemical *in-vitro* assays with recombinant proteins confirm the importance of these domains and hint at an enzymatic function of Exuperantia.

Using transgenes encoding Venus-tagged proteins, I show that residues, which are known to be essential for the catalytic activity of this family of enzymes, are important *in-vivo* for Exuperantia's role in *bicoid* mRNA localization. This suggests that it might be an enzyme with exonuclease activity, which would explain why the protein co-localizes with *bicoid* mRNA only transiently.

Interestingly, *bicoid* mRNA itself does not seem to be the target of this enzymatic activity. The transgenes coding for enzymatic inactive proteins described in this thesis can be used as tools and should allow the identification of the *in-vivo* targets of Exuperantia.

Zusammenfassung

Die anteriore Lokalisierung von *bicoid* mRNA in der Eizelle von *Drosophila* ist eine notwendige Voraussetzung für die Etablierung der anterior-posterioren Achse später im Embryo. Es sind nur wenige Faktoren bekannt, die für diesen Prozess der RNA Lokalisierung essentiell sind. Abgesehen von *swallow*, *staufer* und dem ESCRTII, die für die späteren Schritte der *bicoid* mRNA Lokalisierung notwendig sind, ist der einzig bekannte frühe Faktor *exuperantia*. Frühere Arbeiten zeigten, dass Exuperantia in den Nährzellen der Eikammer aktiv sein muss, um die Lokalisierung von *bicoid* mRNA in der Eizelle zu beeinflussen. In *exu*-mutanten Fliegen wird *bicoid* mRNA noch in die Eizelle transportiert, kann später aber nicht anterior lokalisieren. Die molekulare Funktion von Exuperantia ist bislang nicht verstanden, und es ist nicht bekannt, wie Exuperantia *bicoid* mRNA in den Nährzellen modifiziert. Bisher waren zwei Phosphorylierungsstellen im C-Terminus identifiziert worden, diese sind jedoch entbehrlich für Exuperantias Funktion in der Lokalisierung von *bicoid* mRNA. Außerdem wurde im Jahr 1997 ein Sequenz-Alignment des amino-terminalen Teils von Exuperantia mit Exonukleasen publiziert, was jedoch bislang nicht weiter untersucht worden war.

Im Rahmen dieser Arbeit konnte eine SAM-ähnliche Domäne im mittleren Teil des Proteins identifiziert werden, und es fanden sich Hinweise darauf, dass diese SAM-ähnliche Domäne möglicherweise eine RNA-bindende Funktion hat. Darüber hinaus konnte die Homologie zu Exonukleasen bestätigt werden, und es wurde eine DEDD Exonukleasedomäne (SCOP Familie c.55.3.5) im N-terminalen Bereich von Exuperantia charakterisiert.

Durch die Verwendung von Transgenen konnte nachgewiesen werden, dass Aminosäure-Reste, die für die katalytische Aktivität dieser Enzym-Familie essentiell sind, auch für die *in-vivo* Funktion von Exuperantia eine wichtige Rolle spielen. Die Analyse der transgenen in Fliegen weist darauf hin, dass Exuperantia ein exonukleolytische Enzym ist. Dies könnte erklären, warum Exuperantia nur transient mit *bicoid* mRNA ko-lokalisiert. Interessanterweise haben Versuche innerhalb dieser Arbeit gezeigt, dass *bicoid* mRNA selbst nicht das Ziel dieser enzymatischen Aktivität zu sein scheint. Die hier beschriebenen Transgene, die für katalytisch inaktive Proteine codieren, können in weiteren Versuchen eingesetzt werden, um die *in-vivo* Substrate von Exuperantia zu finden.

Acknowledgement

I would like to thank everybody who supported me during my PhD.

I thank Christiane Nüsslein-Volhard for the opportunity to do my PhD in her lab and for her feedback during progress reports. I thank Christiane Nüsslein-Volhard and Rolf Reuter for the evaluation of this work. Special thanks go to Uwe Irion; it was not always easy but I am thankful for your guidance in the lab, the great support while writing and the encouragement during difficult times. I also want to acknowledge Jana Krauss, for her help in the lab and while drafting the thesis as well as for valuable advice in personal matters. You helped me to be brave enough to go my own way during a turbulent time. Many thanks to the people in the institute who helped me expressing and purifying proteins: Ancilla Neu, Remco Sprangers, Katharina Veith and Fulvia Bono. I also thank Moritz Ammelburg and Andrei Lupas for the *in silico* analysis.

Moritz, my thanks go beyond the protein predictions. Thank you for being a friend.

A big “Thank you” to my lab mates for an encouraging environment. In particular, I would like to thank Vanja and Madeleine for their support, long talks and friendship; Simon, Frauke, Iris, Fabienne, Sabine, Tugba, Mario, Nadine and Yi Yen for all their support and help over the last six years.

Another very special acknowledgement goes to Sören, for help and support in all different situations. Sören, I think we managed well. Thank you!

The work in the lab was tough at times. To keep my spirits up and to get through the difficulties on the way, I was very lucky to find a second family in the “Boulangier”. I do not know how I can put into words how my friends helped me. I thank all of you. Thanks, Henni, Käthe, Andy, Kathrin, Lea K. and Lea A., Milena, Jana, Franziska, all the habitués, and all other friends too numerous to mention individually. All of you helped me in so many different ways. I also want to mention the help of people outside from Tübingen. Thank you Julia, it was very good to know that you are there for me.

Thank you, Jutta and Volker, Ragna, Marvin and Ingmar for the familiar atmosphere whenever I am in Frankfurt.

Very special appreciation goes to my partner Marcel. Thank you for your support and motivation to finish.

Last but not least. Big thanks go to my family. Lars, I was finally able to catch up. Thank you that you are such a great brother, you know I do not say this very often, so savour the flavour. Thank you Claudia, I feel like I have a sister now. Thank you Micha, Alex, Marlen, Melissa and Steffi.

Liebe Mama, Lieber Papa. Vielen Dank für eure Geduld und eure bedingungslose Unterstützung und Liebe. Ich habe euch ganz schön zappeln lassen und eure Nerven teilweise überstrapaziert. Ich bin mir bewußt, dass auch für euch die letzten sechs Jahre nicht leicht waren. Habt vielen Dank!

Table of Contents

1. Introduction	17
1.1. Cell polarity and pattern formation in	17
1.1.1. RNA localization to achieve asymmetry	17
1.1.2. <i>Drosophila</i> as model organism for asymmetry and pattern formation	20
1.2. Early patterning in the <i>Drosophila</i> embryo	21
1.2.1. RNA localization in <i>Drosophila</i> egg chamber	25
1.3. Exuperantia in body patterning	30
1.3.1. Phenotype and alleles	30
1.3.2. General features of Exuperantia protein	33
1.3.3. Model of Exuperantia function	39
2. Results	42
2.1. <i>in-silico</i> analysis of Exuperantia	42
2.2. <i>in vivo</i> Analysis of exonuclease activity of Exuperantia	47
2.3. Expression and analysis of recombinant Exuperantia protein	50
2.3.1. Expression of recombinant protein	50
2.3.2. Functional analysis of recombinant Exuperantia protein	59
2.4. Generation and analysis of new <i>exuperantia</i> alleles	63
2.4.1. EMS mutagenesis and screen for new <i>exuperantia</i> alleles	63
2.4.2. Phenotypic analysis of <i>exuperantia</i> alleles	65
2.4.3. Functional analysis of <i>exuperantia</i> alleles	68
2.4.4. Generation and analysis of <i>exuperantia</i> transgenes	69
2.4.5. Generation of <i>exuperantia</i> transgenic flies	72
2.4.6. Analysis of the rescue potential of the transgenes	72
2.4.7. Localization of Exuperantia fusion protein in mutant background	73
2.4.8. Co-localization of Exuperantia with <i>bicoid</i> mRNA	75
2.4.9. Analysis of exonuclease activity	77
2.4.10. Summary of the transgene analysis	79

3. Discussion	80
4. Material and Methods	87
4.1. Drosophila rearing	87
4.2. EMS mutagenesis and allele screen.....	87
4.3. Western blot.....	89
4.4. <i>in situ</i> hybridization.....	89
4.5. Cuticle preparation	90
4.6. Antibody staining.....	91
4.7. quantitative RT-PCR	91
4.8. Generation of transgenic flies	92
4.8.1. construct generation	92
4.8.2. site directed mutagenesis.....	93
4.8.3. transgenesis	93
4.9. Protein expression	95
4.9.1. generation of constructs.....	95
4.9.2. single step mutagenesis.....	95
4.9.3. general protein expression	96
4.9.4. His-tagged recombinant Exuperantia.....	97
4.9.5. TEV protease cleavage.....	98
4.9.6. GST-tagged recombinant Exuperantia.....	98
4.9.7. HiS-column (ion exchange)	99
4.9.8. Gel filtratrion.....	100
4.10. Fragment analysis	100
4.11. PCR and sequencing	101
4.12. alphabetical list of buffer.....	102
5. Appendix	106
6. References	120

1. Introduction

1.1. Cell polarity and pattern formation in *Drosophila*

Most, if not all, cells are polarized; prominent examples are neurons, epithelial cells or fibroblasts. These cells need to be polarized to fulfill their function in a multi-cellular organism. However, even single cells are polarized, like yeast or *Xenopus* oocytes. Cell polarity is important for many aspects of cellular behaviors, such as migration, signal propagation or the establishment of epithelial barriers. One mechanism for the establishment of polarity within a cell, to achieve the asymmetric distribution of proteins, is the localization of mRNAs. The first localized mRNAs were found in ascidian eggs and localized transcripts have been found since then in many other cell types, like fibroblasts, neurons, yeast and oocytes [1]. Recently, it was shown in early *Drosophila* embryos by an *in situ* hybridization screen, that 71% of the tested transcripts show a specific sub-cellular localization [2].

1.1.1. RNA localization to achieve asymmetry

RNA localization, coupled with localized translation, offers several distinct advantages to cells. Firstly, it is very economic, because each localized mRNA molecule can give rise to many protein molecules. Secondly, it prevents the translation of proteins in regions of the cell where it could be harmful or deleterious. A third advantage is the creation of micro domains with high concentrations of RNAs, facilitating the formation of RNA-protein complexes, which ensures a local concentration of its members. Lastly, RNA localization leads to the decentralization of gene expression by allowing local translational control. E.g. in highly elongated and polarized cells, like neurons, this is a way to ensure fast responses to external signals far away from the cell bodies [3].

The localization of mRNAs requires cis-acting sequences, which are most often found in the 3'UTRs of the RNAs. These sequences are recognized by trans-acting factors like RNA binding proteins for packaging the RNA into RNA-protein complexes (RNP) for transport, translational control and anchoring [4].

Several mechanisms are known to achieve RNA localization within cells [5, 6].

- ❖ Localized synthesis: a rare example of this mechanism is found in the syncytium of the mammalian myofibre, where the δ - and ϵ -subunits of the acetylcholine receptor are only transcribed by the nuclei in close proximity to the neuromuscular junction.
- ❖ Spatially restricted protection from degradation: this mechanism has been shown to restrict mRNAs (*hsp83*, *nanos* and *polar granule component*) to the posterior end of the *Drosophila* egg, where the germ cells will form [7-9]. In the case of *nanos* mRNA only 4% of the transcribed RNA is localized and stable, the rest, which is not localized at the posterior pole, will be rapidly degraded upon the onset of embryonic development [9]. It seems that the local protection from degradation is an evolutionary conserved pathway for germ-line localization, since *nanos* and *vasa* mRNAs are restricted to the primordial germ cells in *Danio rerio* by a remarkably similar process [10].
- ❖ Diffusion and anchoring: this mechanism is also found in pole plasm formation in *Drosophila*. Several RNAs (*nanos*, *germ cell less*, *cyclin B*) are trapped at the posterior pole of the egg after diffusing through the cytoplasm. This process depends on previous localization of *oskar* mRNA and subsequent translation into Oskar protein, which is necessary to hold the RNAs at the posterior pole [11-15].
- ❖ Active transport along the cytoskeleton: this seems to be the predominant mechanism to localize mRNAs in animal cells. This mechanism is based on the cytoskeleton network and the associated motor proteins. A very prominent example is the microtubules and Dynein or Kinesine associated transport in neurons. The localization of *myelin basic protein* mRNA is based on Kinesine, the plus end directed motor protein and microtubules in the hippocampal neurons [16]. Another plus end directed transport, based on the interaction on Kinesine with microtubules is the posterior localization of *oskar* mRNA in the *Drosophila* oocyte [17]. *bicoid* and *gurken* mRNA on the other hand are localized towards the minus end of microtubule network in the oocyte by interaction with Dynein/Dynactin [18, 19]. One of the best understood examples of active mRNA transport along actin is the transport of *Ash1* mRNA in cooperation with Myosin to the bud tip in *Saccharomyces cerevisiae* [20]. *Ash1* mRNA localization is *actin* dependent and requires type-V Myosin4 (in yeast named She1p); She1p is coupled via She2p and She3p to *Ash1* mRNA, where She2p is the RNA

recognition protein. The traffic of *Ash1* along actin cables and with a speed of 200-440nm/sec (consistent with myosin-based motility) has been confirmed by a fluorescent protein-based *in vivo* labeling of *Ash1* mRNA. This *in vivo* tagging method was developed by Bertrand et al. [21]. It was used in *Drosophila* to image *nanos* mRNA localization *in vivo* [2] and was subsequently applied to a number of different mRNAs, including *bicoid* (Fig. 1.1) confirming the localization pattern previously described by *in situ* hybridization [22].

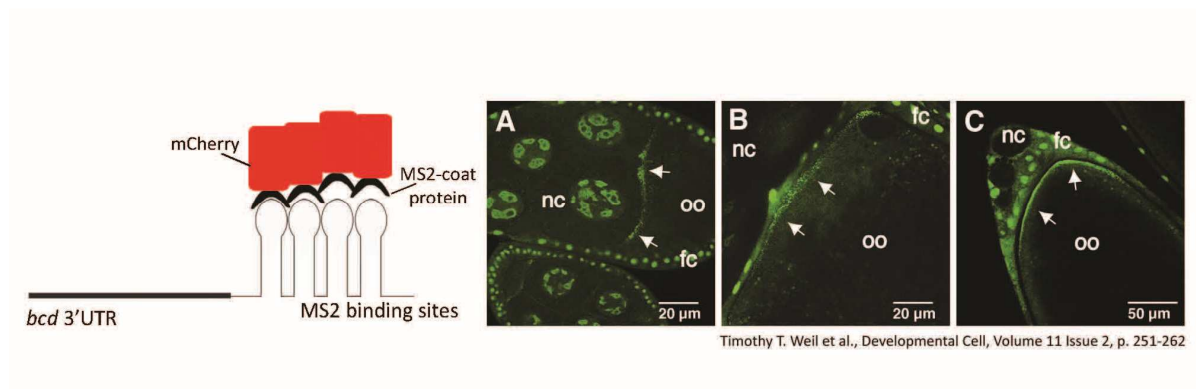


Figure 1.1 MS2 system and *bicoid* mRNA localization.

This method is based on a two plasmid system. One of the plasmids encodes a fusion protein of GFP and the capsid protein, derived from the single stranded RNA phage MS2 (MS2 coat protein). The other plasmid codes for a hybrid RNA containing the RNA localization elements and an array of several MS2 binding sites, a 19 nucleotide RNA stem loop structure, which is recognized by the MS2 coat protein. With these constructs it is possible to follow the RNA of interest in living cells via the GFP fluorescence. Excess GFP-MS2 is kept in the nucleus via a nuclear localization signal (NLS) and only protein bound to RNA is detected in the cytoplasm. The constructs used in this thesis encode a hybrid RNA of the *bicoid* 3'UTR and 10 MS2 binding sites (19 nucleotides long stem loops) and a fusion protein of tandem mCherry and MS2-coat protein. This allows following *bicoid* mRNA localization *in vivo*. **A-C** *bicoid* mRNA is fused to six MS2 binding sites and is recognized by a MS2-coat-GFP fusion protein. This RNA fully rescues the *bicoid* phenotype and localizes normally in egg chambers in stage 7 (**A**), stage 10 (**B**) and stage 12 (**C**). Nurse cells (nc), oocyte (oo) and follicle cells (fc) are indicated. Arrows point on *bicoid* RNA particles.

1.1.2. *Drosophila* as model organism for asymmetry and pattern formation

Drosophila melanogaster is an excellent model organism for RNA localization, it is easy and cheap to culture, its generation time is relatively short and flies can produce a very large number of offspring. The genetics of *Drosophila* has been studied for over a century, resulting in the availability of a well-annotated genome sequence, a plethora of molecular tools and fly stocks carrying mutations in many genes. The *Drosophila* ovary is the single largest organ in the female fly and the oocyte is the single largest cell, growing up to 500µm by 80 µm. As the ovary is a non-essential organ, it is open to manipulation using all the molecular and genetic tools, which have been developed for *Drosophila*, and even very drastic effects can be studied in an otherwise healthy organism. Therefore RNA localization within the oocyte and pattern formation in the resulting embryo has been studied in *Drosophila* intensively. During early embryonic development many transcripts are specifically localized [1], well studied examples include the mRNAs of the pair-rule genes *even-skipped* (*eve*), *hairy* (*h*) and *runt* (*run*) as well as the segment-polarity gene *wingless* (*wg*) [23, 24]. During oogenesis the specific localization of three prominent mRNAs, *gurken* (*grk*), *oskar* (*osk*) and *bicoid* (*bcd*), within the developing oocyte is required to establish oocyte polarity and to determine the axes of the future embryo. A shared machinery for the localization of transcripts in the embryo and the transport of mRNAs from the nurse cells into the oocyte has been identified. The transport of the RNAs towards the minus-ends of microtubules depends on the Dynein/Dynactin motor-complex and the proteins Egalitarian (Egl) and Bicaudal-D (BicD) [23, 25]. Within the oocyte, *gurken* (dorsal-anterior corner) and *bicoid* (anterior) mRNAs continue to be localized by a minus-end directed transport machinery, whereas *oskar* mRNA localization to the posterior pole of the oocyte is plus-end directed and dependent on the molecular motor Kinesin (Fig. 1.2).

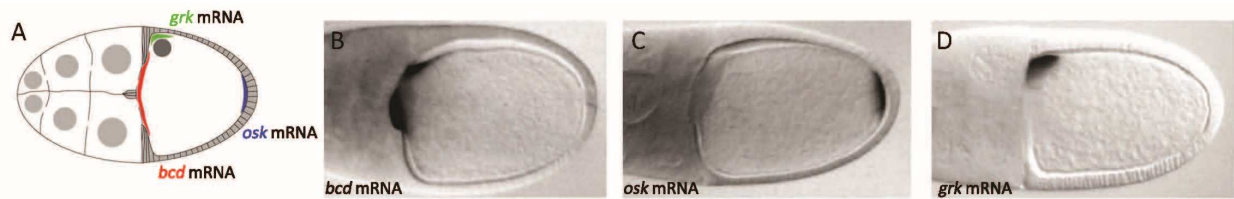


Figure 1.2 RNA localization in a stage 10B *Drosophila* egg chamber.

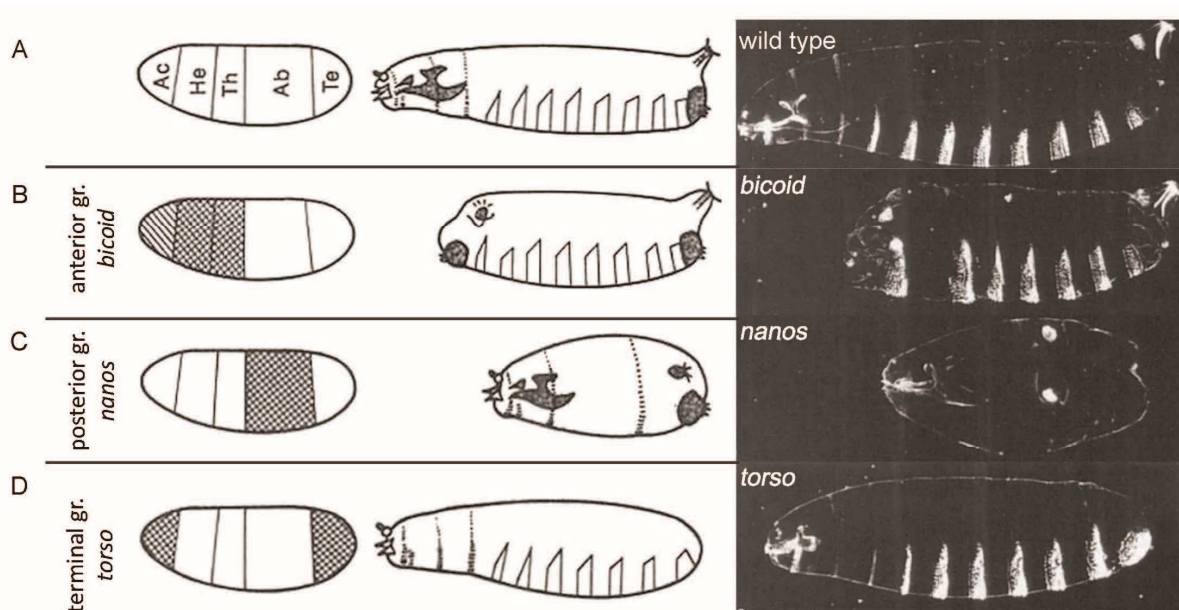
A Schematic overview of a stage 10B egg chamber. Localized RNA are *bicoid* mRNA (red) at the anterior, *oskar* mRNA (blue) at the posterior and *gurken* mRNA (green) in the anterior-dorsal corner. **B-D** *in situ* hybridization in a stage 10B egg chamber of *bicoid* mRNA (**B**), *oskar* mRNA (**C**) and *gurken* mRNA (**D**).

The anterior localization of *bicoid* mRNA is crucial to set up the anterior-posterior axis. Its anterior localization in the oocyte leads eventually to an anterior localization of the Bicoid protein at the anterior pole of the embryo. There, Bicoid acts as anterior morphogen which ensures, by expression control of downstream genes, the pattern formation in the larvae.

1.2. Early patterning in the *Drosophila* embryo

The body plan of the *Drosophila* larva consists of two unsegmented regions at its extremes, the acron at the anterior and the telson at the posterior, and a segmented middle part. The segmental part is composed of 7 head segments, 3 thoracic segments and 8 abdominal segments (Fig. 1.3) [26].

The patterning of the *Drosophila* embryo depends on the formation of the two main body axes, already within the developing oocyte. The dorso-ventral axis is set up in the oocyte by the dorsal-anterior localization of *gurken* mRNA. The anterior-posterior axis is determined by the posterior localization of *oskar* mRNA and the anterior localization of *bicoid* mRNA. Since these transcripts are expressed from the maternal genome and affect zygotic development they are called maternal effect genes. There are three classes of maternal effect genes, which are responsible for anterior-posterior patterning in *Drosophila*. They are distinguishable by the effect mutations have on the embryonic body plan. Mutations in genes of the anterior group (like *exuperantia* and *swallow*) result



adapted from: St Johnston and Nüsslein-Volhard, Cell, 1992, Vol. 68, 201-219

Figure 1.3 Schematic overview of the larval body patterning and examples of cuticle from mutants in the anterior, posterior or terminal group.

A Wild-type larva (scheme and cuticle) with a normal composition of acron (Ac), head (He), thorax (Th), abdomen (Ab) and telson (Te). **B** In anterior group mutants the acron, head and thoracic structures are affected, resulting in larvae with a partially defective or no anterior structures, as in *bicoid* mutants. **C** In mutants of the posterior group abdominal structures are missing, example *nanos* mutant. **D** *torso* as example for the terminal group, the acron and telson are missing.

in embryos with reduced or absent head structures but normal abdomen. Mutations in posterior group genes (like *oskar* and *nanos*) lead to normally developed anterior structures of the embryo but a missing abdomen. The third group of genes, the terminal group (like *torso* and *torso-like*), is necessary for the formation of specialized structures at the poles of the embryo, the acron and the telson (Fig. 1.3) [26].

So far, four genes belonging to the anterior group, *exuperantia* (*exu*), *swallow* (*swa*), *staufer* (*stau*) and *bicoid* (*bcd*) are known. Mutations in these genes lead to a lack or reduction of head and thoracic structures (Fig. 1.3). *bicoid* encodes the anterior determinant, the other factors are important to localize *bicoid* mRNA to the anterior of the oocyte. In *bicoid* loss-of-function mutants no anterior structures are present and the telson is duplicated instead of the [27]. The phenotype of *exuperantia*, *swallow* and

staufen mutants is less severe, but clearly affects anterior structures. After fertilization *bicoid* mRNA, which is restricted to the anterior of the embryo, is translated into protein. Bicoid protein forms a gradient in the embryo with the highest levels at the anterior (Fig. 1.4). It is a homeodomain containing transcription factor that acts as a morphogen, controlling expression of zygotic target genes in a concentration dependent manner. The first of these target genes are the gap genes, e.g. *hunchback*, *Krüppel*, *knirps* and *giant*. In addition, Bicoid is also a translational repressor of *caudal* mRNA, leading to a Caudal protein gradient forms from the posterior towards the anterior (Fig. 1.4) [26]. The posterior group genes specify the posterior part of the embryo. Mutations in this group of genes result in embryos lacking abdominal structures (Fig. 1.3) [26]. Genes belonging to the posterior group, like *oskar*, are essential to ensure the posterior localization of *nanos (nos)* mRNA, which is the posterior determinant in the embryo. They also specify the pole plasm at the very posterior pole, which will be incorporated into the germ cells. Like *bicoid*, *nanos* is translated after fertilization and forms a protein gradient with the highest level at the posterior pole. In contrast to Bicoid, Nanos does not act as a morphogen; it rather acts as a translational suppressor of the evenly distributed maternal *hunchback* mRNA leading to a gradient of the Hunchback protein complementary to the Nanos protein gradient. This Hunchback gradient is further amplified by the activation of zygotic *hunchback* at the anterior by Bicoid (Fig. 1.4).

The gap genes, like *hunchback*, *Krüppel*, *knirps* and *caudal* are the first genes transcribed in the zygote. They all encode transcription factors and their expression pattern is determined by the transcriptional activation or repression via the anterior and posterior determinants (Fig. 1.4).

The gap genes transcription factors subsequently regulate, together with the maternal determinants the expression of the pair-rule genes (e.g. *even-skipped (eve)*, *runt* and *fushi-*tarazu**, *odd-skipped*, *paired*, and *odd-paired*). The pattern of pair-rule gene expression is the first signs of segmentation in the *Drosophila* embryo. This changes the spatial framework from the aperiodic regionalization before (maternal effect genes and gap genes) to a periodic one. They arise in evenly spaced stripes along the body axis in the cellular blastoderm stage. Each stripe is specifically controlled by a combination of maternal morphogen and gap gene activity (Fig. 1.4).

In conclusion, the positioning of maternally provided determinants is a key prerequisite for pattern formation in the *Drosophila* embryo. All following steps in pattern formation are built on the initial determination of the axis.

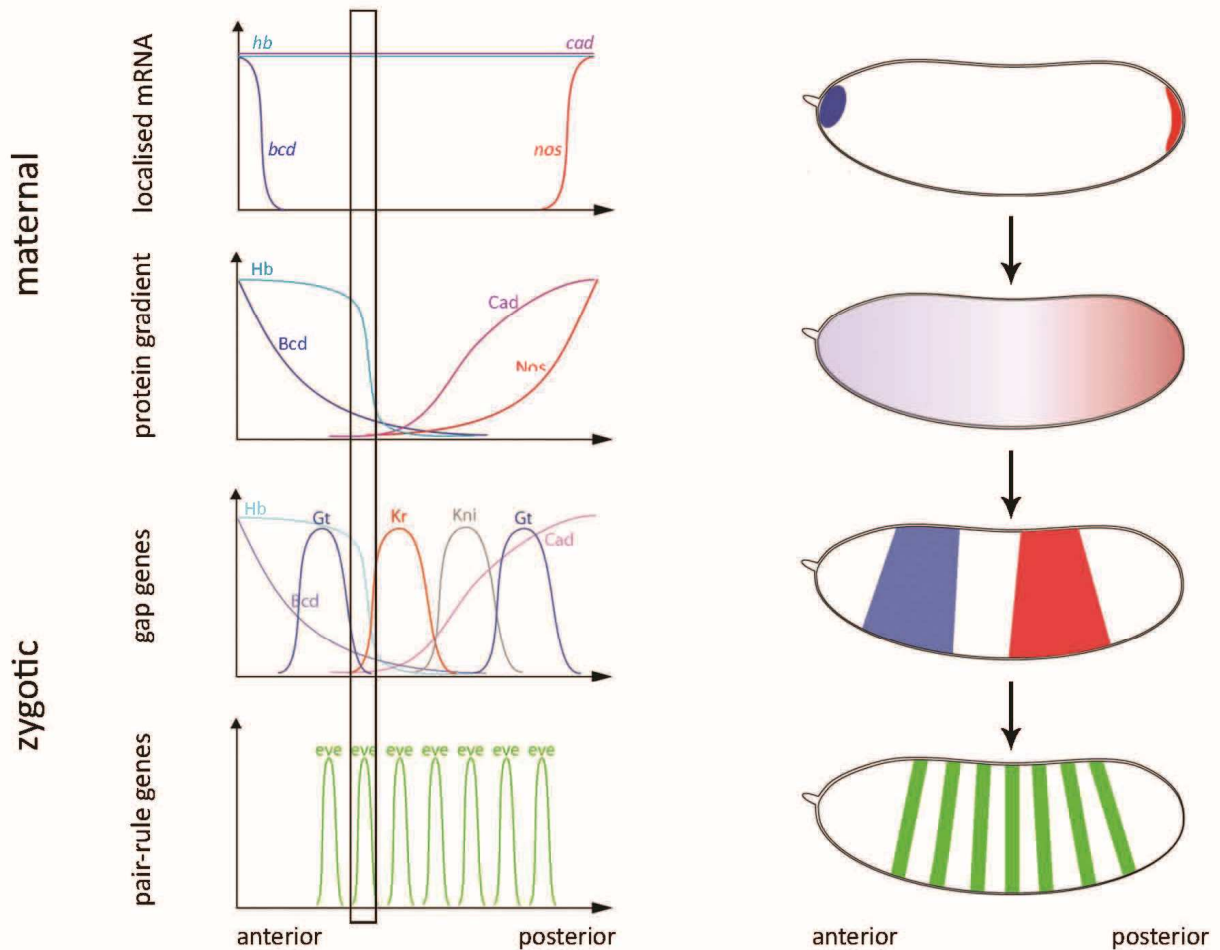


Figure 1.4 Schematic overview of maternal effect genes and zygotic gap genes and pair-rule genes in the *Drosophila* embryo.

RNA or protein levels along the anterior-posterior axis of an embryo in a graph (left) or an embryo (right). The black frame highlights the combination of maternally provided genes and gap genes which lead to the expression of the second *eye* stripe.

1.2.1. RNA localization in *Drosophila* egg chamber

Mis-localization of *bicoid* mRNA in the oocyte affects the Bicoid morphogen gradient in the embryo, which results in a less pronounced *hunchback* expression and reduced *caudal* repression. This leads necessarily to a shift and mis-expression of the gap genes and subsequently the pair-rule genes. The whole further patterning is disturbed. To ensure the localization of RNAs the oocyte needs to be polarized.

Polarity in the egg chamber and oocyte

Each ovary of a *Drosophila* female is made of 15-20 ovarioles (Fig. 1.5 A), which are functional units containing a sequence of egg chambers with increasing stages of development (Fig. 1.5 B). Each egg chamber consists of 16 germ-line cells, one oocyte and 15 nurse cells, surrounded by a single epithelial layer of somatic follicle cells (Fig. 1.5 B). Due to incomplete cytokinesis all 16 germ-line cells of the egg chamber, the cystocytes, are interconnected via cytoplasmic bridges, the so called ring canals [28]. Adjacent egg chambers within one ovariole are connected by specialized follicle cells, the stalk cells. At the anterior tip of each ovariole is the germarium, which contains, besides the somatic follicle cell stem cells, 2-3 germ-line stem cells and the earliest stages of oogenesis.

The proper composition and polarity of the egg chamber is highly dependent on a membranous branched structure called the fusome [29], which is distributed asymmetrically during the first division and already determines the later polarity [30]. The asymmetric distribution of the fusome specifies the later oocyte; the other 15 germ-line cells will develop into nurse cells. The future oocyte is positioned at the posterior of the egg chamber; this is additionally enforced by external cues coming from the interaction with the follicle cells [28, 31]. The initial polarity of the oocyte is also determined by the microtubule organization center (MTOC), which lies in the oocyte between the ring canals and the nucleus. Factors from the nurse cells are transported into the oocyte along microtubules in a dynein dependent manner and accumulate at the anterior. These include the centrosomes, the proteins Egalitarian, Bicaudal D,

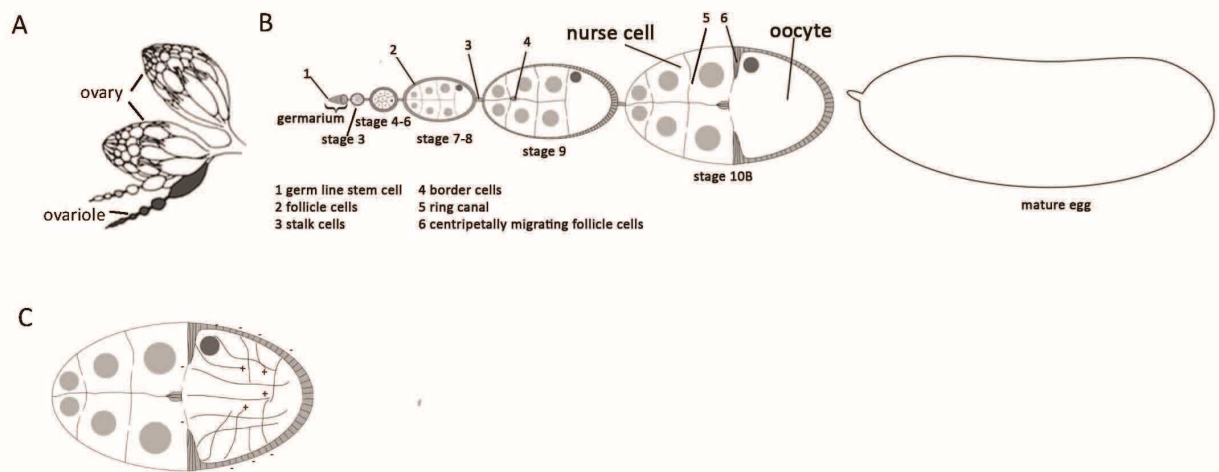


Figure 1.5 Schematic overview of *Drosophila* ovary and egg chamber composition.

A One *Drosophila* ovary consists of 15-20 ovarioles. **B** Scheme of an ovariole containing different stages from the stem cells in the germarium to the mature egg. **C** Egg chamber in stage 10B, depicted is the microtubule network. The minus ends of the microtubule pointing to the cortex, except the most posterior cortex. Plus ends of the microtubule are located in the middle of the oocyte.

oo18 RNA-binding protein and Cup as well as *oskar*, *gurken* and *orb* mRNAs (Balbiani body) [26, 29, 30]. Stage 3 egg chamber enters the vitellarium after enveloping of the cyst by follicle cells and positioning of the oocyte at the posterior. With that a reorganization of the microtubule network occurs. The MTOC, centrosomes, RNAs and proteins are re-localizing to the posterior of the oocyte. As in many other organisms [32, 33], one of the main internal polarization cues of the *Drosophila* oocyte is the localization of Par proteins. Par-1, a serine/threonine kinase, initially localizes with the fusome and is restricted to the oocyte in a microtubule dependent manner [30], it co-localizes with the MTOC at the anterior and is later transferred to the posterior together with the Balbiani body. This re-localization requires Par-1 itself as well as Bazooka (Baz), the Par-3 homologue of *Drosophila*, which remains at the anterior pole. The localization of these two proteins within the oocyte is mutually exclusive. Par-1 phosphorylates Baz leading to the recruitment of 14-3-3 proteins (Par-5); this blocks the formation of a Baz/Par-6/aPKC complex at the posterior, by inhibiting the oligomerization of Baz. In mammalian cells a homologue of aPKC is known to

phosphorylate Par-1, which leads to the inhibition of its kinase activity. This mutual antagonism could explain how these complementary domains in polarized cells in general, and in the *Drosophila* oocyte specifically, are ensured [28]. The link between Par-1 and the microtubule network could be direct; the mammalian homologue of Par-1, MARK, is known to regulate microtubule dynamics by phosphorylating microtubule associated proteins [34-36].

An unknown signal from the follicle cells triggers the re-polarization of the microtubule network within the oocyte at stage 7. This leads to a disassembly of the posterior MTOC and the migration of the nucleus towards the anterior. The position of the nucleus in one anterior corner determines the future dorsal side of the embryo. Subsequently to the disassembly of the MTOC new microtubules emanate from the anterior and lateral cortex, projecting towards the center of the oocyte. No microtubules emanate from the most posterior cortex (Fig. 1.5 C) [37, 38]. This highly organized microtubule network and the establishment of polarity within the egg chamber is a prerequisite for the proper body patterning of the future embryo.

***oskar* mRNA localization**

Within the egg chamber *oskar* mRNA is transcribed in the nurse cells and accumulates in the early oocyte shortly after its specification. This accumulation is mediated by microtubules and occurs through the ring canals. In the oocyte *oskar* mRNA localizes transiently to the anterior and later, from stage 9 onwards, becomes restricted to the posterior pole. Since *oskar* mRNA localization is strongly affected in *kinesin heavy chain* mutants, Kinesin I is the motor protein implicated in this process [17]. A number of other factors are known to be involved either in translational repression, in localization or in anchoring of *oskar* mRNA. Egalitarian and Bicaudal D are necessary for the transport of *oskar* mRNA from the nurse cell to the oocyte [39]. Staufén, Hrp48, Squid and Glorund are RNA binding proteins associated with *oskar* mRNA [40-42]. So is the exon junction complex (EJC), consisting of Barentz, MagoNashi, Y14 and eIF4aIII [43, 44]. This complex is loaded onto the mRNA upon splicing. It has been shown that, splicing of the first intron of *oskar* is essential for its localization [45]. During transport to

the posterior pole of the oocyte translation of *oskar* mRNA must be repressed. In mutants where *oskar* is prematurely translated, while the mRNA is still transported, e.g. *Bruno*, *cup*, *Me31B*, localization is defective. Other factors, essential for *oskar* mRNA localization affect oocyte polarity or the microtubule cytoskeleton, e.g. Par-1, Lkb-1 or Cappuccino and Spire [38]. The anchoring of *oskar* mRNA at the posterior cortex is another very important step in localization, it is ensured by Oskar protein itself [4, 40].

***bicoid* mRNA localization**

In contrast to the large number of factors known for *oskar* mRNA localization, just four are known to be essential for *bicoid* mRNA localization, *swallow*, *staufer*, *ESCRTII* and *exuperantia*. After transcription in the nurse cells, small amounts of *bicoid* mRNA are already detectable in stage 6 oocytes. The RNA starts to be localized at the anterior margin in a ring shape around stage 8. In stage 9 egg chambers perinuclear cluster of *bicoid* mRNA are detectable in the nurse cells. At stage 10B the localization of the RNA changes from a ring-like structure into a disc-shape. The clusters in the nurse cells are completely released during stage 12 and transported into the oocyte through the ring canals, and no *bicoid* RNA is detectable in the nurse cells anymore. In the oocyte *bicoid* mRNA is tightly localized at the anterior cortex until the egg is laid [46].

In *staufer* mutants *bicoid* RNA localization beyond stage 10B is disturbed, resulting in a *bicoid* mRNA gradient, which subsequently leads to a shallow Bicoid protein gradient in the embryo. Staufen protein co-localizes with *bicoid* mRNA from stage 10B of oogenesis onwards [47]. It has known RNA binding domains, and the *bicoid* 3' UTR, when injected into the early embryo, recruits Staufen into particles, which move along microtubules, indicating that Staufen binds to *bicoid* RNA under these circumstances [47, 48]. However, Staufen also binds *oskar* mRNA and is associated with it throughout oogenesis, therefore it cannot provide specificity for the anterior localization of *bicoid* mRNA.

The recruitment of Staufen to the *bicoid* RNA complex is dependent on the ESCRTII complex, which is a component of the endosomal sorting pathway. *bicoid* mRNA localization is defective in mutants of all subunits of the ESCRTII. The role of ESCRTII

in this process seems to be independent of endosomal sorting, since mutants in other components of this pathway do not show any *bicoid* mRNA localization phenotype. Furthermore, Vps36, a subunit of the ESCRTII is the first sequence-specific RNA-binding protein known so far in *bicoid* mRNA localization [49].

The formation of particles in the nurse cells, the transport from the nurse cells into the oocyte, as well as the initial localization of *bicoid* mRNA in the oocyte are unaffected in *swallow* mutants, but at stage 10B the localization of *bicoid* mRNA starts to fail. This coincides with the co-localization of *bicoid* mRNA and Swallow at the anterior cortex, which is microtubule dependent but not dependent on *bicoid* mRNA localization itself. It is associated with the change from the ring-like localization of *bicoid* into a disc shaped cap. It is thought that this is connected to a reorganization of the microtubule network and a formation of the MTOC in the middle of the anterior pole. This MTOC interacts with Swallow [50, 51].

Beside the GLUE domain of VPS36 of the ESCRTII complex [49] no *bicoid* specific RNA binding proteins have been identified so far. Unspecific RNA binding proteins (PolyA binding protein (PABP), Modulo and Smooth) involved in the process of *bicoid* mRNA localization have been found in a protein complex from ovaries purified using a minimal *bicoid* localization element (BLE) [52]. However, none of these proteins, show sequence specificity for *bicoid*. Therefore they cannot be responsible for the specificity of the complex.

The influence of the earliest known factor in *bicoid* mRNA localization, *exuperantia* will be discussed in more details in the following chapter.

1.3. Exuperantia in body patterning

1.3.1. Phenotype and alleles

exuperantia (*exu*) has been known for more than 25 years to play a crucial role in *Drosophila* early patterning. It was isolated in a screen for maternal-effect mutations that alter the body patterning of the embryo. Embryos derived from homozygous *exu*-mutant females show reduced head structures and an expanded thorax but a normal abdomen, indicating a defect in anterior patterning (Fig. 1.6 A) [53-55]. Since *bicoid* loss of function mutants show a more severe phenotype than *exu*-mutants some residual *bicoid* activity must still be present (Fig. 1.6 B).

Besides its function in oogenesis, *exuperantia* is also required for spermatogenesis, although the precise role in this process is not understood [56-58]. Males mutant for *exuperantia* are sterile, their spermatids are not motile and never reach the seminal vesicle of the testis [56]. It was shown that *exuperantia* mRNA is alternatively spliced, resulting in male and female specific transcripts, which differ in their 5' and 3' UTRs but not in the protein coding sequence [58].

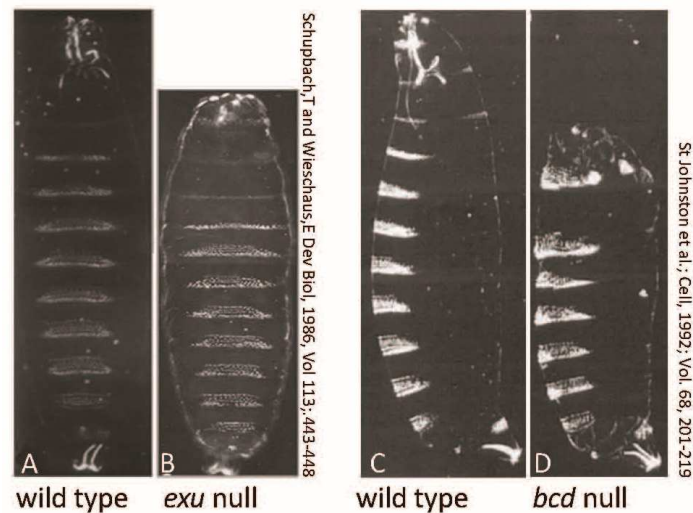


Figure 1.6 Cuticle of *exuperantia* and *bicoid* mutants.

A,B cuticle of a wild-type larva (**A**) in comparison to an *exu*-mutant larva (**B**). The head skeleton is reduced, but posterior structures are fine. **C,D** cuticle of wild-type (**C**) and *bicoid* mutant larva (**D**). Note the complete loss of anterior structures.

So far, eight mutant alleles for *exuperantia* have been described (Table 1.1). Flies homozygous for one of the following five alleles, *exu*^{SCO2}, *exu*^{XL1}, *exu*^{XL2} and *exu*^{VL75}, do not produce detectable amounts of RNA [52, 56, 59]. *exu*^{DP3} is a male specific allele, resulting exclusively in male infertility; it has no effect on oogenesis [60]. Analysis of this allele showed that part of the male specific 3' UTR is deleted, which results in a smaller and less abundant mRNA. This mRNA leads to a normal sized protein, with consistently reduced expression but normal localization.

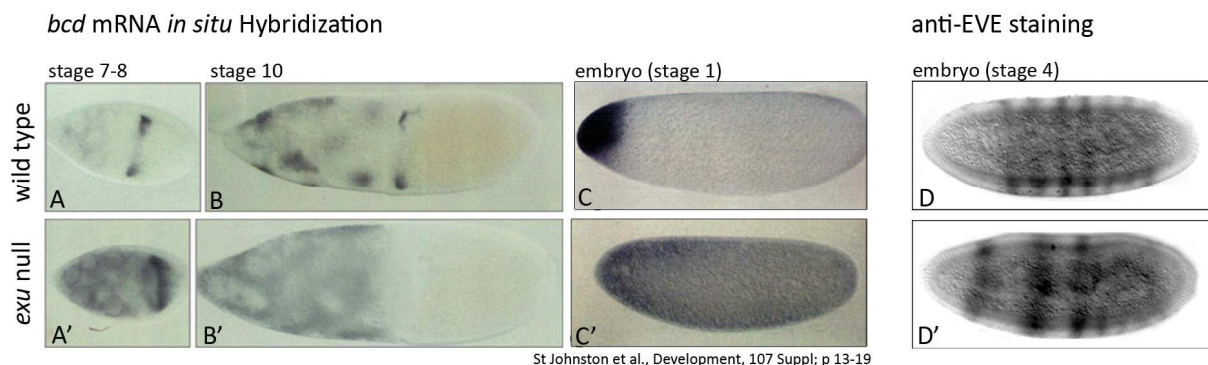
In addition to the male specific and the RNA/protein null alleles, three other alleles with point mutations have been described. *exu*⁴, which carries an early nonsense mutation (Gln⁵³Stop), is presumably also a protein null allele; however no functional data on this allele have been published [61]. Both, *exu*^{PJ42} and *exu*^{QR9}, carry mis-sense mutations and lead to stable proteins that can be detected on Western blots [59]. The spermatogenesis phenotype of the *exu*^{PJ42}-allele is described to be temperature sensitive leading to a more severe phenotype at 18°C than at 25°C. Nevertheless, embryos laid by flies homozygous for this allele still do not hatch at room temperature [56]. In *exu*^{PJ42} Arg³³⁹ is mutated to Ser. In *exu*^{QR9} sequencing showed that Gly⁴⁴ is changed to Gln. All mutant *exu*-alleles have been described as leading to the same severity of anterior patterning defects; no hypomorphic alleles exist.

name	description	phenotype	reference
<i>exu</i> ^{PJ42}	Arg ³³⁹ Ser	amorph	[56]
<i>exu</i> ^{QR9}	Gly ⁴⁴ Gln	amorph	[56]
<i>exu</i> ⁴	Gln ⁵³ Stop	amorph	[61]
<i>exu</i> ^{DP3}	deletion of male specific 3'UTR	male phenotype only	[60]
<i>exu</i> ^{XL1}	X-ray induced, RNA level reduced to 5%	amorph	[56]
<i>exu</i> ^{XL2}	EMS induced, no RNA detectable	amorph	[56]
<i>exu</i> ^{VL57}	700bp deletion, no RNA	amorph	[56]
<i>exu</i> ^{SCO2} / <i>exu</i> ^{SC}	RNA level reduced to 30-40%	amorph	[56]

Table 1.1 Summary of known *exuperantia* alleles.

***bicoid* mRNA localization in *exu*-mutants**

As described above, *bicoid* mRNA is transcribed in the nurse cells and transported into the oocyte. In wild-type egg chambers it can be detected by *in situ* hybridization in the nurse cell cytoplasm and at the anterior cortex of oocytes from stage 7 onwards. In embryos the RNA forms a cap at the anterior pole of (Fig. 1.7 A - B) [46, 54]. In all *exu*-mutants, except *exu*^{DP3}, which has no effect in oogenesis, the anterior localization of *bicoid* mRNA is defective. The RNA is transcribed in the nurse cells and transported into the oocyte, but it localizes more diffusely within the oocyte compared to wild-type. From stage 10 onwards the localization defects becomes more pronounced, resulting in an even distribution of *bicoid* in the embryo (Fig. 1.7 A' – C') [46, 54]. This lead to the conclusion, that *exuperantia* is necessary to promote anterior localization of *bicoid* mRNA [46].



St Johnston et al., Development, 107 Suppl; p 13-19

Figure 1.7 *bicoid* *in situ* hybridization and anti-Eve staining in wild-type and *exu*-mutant egg chambers and embryos.

bicoid mRNA *in situ* hybridization in wild-type (A-C) and *exu*^{PJ42} mutant (A'-C') egg chambers and embryos. In stage 7 egg chambers *bicoid* mRNA localization is diffuse in *exu*-mutants in comparison to wild-type (A,A'). This weak localization is lost in *exu*-mutant egg chambers at stage 10 (B') and in embryos (C'). In wild-type embryos *bicoid* mRNA appears as a anterior cap (C). D The first Eve stripe appears in wild-type embryos around 32% of the egg length (anterior: 0%; posterior: 100%) (D). In *exu*-mutant flies (*exu*^{VL}/*exu*^{PJ42}) the first stripe is shifted towards the anterior (D').

1.3.2. General features of Exuperantia protein

Exuperantia is first detectable at low levels in stage 4 egg chambers. It starts to accumulate around the nurse cell nuclei at stage 7. In stage 10 the expression increases slightly [59, 61, 62]. A more detailed analysis of the sub-cellular distribution of Exuperantia protein was possible after Wang and Hazelrigg in 1994 generated the first *Drosophila* GFP-fusion protein by creating a transgene where the coding sequence for GFP is coupled to Exuperantia coding sequence [63]. Regardless of whether the GFP sequence was fused to the N-terminal or C-terminal end of Exuperantia, both chimeric proteins were able to rescue the *exu*-mutant phenotype and show the same localization: A diffuse, sometimes patchy localization in the nurse cells and an early anterior localization of Exuperantia in stage 7 oocytes, which disappears in later stages (stage 10).

Additionally, there is a consistent posterior localization of Exuperantia in the oocyte which persists until late stages. Furthermore, it was shown that Exuperantia is found in particles at the ring canals, which were proposed to be mRNA containing particles (RNPs) [63]. These particles are sensitive to treatment with colchicine or taxol. Wilsch-Bräuninger et al. provided support that these particles contain Exuperantia protein and RNA by using electron microscopy [62]. They described nurse cell-specific sponge-like structures (sponge bodies) which are highly enriched for Exuperantia protein and contain RNAs. However, the presence of *bicoid* mRNA in sponge bodies could not be shown. In 1989 St. Johnston et al. described patchy *bicoid* mRNA localization in nurse cells of stage 10 egg chambers, comparable to the Exuperantia particle described by Wang et al. and Wilsch-Bräuninger et al. [46, 62, 63].

Very little is known about the protein structure of Exuperantia. *exuperantia* encodes a basic protein of 532 amino acid residues. It was shown to carry two motifs with phosphorylation sites (aa⁴³⁴ - aa⁴⁴⁰ and aa⁴⁵³ - aa⁴⁵⁹), which, when phosphorylated could serve as 14-3-3 binding sites (Fig. 1.8). 14-3-3 proteins are known to promote protein-protein interactions. These motifs have been shown to be phosphorylated by the Par1 kinase *in vitro* [64]. However, mutations of all serine residues in these motifs to alanine only result in a weak defect in *bicoid* mRNA localization and no severe change

in pattern formation in the embryo was described [64]. This indicates that the putative 14-3-3 binding sites in Exuperantia are not essential for *bicoid* mRNA localization.

Immunoprecipitation of Exuperantia showed that it is part of a RNA sensitive complex that contains several proteins [65]. A direct interaction was shown for the cold-shock protein Ypsilon Schachtel (Yps). However, only *oskar* mRNA was found in the complex, no *bicoid* mRNA [65].

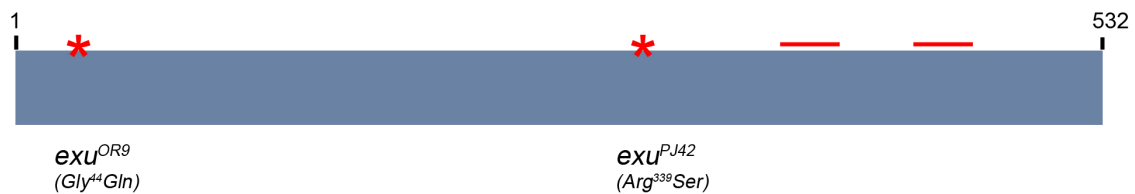


Figure 1.8 Exuperantia protein.

Exuperantia is a basic protein with 532 amino acid residues. Described features are two phosphorylation sites (aa⁴³⁴-aa⁴⁴⁰ and aa⁴⁵³-aa⁴⁵⁹), which, if phosphorylated, become putative 14-3-3 binding sites (lines) and two point mutations (Gly⁴⁴Gln and Arg³³⁹Ser) which cause an amorphic phenotype (stars).

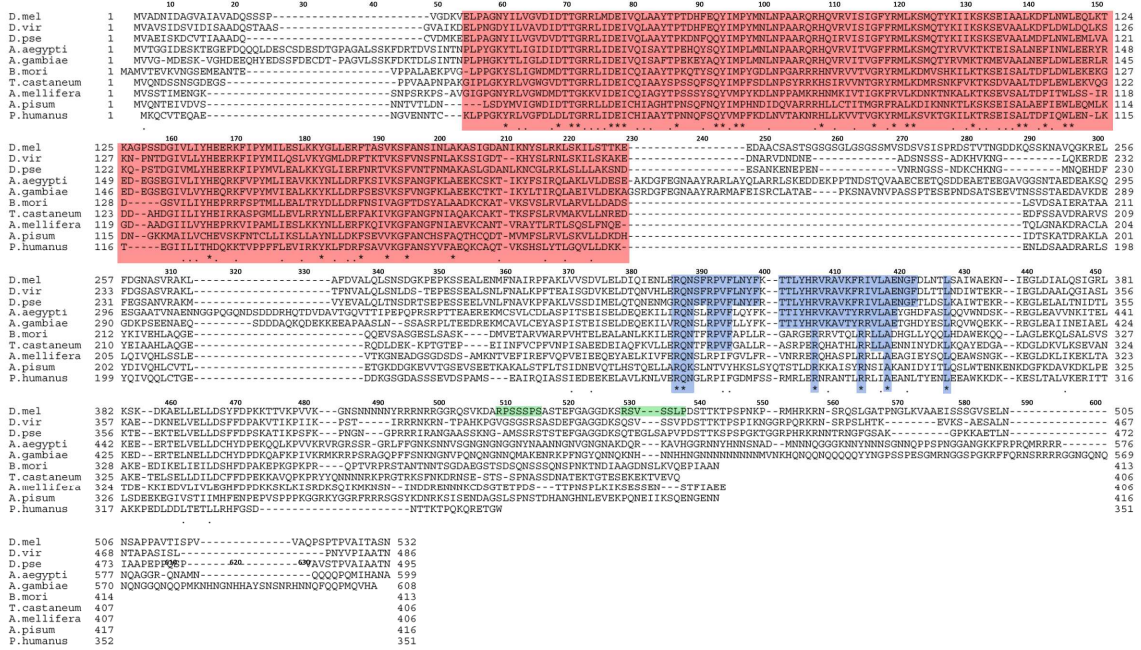
Conservation of Exuperantia protein in insects

In contrast to *bicoid*, which is not conserved outside higher dipteran flies, homologues of Exuperantia can be found in all insects. The protein sequences of Exuperantia show a high degree of conservation in the N-terminal region (Fig. 1.9 A, red box aa⁵³ - aa²²⁹). This part of Exuperantia has also been aligned with DEDD exonucleases ([3] and see below). In the central part of Exuperantia (aa²⁷⁰ - aa⁴¹⁵ in *D. melanogaster*) a domain with a lower degree of conservation can be identified. It is characterized by a number of invariant residues in all insects (Fig. 1.9 A, blue boxes between aa³⁸⁰ and aa⁴⁷⁰). The previously described phosphorylation sites in the C-terminal part of Exuperantia [2] are not conserved (Fig. 1.9 A green bars).

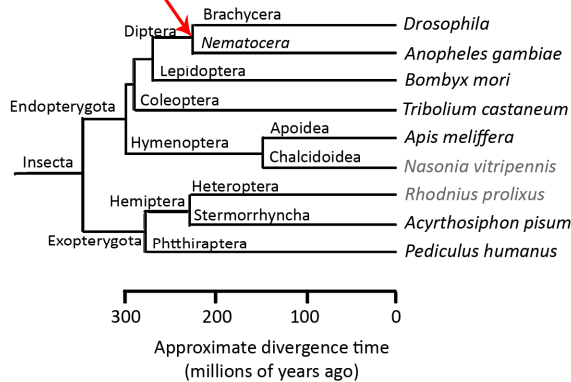
It is not known, why *exuperantia* is more widely conserved than *bicoid* (Fig. 1.9 B). It could be that Exuperantia has a role in *oskar* mRNA localization, since it co-localizes with *oskar* mRNA throughout oogenesis in *Drosophila* [4] and *oskar* mRNA can be in co-immunoprecipitated with Exuperantia [65], however, *oskar* mRNA localization is not

affected in *exu* null mutants [5]. If *Exuperantia* has a function in *oskar* mRNA localization it is not essential and probably redundant. Alternatively, *Exuperantia*'s essential role in spermatogenesis [6] could be the reason for its conservation.

A



B



adapted from: *Apis* genome | Nature 443 | 26 October 2006

Figure 1.9 Exuperantia alignment of insects.

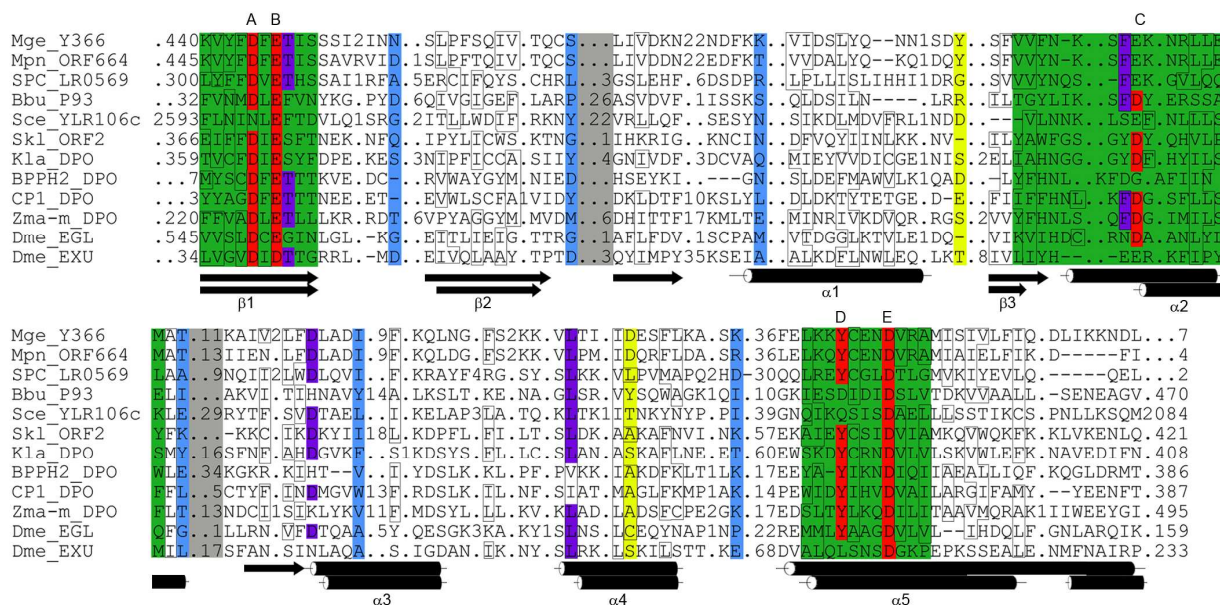
A ClustalW generated alignment of selected protein sequences of *Exuperantia* homologues from different insect species. The region of exonuclease homology in red, central part with highly conserved residues in blue, previously described 14-3-3 binding sites in green. **B** Phylogenetic tree of insects based on genome sequence (adapted from *Apis* genome). Red arrow indicates the appearance of *bicoid* in higher dipterans.

Is Exuperantia an exonuclease?

A surprising finding about Exuperantia was made by Moser et al. (1997). With the aim to identify more proteins containing an RNase D 3'-5' exonuclease domain they used a hidden Markov model (HMM) and phylogenetic studies to find and characterize other proteins containing this domain, later named DEDD exonuclease domain [66].

Two *Drosophila* proteins (Exuperantia and Egalitarian) were aligned with these exonucleases (Fig. 1.10) showing the main characteristics of the domain. The exonuclease features of Egalitarian have been studied already [66]. Egalitarian is known to interact with Bicaudal D and to play an important role in targeting RNAs to the minus ends of microtubules in *Drosophila*. Deletion of the exonuclease homology region of Egalitarian leads to a strong reduction of its ability to interact with RNA but not with Bicaudal D, indicating this domain is involved in RNA binding [67]. However, substitutions of the name giving residues, known to be important for enzymatic function of DEDD domains (Asp⁵⁶¹, Glu⁵⁶³, Asp⁶²¹, and Asp⁷⁰⁸ in Egalitarian) into alanine, did not result in defective Egalitarian function during oogenesis [67] [66].

This study showed that the exonuclease domain of Egalitarian is necessary for RNA binding but it is unlikely to have enzymatic activity, even though all catalytic residues and motifs are still conserved. In Exuperantia, in which the catalytic residues are also conserved, the catalytic activity has not been studied so far.



adapted from: Moser et al. Nucleic Acid Research, 1997, 25/24 p. 5110-8

Figure 1.10 An HMM-generated alignment of selected exonuclease domains. Amino acids conserved in the majority of the sequences are highlighted and predominantly hydrophobic residues are boxed. Full points indicate insertions, numbers indicate the size of inserted residues. Exo I - III domains are indicated in green, catalytic residues are red (A-E). Residues preceding insertions longer than 10 amino acids are blue, yellow columns indicate Cys¹¹² and Cys¹⁶⁸ in *E.coli* RNase T and magenta columns are conserved residues. Secondary structures, like β -sheets (β 1 - β 3) and α -helices (α 1 - α 5) are indicated below. Sequences used for this alignment are listed in Appendix A.

DEDD Exonucleases

Exonucleases have been grouped into six superfamilies based on extensive sequence analysis and their catalytic properties [68]. One of the superfamilies is the DEDD 3'-5' hydrolytic exoribonuclease family. Examples of this family are RNase D, RNase T, Oligoribonuclease, Rex2, Klenow fragment and DNA polymerase [68]. Members of this family show a distributive catalytic activity from the 3' end towards the 5'. Besides RNase activity, some proteins of this family show additional DNase activity. Enzymes of this family share a common catalytic mechanism involving two metal ions (Mg²⁺, Mn²⁺ or Zn²⁺) [69]. The family has been named after the sequence of the four invariant acidic amino acid residues originally described in DNA polymerase [70]. These residues have been shown to be important for catalytic activity of the enzyme, but to be not essential

for substrate binding in RNase T [71]. Although the overall sequence similarity in proteins of this family is not very high, the four highly conserved acidic residues reside in three conserved segments (Exo I – III). The Exo I segment, the most N-terminal one, contains the first two characteristic residues and is involved in binding of the metal ion A (Fig. 1.11). For the Klenow fragment it was shown that Exo I segments is critical for the binding of metal ion A, which is necessary for substrate binding by direct interaction with the phosphodiester bond to be hydrolyzed [72]. The Exo II motif contains the third name giving residue and is needed for binding metal ion B. Although it is not crucial for the substrate binding, it is essential for the catalytic activity of the enzyme. Two subfamilies of DEDD exonucleases can be distinguished by the different sequence motif in the Exo III part. The DEDDy family contains the sequence Y-x(3)-D, while the DEDDh family is characterized by H-x(4)-D. The significance of the difference is so far not understood, it cannot be responsible for the differentiation in RNases and DNases since both classes are found in both subfamilies [68]. The enzymatic activity of exonucleases of the DEDD super-family varies from 3' maturation of highly structured RNAs, like ribosomal or transfer RNAs (bacterial RNase T or eukaryotic Rex proteins) to shortening of PolyA-stretches (Poly(A)-specific ribonuclease (PARN) or Poly(A) specific ribonuclease subunit (Pan2)). This can either lead to the maturation of RNA or to the decay of the RNA. Most DEDD exonucleases are not sequence-specific, they are most often directed to their targets through interactions with other sequence- or structure-specific RNA-binding proteins [73]. These features could allow the analysis of the enzymatic activity *in vitro* even without knowing the *in vivo* target.

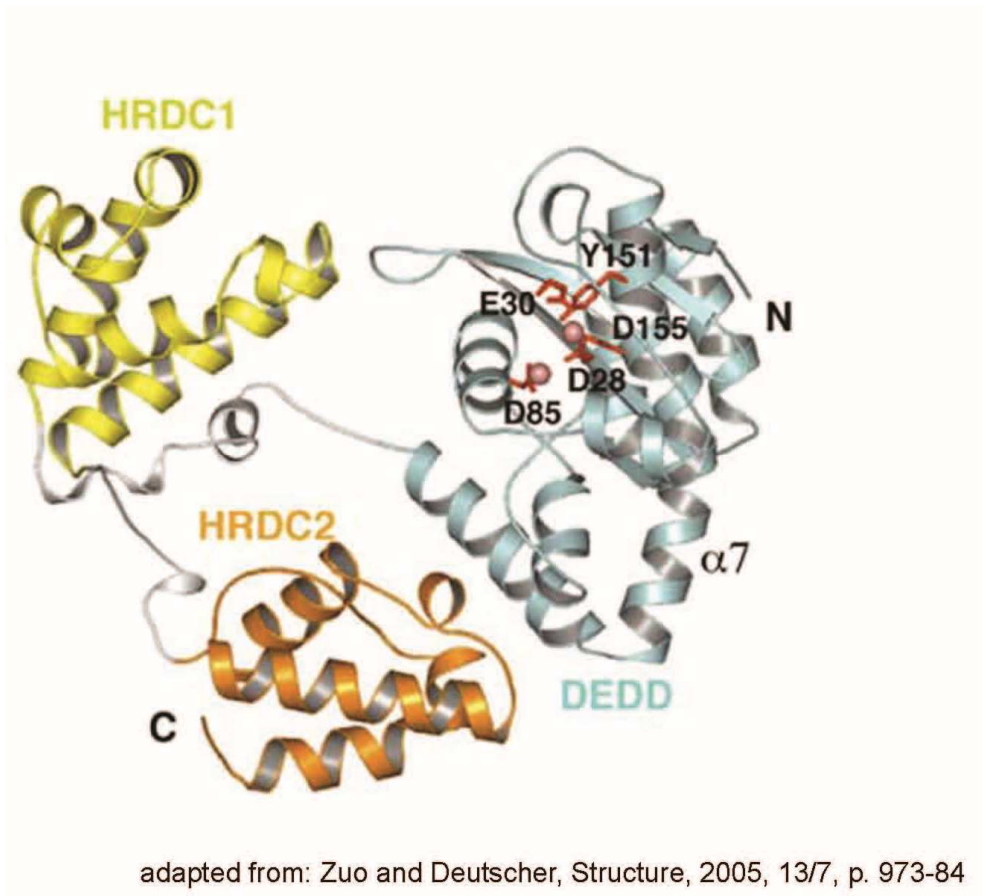


Figure 1.11 A ribbon representation of RNase D.

In grey, the DEDD exonuclease domain, red sticks are the catalytic residues of RNase D and the balls represent the position of the metal ions.

1.3.3. Model of Exuperantia function

Even though *exuperantia* is essential for the proper localization of *bicoid* mRNA, the mechanism of Exuperantia function is still unknown.

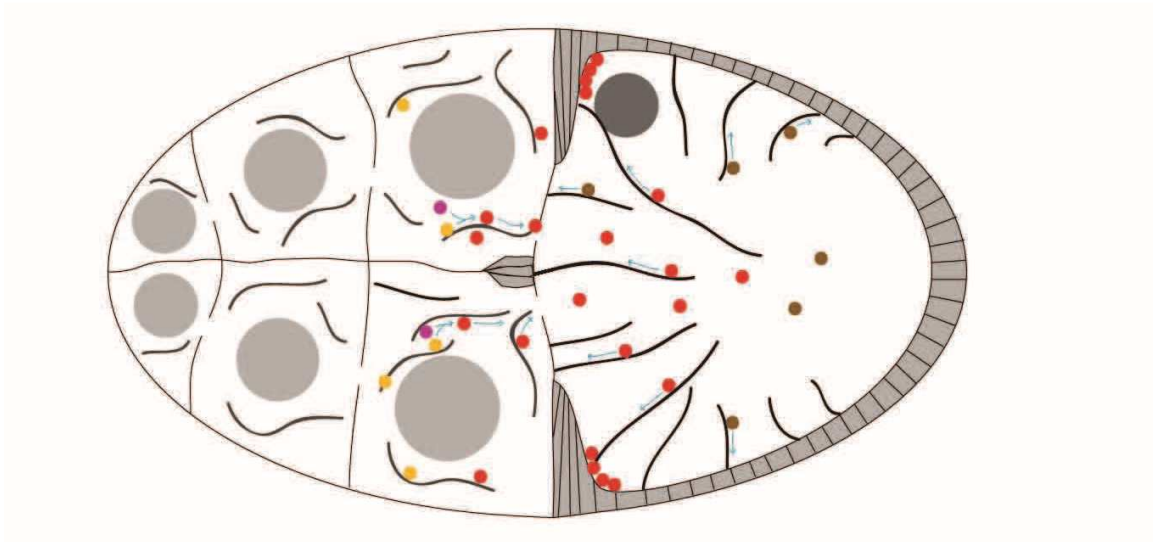
A model for Exuperantia function was proposed based on RNA injection experiments by Cha et al. [74]. By injection of *in vitro* generated fluorescently labeled *bicoid* mRNA into isolated egg chambers they could show that *bicoid* RNA needs to pass through the nurse cells to gain competence to localize to the anterior cortex in the oocyte. RNA injected directly into the oocyte localizes unspecifically to the nearest cortical region.

RNA injected into a wild-type nurse cell forms particles within 30 seconds, and, if withdrawn and re-injected into a wild-type oocyte the RNA always localizes to the anterior cortex (wt→wt). This result indicates that the nurse cells contain a factor promoting anterior localization. To study the role of *exuperantia* in this context Cha et al. performed reinjection experiments also with *exu*-mutant egg chambers. After injecting *bicoid* RNA into a wild-type nurse cell, withdrawal and re-injection into an *exu*-mutant oocyte (wt→*exu*) *bicoid* RNA localizes to the anterior cortex, indistinguishable from the wt→wt experiment.

If the RNA is injected into an *exu*-mutant nurse cell, withdrawn and re-injected into a wild-type oocyte (*exu*→wt) it localizes unspecifically to the nearest cortex, comparable to the direct injection of RNA into the oocyte without passing through a nurse cell before. These experiments show that *exuperantia* is a key player in modifying *bicoid* RNA or factors of the *bicoid* RNP within the nurse cells to promote specific anterior localization in the oocyte (Fig. 1.12).

Injection of *bicoid* RNA into an *exu*-mutant nurse cell followed by re-injection into an *exu*-mutant oocyte (*exu*→*exu*) resulted in the disappearance of the RNA without cortical localization in the oocyte. This could be explained by an additional stabilizing function of Exuperantia. These experiments also showed that the transport of *bicoid* mRNA from the nurse cells into the oocyte does not depend on *exuperantia*, since the RNA, when injected into *exu*-mutant nurse cell is transported into the oocyte but fails to localize there anteriorly.

In summary, direct visualization of *bicoid* mRNA in egg chambers and the study of its behavior in *exu*-mutant or wild-type environment led to a model, in which Exuperantia protein is required in the nurse cells to promote, by a so far unknown mechanism, *bicoid* mRNA localization in the oocyte [74]. This supposedly happens within RNA-protein complexes in the nurse cells [74], which have been described as sponge bodies before [62]. However, a direct interaction of Exuperantia with *bicoid* mRNA has not been shown, so far.



adapted from Cha et al. Cell 2001, 106 p. 35-46

Figure 1.12 Model of Exuperantia function.

Within the nurse cell cytoplasm the *bicoid* mRNA form particle (pink dots). In a microtubule dependent manner Exuperantia (yellow dots) modifies these RNPs (red dots). This interaction with Exuperantia promotes the proper anterior localization in the oocyte. The transport into the oocyte is not dependent on Exuperantia, but RNPs which have not seen Exuperantia in the nurse cell (brown dots) localize unspecifically to the nearest cortex.

To understand more about the function of Exuperantia in *bicoid* mRNA localization, we addressed the following questions.

- ❖ Can we identify additional structural elements in Exuperantia?
- ❖ If so, what are the functions of these structural elements?
- ❖ Does the N-terminus of Exuperantia act as an active DEDD exonuclease?

2. Results

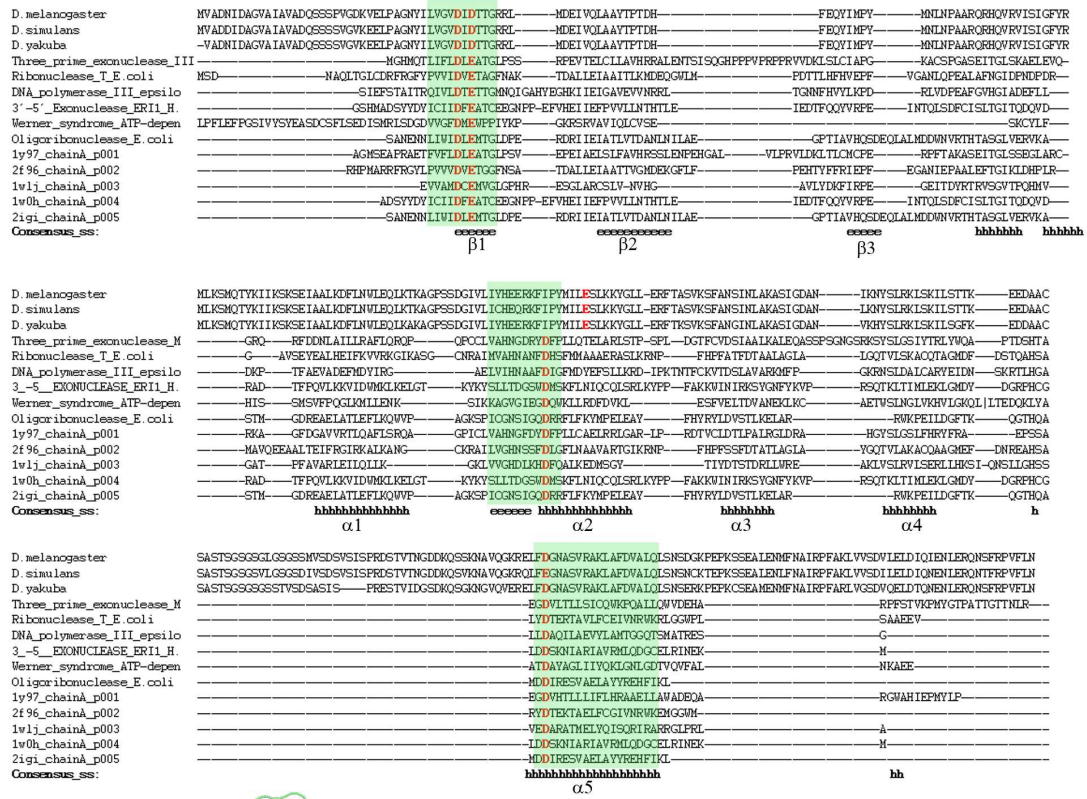
2.1. *in silico* analysis of Exuperantia

Exuperantia is an important factor in *bicoid* mRNA localization; it was shown, that Exuperantia modifies either *bicoid* mRNA itself or the *bicoid*-RNPs in the nurse cells to ensure the proper anterior localization of the mRNA within the oocyte [74]. How Exuperantia achieves this is not understood, so far. In the past, two regions of the protein have been described: a serine rich stretch (aa⁴³⁴-aa⁴⁴⁰ and aa⁴⁵³-aa⁴⁵⁹), which, upon phosphorylation, might act as 14-3-3 binding motifs, but, when mutated, shows only a weak *bicoid* mRNA localization defect [64]; and in 1997 the N-terminal part of Exuperantia was aligned with RNaseD-like exonuclease domains [66], a finding which has never been followed up.

To gain a better understanding of the molecular functions of Exuperantia, the amino acid sequence was re-analyzed using the HHpred tool from the MPI-toolkit (<http://toolkit.tuebingen.mpg.de/hhpred>) [75]. This program is based on the pair wise comparison of hidden Markov models (HMMs) and is currently the most sensitive method to detect remote homologies. In contrast to other algorithms, which search sequence archives, e.g. UniProt, HHpred searches in alignment databases like Pfam or SMART. Using this sensitive approach the confirmation of the homology to a 3'-5' exonuclease domain located at the N-terminus (aa¹ - aa²⁹⁶) of the protein was possible although the overall sequence identity is only 15%. Besides this, HHpred could not identify other characteristic domains. The homology of the N-terminus of Exuperantia to DEDD 3'-5' DnaQ-like exonucleases (SCOP family c.55.3.5) was corroborated by several features. Besides the secondary structure similarity detected by HHpred, the four amino acid residues important for the catalytic activity of these enzymes are conserved (Asp³⁹, Asp⁴¹, Glu¹⁵⁰ and Asp²⁵⁸ in Exuperantia Fig. 2.1 A). The normal sequence of the catalytic residues in this kind of exonucleases is D-E-D-D. However, the first two of these residues are interchanged in Exuperantia. This change leaves the geometry of the catalytic center intact, so it is presumably due to compensatory

mutations. Additionally, the third residue, E¹⁵⁰, is shifted by six positions in the α -helix 2 (Fig. 2.1 A), again preserving the geometry of the catalytic center. This combination of conservation and compensatory mutations of catalytic residues argues for the retention of an enzymatic activity in Exuperantia, as opposed to a mere RNA binding functionality of an exonuclease-like domain. On the other hand, Egalitarian also contains a domain similar to DEDD exonucleases, with conserved catalytic residues. However, it was shown that these residues are dispensable for the function of the protein [76].

A



B

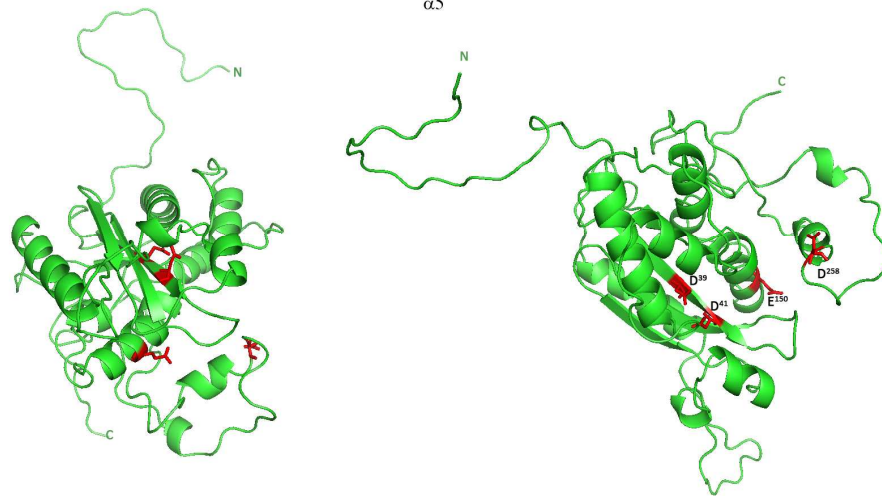


Figure 2.1 HHpred alignment of DEDD exonucleases and derived structural model of N-terminus of Exuperantia.

A HHpred alignment of selected DEDD exonucleases and three Exuperantia sequences from different *Drosophila* species. Highlighted in green are Exo motifs I-III, in red the four catalytic residues. All *Drosophila* Exuperantias show the compensatory mutation from DEDD to DDED. The consensus secondary structure (ss): e = extended for β -sheet and h = α -helix. **B** Model of the DEDD domain of Exuperantia (aa¹ - aa²⁹⁶) side view (left) and top view (right). Highlighted in red are the four acidic residues (amino acid number is indicated in the right picture).

Apart from this N-terminal domain, a SAM-like domain in the middle part (aa³²⁶ - aa³⁸⁷) of the protein was identified (Andrei Lupas, personal communication). SAM domains are characterized by five α -helices, which are arranged in a globular bundle enclosing a hydrophobic core, and are known to serve mainly as protein-protein-interaction modules mediating both homo- and heterotypic interactions [77]. In a manually generated sequence alignment of Exuperantia central domains (aa³²⁶-aa³⁸⁷) with several SAM domains (Fig. 2.2 A), the secondary structure similarity can be shown by the presence of the five α -helical bundles characteristic for SAM domains. Interestingly, two of the aligned SAM domains are known to bind RNAs, VTS1 from *S. cerevisiae* (PDB-ID 2D3D [78]) and Smaug from *D. melanogaster* (PDB-ID 1OXJ [79]). Both bind RNA mainly through a conserved motif of positively charged residues (Fig. 2.2 A red asterisk) [80]. Most of these residues are conserved in Exuperantia proteins, suggesting that it also might be capable of binding nucleic acids. Furthermore, this motif includes the Arginine³³⁹ residue (Fig. 2.2 highlighted in red), which is known to cause an amorphic phenotype when mutated to serine (*exu*^{PJ42} [59]). A homology model of the putative SAM domain of Exuperantia (Fig. 2.2 B, C) shows the five canonical α -helices and emphasizes that the side chains of the potential RNA binding residues are surface exposed, which would allow nucleic acid binding.

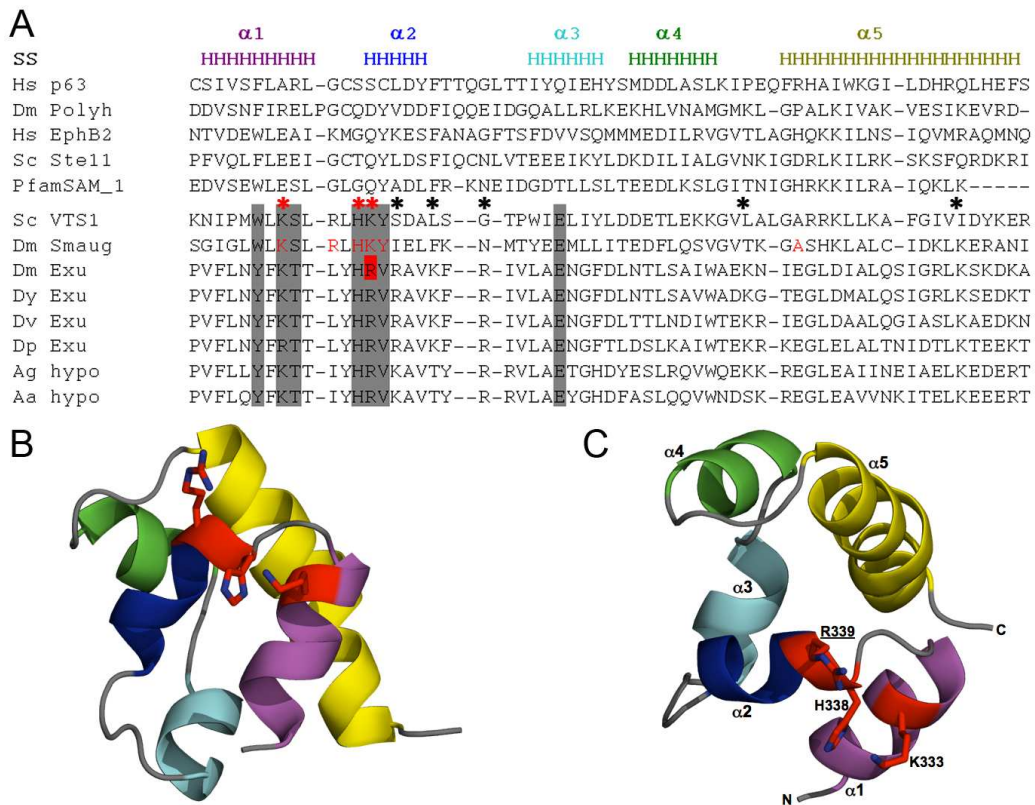


Figure 2.2 Prediction of a RNA-binding SAM domain in Exuperantia.

A Manually generated multiple sequence alignment of SAM-like domains of Exuperantia from selected species and other SAM domains. It contains several SAM domains with known structures. VTS1 from *S. cerevisiae* and Smaug from *D. melanogaster* are known to bind RNA mainly through a conserved motif of positively charged residues (red residues in Smaug have been shown to disrupt RNA binding, when mutated). Most of these residues are conserved in Exuperantia. The helices 1 to 5, characterizing SAM domains, are indicated above the alignment. The highlighted residue (boxed in red) is Arg³³⁹, which is mutated in *exu*^{PJ42}-allele into serine. Residues highlighted in grey are conserved or very similar in Exuperantia and RNA-binding SAM domains. The asterisks indicate positively charged residues (red - conserved in Exuperantia, Smaug and VTS1; black reserved at least in Exuperantia). Side **(B)** and top **(C)** views of the structural model of the putative SAM domain of Exuperantia. The homology model was built with Modeller using the SAM domain of Smaug as a template. It shows the five canonical α -helices of the SAM domain. In the top view **(C)** the side chains of the residues, which are potentially relevant for RNA binding, are numbered (colored in red in the alignment).

2.2. *in vivo* Analysis of exonuclease activity of Exuperantia

The *in silico* analysis of Exuperantia revealed similarity to DEDD exonucleases and the conservation of the four name giving acidic catalytic residues; facts arguing for the presence of a catalytic activity in Exuperantia protein. In the nurse cells Exuperantia is found in RNA rich sponge bodies [62], which are similar to *bicoid* mRNA accumulations that had been described earlier [46]. This could point to a direct interaction of Exuperantia and *bicoid* mRNA in the nurse cell cytoplasm. Since DEDD exonucleases degrade nucleic acids from the 3'end towards the 5'end I examined the 3'UTR of *bicoid* mRNA for alterations dependent on Exuperantia. For that purpose I performed PCR on mRNA-derived cDNA obtained from ovaries of wild-type and *exu*-mutant flies (*exu*^{VL57}/*Df(2R)exu1*) to analyze the length and sequence of the *bicoid* 3'UTR. In this PCR assay, the forward primer anneals 5' of the last intron in the *bicoid* gene, thus allowing a differentiation between cDNA and a potential contamination with genomic DNA. In addition to this primer I designed four reverse primers. As internal control a reverse primer was used, which anneals to the known 3'UTR. The other three reverse primers were designed to anneal 5' to computer-predicted additional PolyA signals, which are found further downstream of the known *bicoid* 3'UTR (Fig. 2.3 B). I was able to amplify the control-fragment spanning the known 3'UTR (Fig. 2.3 B reverse primer #1, B' lane #1), as well as the longest fragment with the most downstream reverse primer (Fig. 2.3 B reverse primer #4, B' lane #4) from ovarian cDNAs of wild-type and *exu*-mutant flies. The intensity of the two fragments amplified, using reverse primers #2 and #3, is much weaker. This indicates varying amplification efficiencies for the different primer combinations and probably a very weak efficiency for primers 2 and 3. Importantly, there was no difference detectable between wild-type and mutant flies; except for a slight contamination with genomic DNA in the ovarian cDNA from wild-type flies, which lead to the generation of a longer PCR product (Fig. 2.3 B'). Furthermore, sequencing of the amplified RT-PCR products revealed no difference between wild-type and mutants.

To test if the quantities of the longer fragments differ between *exu*-mutant ovaries and wild-type I used quantitative real time PCR (qRT-PCR). For that I used as the internal control a primer pair which anneals to the known 3' UTR (Fig. 2.3 C "std"). Three additional primer pairs downstream of the known *bicoid* UTR were designed (Fig. 2.3 C #1 - #3), which bind upstream of potential PolyA signals. The graph in Fig. 2.3 C' shows the changes in the amounts of the amplification products corresponding to the three different 3'UTRs. All values are normalized against the known 3'UTR fragment and then presented as fold-changes in *exu*-mutants vs. wild-type. The numbers in the graph (Fig. 2.3 C' #1 - #3) correspond to the primer pair numbers indicated in the scheme (Fig. 2.3 C #1 - #3). No significant difference in the amounts of transcripts between wild-type and *exu*-mutant ovaries could be detected. Taken together these results indicate that Exuperantia does not affect the length, the amount nor the base composition of the *bicoid* 3'UTR.

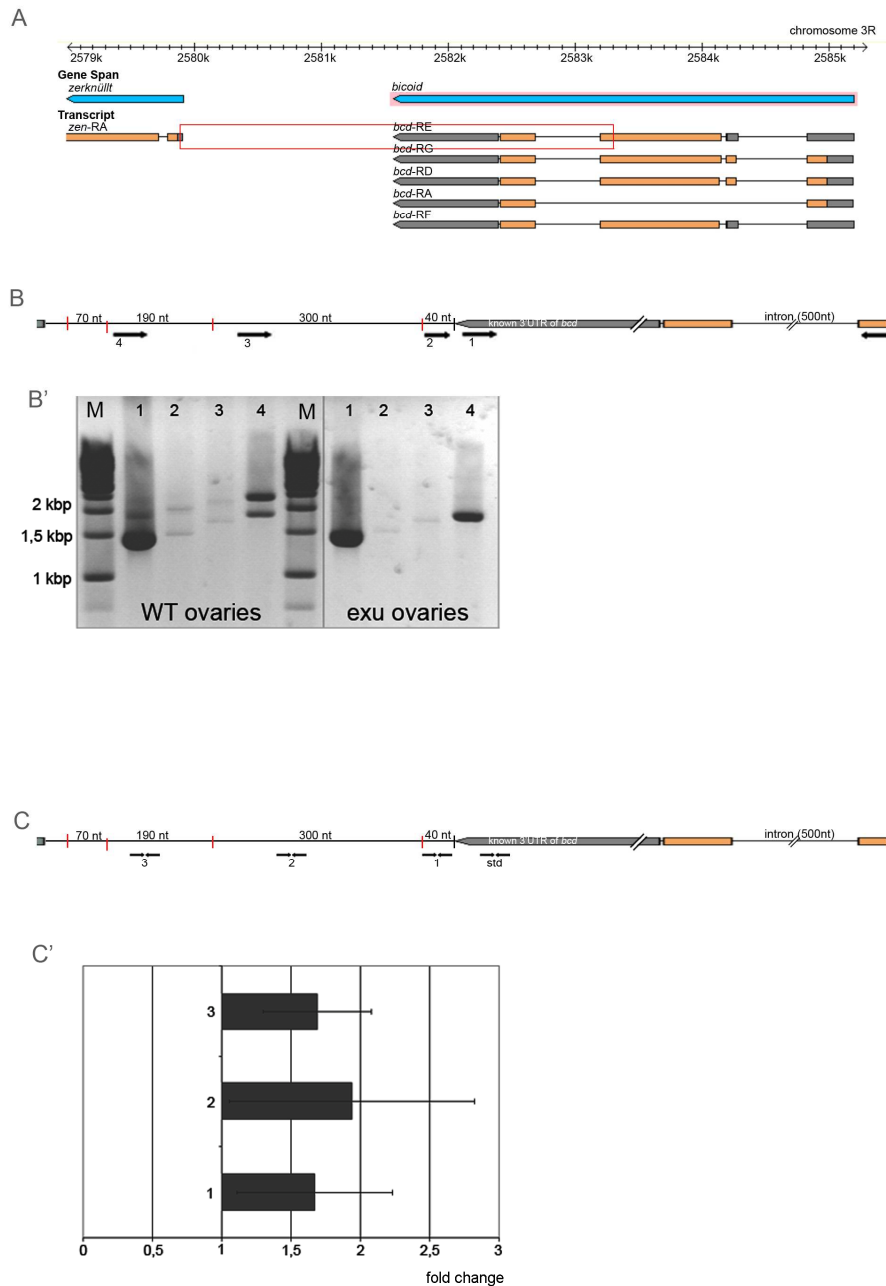


Figure 2.3 *bicoid* 3' UTR length assay.

A Overview of *bicoid* in flybase. The red boxed part is enlarged in **B** and **C**. **B** Scheme of the PCR performed to assay the length of the 3' UTR of *bicoid*. The forward primer was the same in all reactions. Reverse primers were chosen to anneal either in the known 3' UTR (1) or in front of predicted Poly A signals (2-4). **B'** Gel image of amplified fragments. The numbering corresponds to the numbers of the reverse primers in **B**. **C** Scheme of the qPCR to examine the amount of longer 3' UTRs in *exu*-mutant flies compared to wild-type flies. **C'** Graph shows the fold change of fragments, brought in relation to known 3'UTR fragment ("std"). Numbers of bars indicate the corresponding primer pairs shown in **C**. M = size marker

2.3. Expression and analysis of recombinant Exuperantia protein

2.3.1. Expression of recombinant protein

In order to test Exuperantia in biochemical *in vitro* assays I cloned the coding sequence of *exuperantia* from wild-type flies to express recombinant protein in *E. coli*. Since our foremost interest was to test for a potential exonuclease activity of the N-terminal part, with high homology to DEDD domains, I generated a series of full-length and truncated expression constructs. To analyze the potential catalytic activity of Exuperantia I introduced site specific mutations, which alter the first acidic residues (Asp³⁹ and Asp⁴¹) into asparagines (D^{39/41}N). In the case of RNase T it has been shown that a change of these residues into alanines destroys the catalytic activity of the enzyme but does not change target binding [71]. Below, I will call this modification “catalytically dead”, being aware that no proof exists so far, that wild-type Exuperantia protein is indeed an active exonuclease. All constructs encode either the wild-type DEDD domain or the “catalytically dead” version. The expression of all fusion proteins is driven by the T7 RNA polymerase, which is inducible by IPTG. As expression system I used various derivatives of the *E. coli* strain BL21(DE3).

Expression of His-tagged Exuperantia

For purification of the recombinant proteins I used an expression vector, which results in N-terminally His-tagged fusion proteins. I generated six different constructs: full length Exuperantia (His:Exu), a C-terminally truncated version, in which I deleted the putative 14-3-3 binding motifs (His:Exu^{ΔC}), and a further C-terminally truncated protein where additionally the SAM-like domain was deleted (His:Exu^{ΔS,ΔC}). All these proteins were also expressed as “catalytically dead” versions (His:Exu^{D39/41N}, His:Exu^{D39/41N,ΔC}, His:Exu^{D39/41N,ΔS,ΔC}) (Fig. 2.4 A).

To express the proteins I started with standard methods and the BL21(DE3) strain. Even at lower temperatures it was not possible to reliably induce expression. To rule out

low expression levels due to codon bias differences between *E. coli* and *Drosophila* I used the bacterial strain BL21(DE3)RIPL, which carries additional tRNA genes for arginine (R), isoleucine (I), proline (P) and leucine (L) most frequently limiting translation in *E. coli* [81]. The use of this strain also did not give sufficient and reproducible expression. Another reason for low expression could be toxic effects of the recombinant protein on the cells. To overcome this I used the *E. coli* strain BL21(DE3)pLysS. Cells of this strain express T7 lysozyme that reduces the basal activity of the T7 RNA polymerase and thereby further reduces expression of the recombinant protein before induction by IPTG. Additionally C41(DE3) cells were used to express recombinant Exuperantia proteins. This bacterial strain is derived from BL21(DE3) but has uncharacterized mutations that prevent cell death associated with the expression of toxic proteins [82]. Using these two strains I was able to express the different Exuperantia proteins, however they were insoluble.

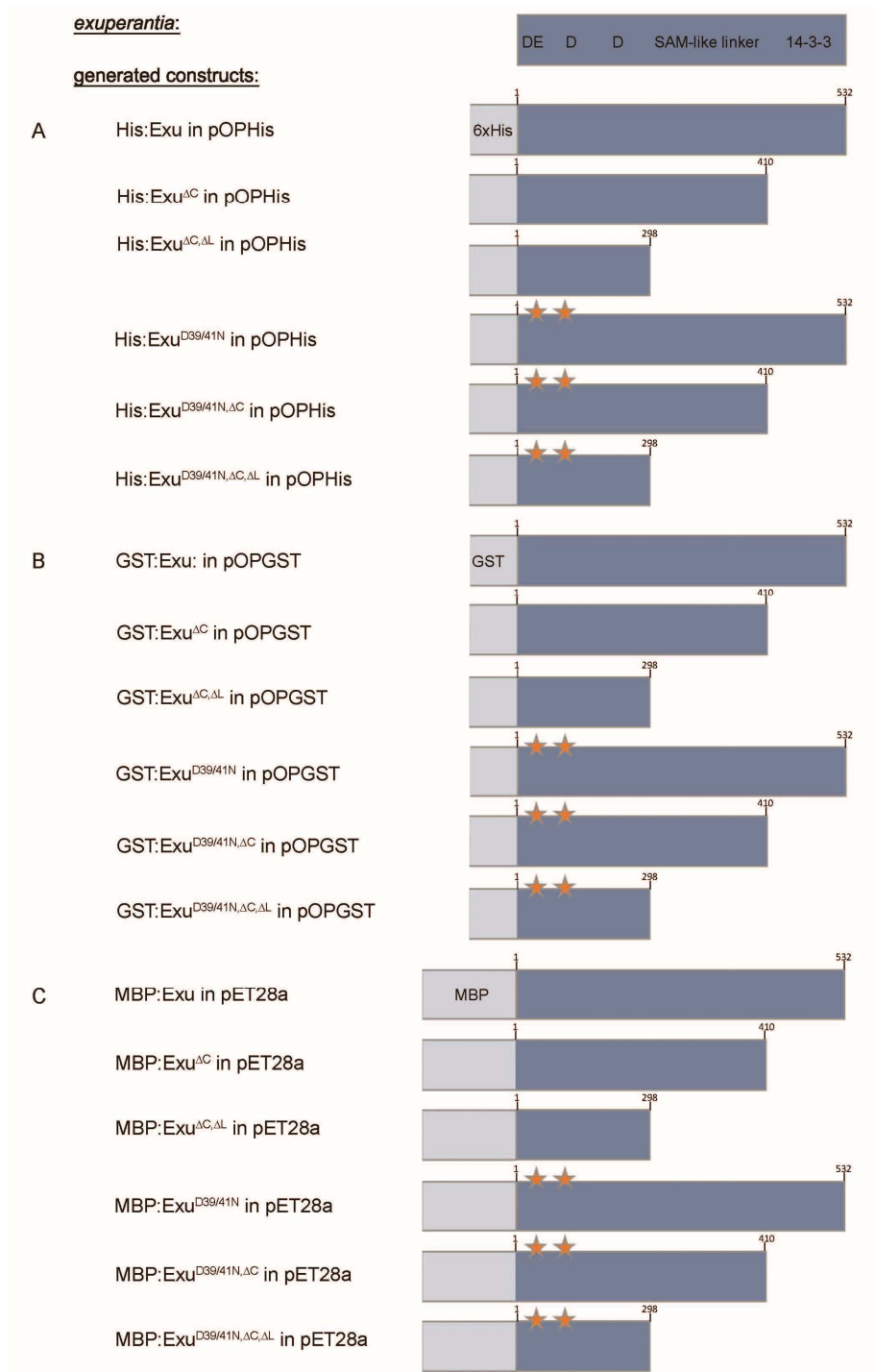


Figure 2.4 Constructs to express recombinant Exuperantia protein. The coding sequence of *exuperantia* was N-terminally fused to the indicated tags. **A** 6xHis, **B** GST, **C** Maltose Binding Protein (MBP). Truncations and modifications were generated as depicted. Stars indicate mutation of Asp³⁹ and Asp⁴¹ to asparagine.

Expression of GST- and MBP-tagged Exuperantia

To obtain soluble, non-aggregated recombinant Exuperantia protein I used a GST-tag as solubility tag [83]. Six different constructs were generated: the full length version (GST:Exu), a C-terminally truncated construct, lacking the putative 14-3-3 binding motifs (GST:Exu^{ΔC}) and a further C-terminally truncated construct where additionally the SAM-like domain was deleted (GST:Exu^{ΔS,ΔC}). All three constructs were also generated with the “catalytically dead” mutations (GST:Exu^{D39/41N}, GST:Exu^{D39/41N,ΔC}, GST:Exu^{D39/41N,ΔS,ΔC}) (Fig. 2.4 B). Due to previous experiences I used again the BL21(DE3)pLysS strain to express the proteins. Different methods for cell lysis including sonication, French Press and lysozyme treatment were used. Also the GST-Exuperantia proteins remained largely insoluble.

Another approach to generate soluble and purified recombinant protein was the use of a Maltose Binding Protein (MBP) -tag. MBP-tags are known to increase the solubility of recombinant proteins [83]. Building on the previous experiences I used the BL21(DE3)pLysS strain to express the MBP-tagged proteins. Again six constructs were generated: three construct with different length, as described before (MBP:Exu, MBP:Exu^{ΔC}, MBP:Exu^{ΔS,ΔC}) and the “catalytically dead” versions (MBP:Exu^{D39/41N}, MBP:Exu^{D39/41N,ΔC}, MBP:Exu^{D39/41N,ΔS,ΔC}) (Fig. 2.4 C). Use of the MBP-tag did not result in improved solubility of recombinant Exuperantia.

Expression of His-MBP-TEV-tagged Exuperantia

To overcome the insolubility problem I decided to express the DEDD domain alone and to vary its length slightly, since it is known that difference of a few amino acids can already have a big influence on the solubility of a truncated protein. The five different constructs are depicted in Figure 2.5 A.

Between the His-MBP-tag and the protein of interest there is a TEV-protease cleavage site allowing the release of the un-tagged recombinant protein. Exuperantia versions, except A were expressed and soluble. However, during gel filtration the proteins still

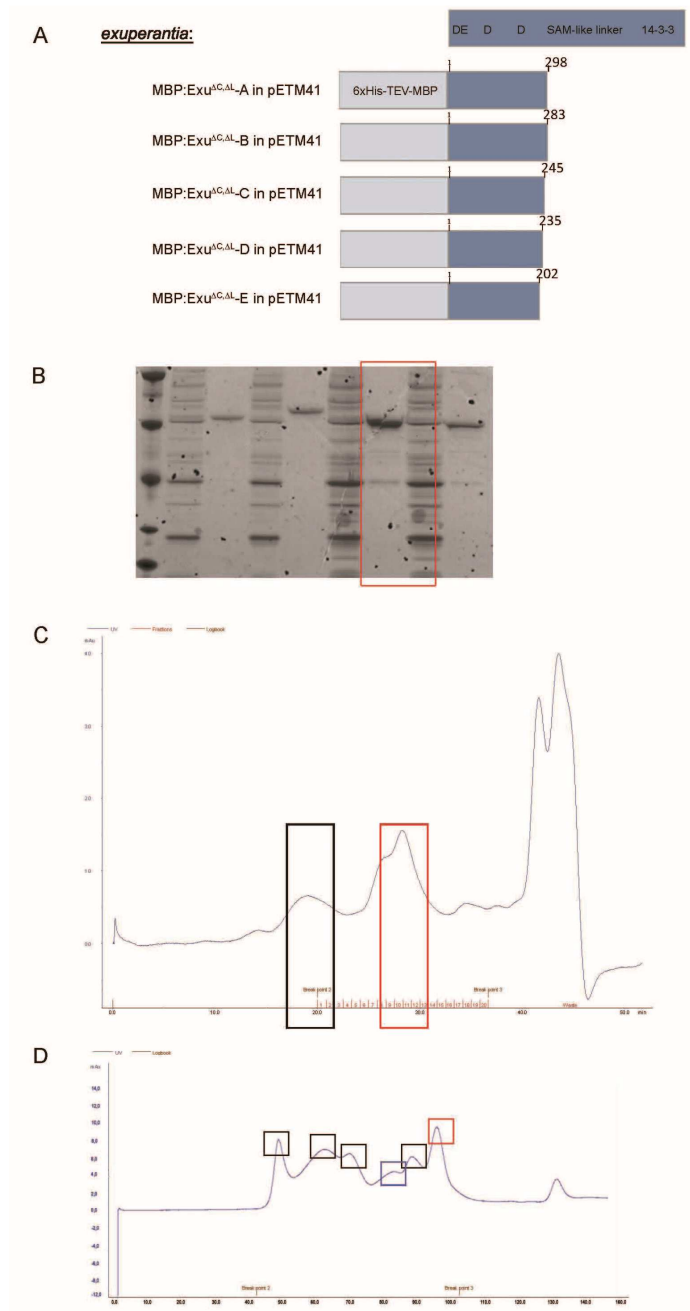


Figure 2.5 Expression and gel filtration of His-MBP-TEV-tagged Exuperantia. **A** Constructs of the DEDD domain alone with different C-termini to test solubility. The constructs are tagged with a TEV-cleavable His-Maltose Binding Protein tag. **B** All four proteins except version A are expressed and soluble. **C** Gel filtration of MBP-tagged Exuperantia version E. The red rectangle shows the DEDD protein peak, which elutes from the column earlier as expected, indicating oligomerization. A part of the protein elutes in the first fraction (black rectangle) indicating aggregation. **D** Gel filtration after TEV-protease cleavage. TEV-protease (black squares), MBP (blue square) and DEDD-E (red square) peaks are highlighted.

behave like high molecular weight complexes, most likely soluble aggregates. An example is given in Fig. 2.5 C for Exuperantia version E. A considerable amount of the protein elutes from the gel filtration column in the first few fractions (Fig. 2.5 C black rectangle) indicative of very large complexes. The remaining Exuperantia elutes later. However, still earlier than expected for monomeric Exuperantia (Fig. 2.5 C red rectangle), which indicates towards an oligomerization. To further decrease the aggregation tendencies of the proteins I cleaved the MBP-tag using TEV-protease. After cleavage and gel filtration only small amounts of soluble recombinant protein could be recovered (Fig. 2.5 D red rectangle). Most of the peaks detected correspond to TEV-protease, which remained in solution (Fig. 2.5 E black square), or the MBP-Tag (Fig. 2.5 E blue square). Only 1ng of soluble recombinant protein could be purified by this method. This is too little protein for further applications.

Expression of GST-tagged full length Exuperantia

At the same time a protocol for expression and purification of recombinant GST-tagged full-length Exuperantia was developed in Fulvia Bono's group at our institute. To follow this protocol I generated two constructs: wild-type (GST:Exu) and "catalytically dead" (GST:Exu^{D39/41N}) full length Exuperantia with N-terminal GST tags (Fig. 2.6 A). For the expression I used the *E. coli* strain BL21(DE3)gold.

The recombinant protein was purified using glutathione-beads. The eluate from the beads was then further purified using a Hi-S column (Fig. 2.6 B,C and B',C'). Surprisingly, the protein eluted from the column only at the maximum salt concentration of 1300mM NaCl. This could be the reason for the very low yields in the previous experiments. However, again only a minor fraction of the protein eluted as monomer (Fig. 2.6 B,C red rectangle). The collected fractions (Fig. 2.6. B',C') were pooled and then further purified by gel filtration (Fig. 2.6 B'',C'' and B''',C'''). For wild-type Exuperantia 7,3mg of protein were (Fig. 2.6 B''). For the "catalytically dead" Exuperantia, less protein was recovered (1,37mg) and the protein was less (Fig. 2.6 C''). The proteins in the eluates appeared to be monomeric and non-aggregated and were used in further biochemical assays.

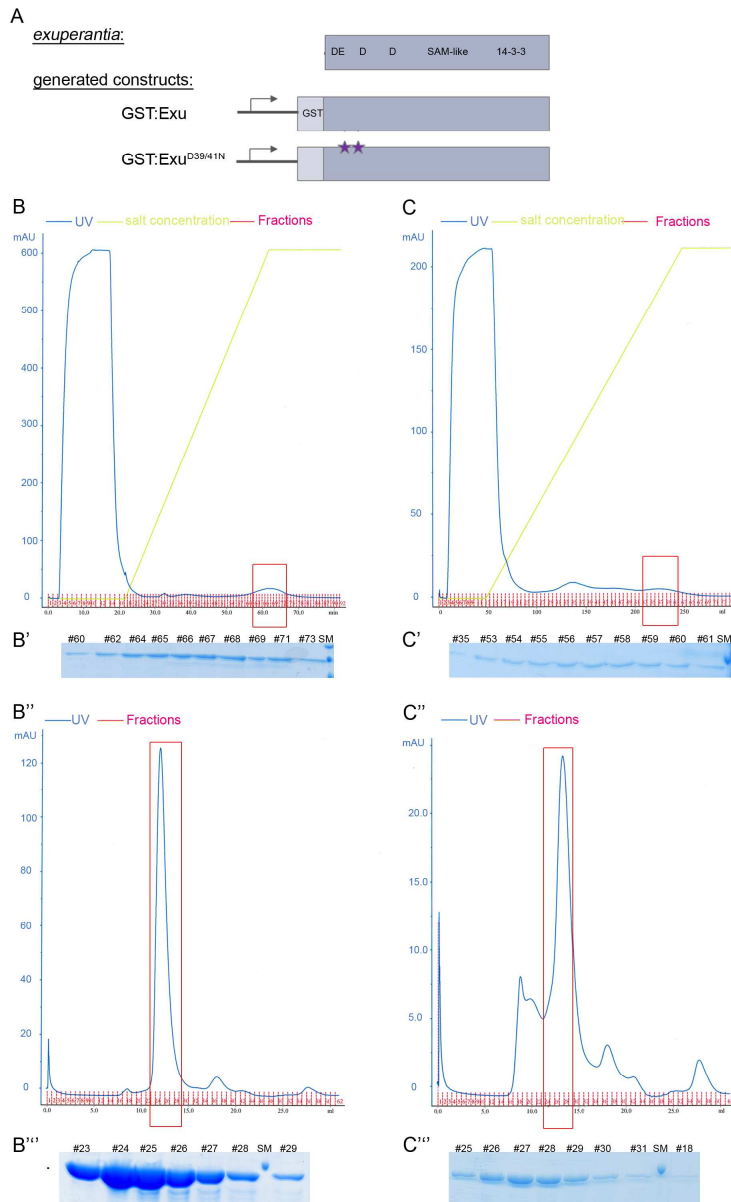


Figure 2.6 Purification of recombinant GST:Exu.

A GST:Exu full length wild-type and “catalytically dead” constructs. Purification of Exuperantia full length wild-type (**B-B'''**) and “catalytically dead” (**C-C'''**). **B,C** HiS-column protein purification. Blue line shows the UV absorption at 280nm, the yellow line shows the increasing salt concentration from 300mM to 1300mM NaCl. The red boxes indicate the Exuperantia-protein peaks. **B',C'** The presence of the protein was verified by SDS-page and Coomassie staining, numbers indicate fractions. **B'',C''** Gel filtration of the pooled Exu-fraction from the HiS purification. The red boxes indicate monomers of the recombinant proteins. **B''',C'''** The presence of the protein was verified by SDS-page and Coomassie staining, numbers indicate the fractions. Note the difference in the scale of the Y-axis.

Expression of His-NusA-tagged Exuperantia

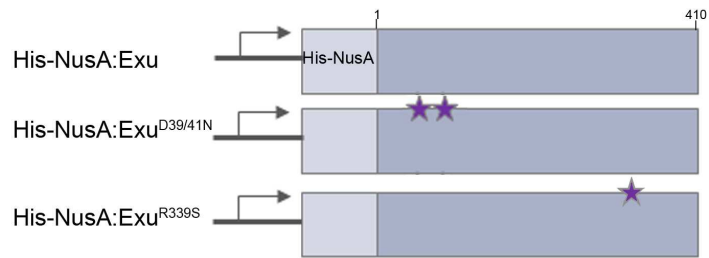
Another solubility tag, leading to the purification of recombinant monomeric Exuperantia, was the NusA protein. I used a version of Exuperantia in which I deleted the C-terminal part of the protein which contains the putative 14-3-3 binding motifs (Fig. 2.7 A), since this unstructured part could be a cause for the previous aggregation problems and transgene rescue experiments (see 2.4.2.2) showed that it is not essential for Exuperantia's function. The SAM-like domain was retained in these constructs. I decided to mimic the amorphic *exu*^{PJ42} allele (see Fig. 2.2) in the NusA-tagged Exu^{ΔC} to probe for the RNA binding ability of the SAM-like domain (NusA:Exu^{ΔC,R339S}). In addition I also expressed the "catalytically dead" version (NusA:Exu^{D39/41N,ΔC}). All three proteins were soluble when expressed in the *E. coli* strain BL21(DE3)pLysS (Fig. 2.7 B-B"). In all three cases there are similar background bands on Coomassie gels after affinity purification (Fig. 2.7 B-B" asterix). I purified the proteins using the N-terminal His-tag. I did not purify the eluates from the Ni-NTA-columns further but used the eluate directly (as shown in Fig. 2.7 B-B"); these proteins did not seem to aggregate anymore and were used in *in vitro* assays (see section 2.3.2).

A

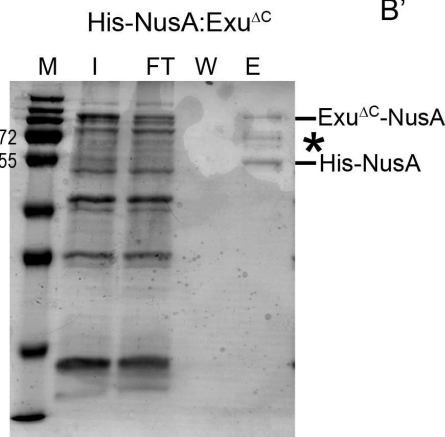
exuperantia:



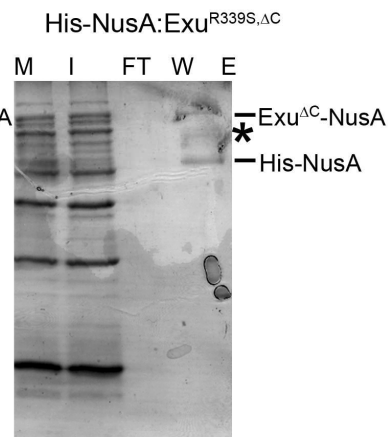
generated constructs:



B



B'



B''

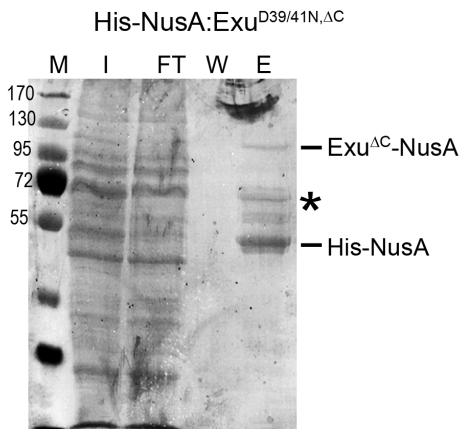


Figure 2.7 Expression of NusA-tagged Exuperantia.

A Schematic overview of His-NusA:Exu constructs. **B** The purification of all NusA-tagged proteins is comparable (**B-B''**). The only weakly expressed proteins give a faint band in the eluates. Most of the protein seems to be degraded. Some degradation products are visible (asterisk). M - weight marker, I - input, FT- flow through, W - wash, E - elution.

2.3.2. Functional analysis of recombinant Exuperantia protein

RNaseT, one of the best studied proteins with a DEDD domain, shows DNase activity *in vitro*, although *in vivo* the enzyme has been shown to only process tRNAs [13]. With this knowledge of a possible low substrate-specificity of DEDD exonucleases *in vitro* I developed an assay to analyze the potential exonuclease activity of Exuperantia. One important consideration in the development of this assay was the fact that DEDD exonucleases can have very different processivities, ranging from several hundred nucleotides (e.g. the Pan2 de-adenylase) to few or only one nucleotide (e.g. RNaseT) [73]. This necessitated the use of an assay with single-nucleotide sensitivity. Most DEDD exonucleases are sequence independent, they are often targeted to their substrates by other RNA-binding domains within the protein or by protein-protein interactions with other target specific RNA-binding proteins. This sequence independence allows an exonuclease assay, without knowing the *in vivo* target.

For the *in vitro* assay single- and double-stranded RNA oligonucleotides were used as substrates and incubated with purified recombinant proteins. The RNA oligonucleotides were fluorescently labeled at their 5'-ends and exonucleolytic degradation was analyzed by capillary electrophoresis. The sensitivity of the method was tested with two RNA oligonucleotides differing in length by only one base. To establish the assay I chose a reaction buffer, which had been described for an *in vitro* exonuclease assay for RNaseT [84]. As negative control the 26nt RNA oligonucleotide substrates were incubated without adding any protein. Multiple peaks, similar to the untreated substrate, are detected (compare Fig. 2.8 A and B a). This probably indicates partial degradation of the substrate, or a mixture of synthesis products. As positive control RNase1 was used. After adding RNase1 the degradation of the RNA is easily visible, the main peak corresponds now to one nucleotide in size (Fig 2.8 B b). For the experiment I used either wild-type (Fig. 2.8 B c) or the "catalytically dead" GST tagged full length Exuperantia (Fig. 2.8 B d) proteins. If Exuperantia has exonuclease activity, I would expect that incubation with the wild-type recombinant protein leads to a shift of the RNA peak. If the activity is based on the DEDD domain, RNA which is incubated with the "catalytically dead" recombinant protein should stay stable. In the assay, incubation with

either protein resulted in the disappearance of the input-peak corresponding to the 27nt substrate (Fig. 2.8 B c,d; green triangle indicates expected input peak, green asterix indicates position of 1 nucleotide degradation product of RNase1). However, no degradation products are visible. Surprisingly, the size standard (labeled DNA oligonucleotides; in Fig. 2.8 orange) disappeared, too (Fig. 2.8 B d,c). This could be due to an unspecific binding of labeled oligonucleotides by the Exuperantia proteins and possibly the formation of larger aggregates, which will not enter the capillaries. To release the oligonucleotides again and be able to analyze their sizes I treated the RNA/protein mixture with proteinase K prior to electrophoresis. As shown in Figure 2.8 (B a'-b'') this treatment does not interfere with the positive or negative controls, as they give comparable results in both assays (compare Fig. 2.8 B a,b and a',b'). The Exuperantia treated RNAs and the DNA markers are released, as indicated by the re-appearance of the peaks after capillary electrophoresis (compare Fig. 2.8 B c,d and c',d'). This strongly suggests the formation of protein-nucleic acid aggregates promoted by GST-full length Exuperantia. However, in this assay no differences between wild-type and "catalytically dead" Exuperantia could be detected.

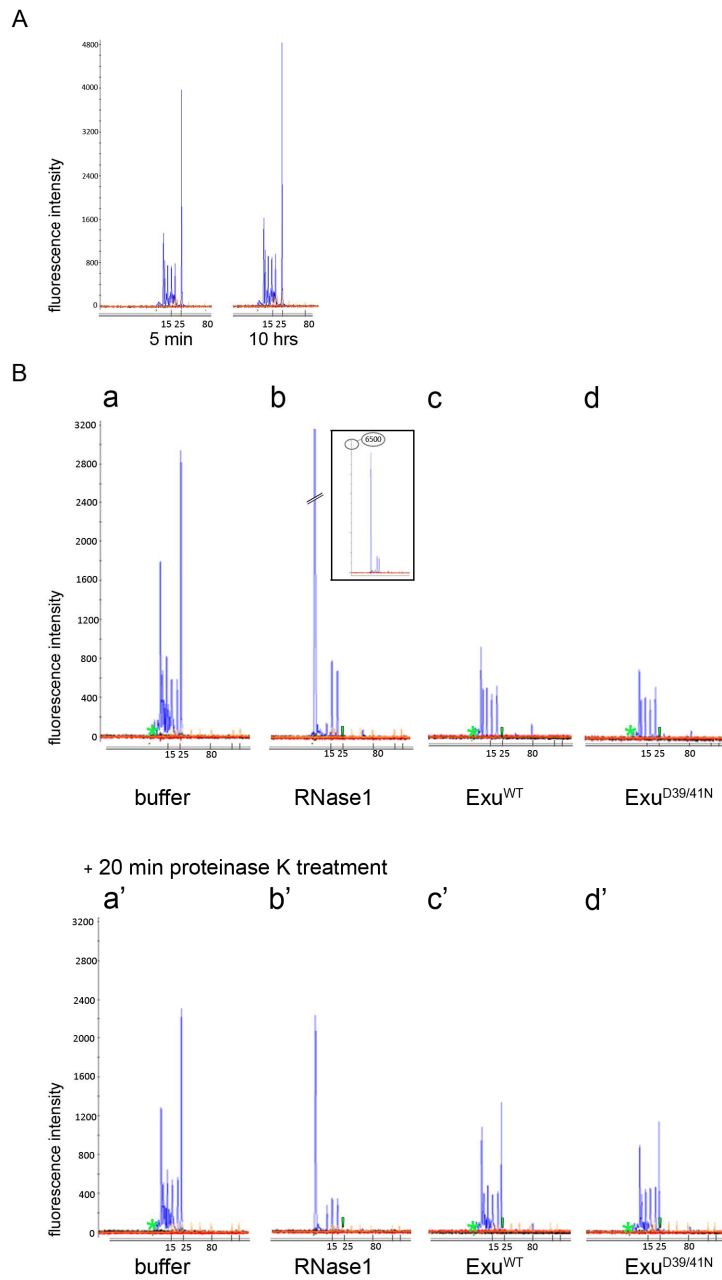


Figure 2.8 Fragment analysis using capillary electrophoresis with GST:Exuperantia.

A Capillary electrophoresis of labeled RNA (blue peaks) oligonucleotide after 5 min and 10 hrs incubation. **B** Fragment analysis of labeled RNA oligos (blue peaks) compared to a DNA-marker (orange) after treatment with no protein (neg. control **B a,a'**) RNase 1 (pos. control **B b,b'**) GST:Exuperantia wild-type (**B c,c'**) and “catalytically dead” (**B d,d'**). With (**a-d**) and without (**a'-d'**) 20 min proteinase K treatment. 1 nucleotide size degradation fragments are indicated by green asterisk, green triangle indicates position of the input oligonucleotide

To avoid formation of aggregates, I used C-terminally truncated Exuperantia with NusA as solubility tag (see 2.3.1 f). Besides the wild-type Exu^{ΔC} and the “catalytically dead” Exu^{D39/41N,ΔC}, I also mimicked the amorphic *exu*^{PJ42}-allele Exu^{R339S,ΔC}. These recombinant proteins do not form aggregates with the oligonucleotides, and no proteinase K treatment is necessary before capillary electrophoresis. I incubated the RNA oligonucleotides in different reaction buffers without protein (negative control), Exu^{ΔC}, Exu^{D39/41N,ΔC} and Exu^{R339S,ΔC} proteins. I tested several different buffers with varying pH and different combinations of salts (see Appendix B). With one buffer promising results were obtained (Fig. 2.9), the RNA peak after treatment with Exu^{ΔC} protein is partially shifted from 26nt to much smaller size (Fig. 2.9 most left, arrow). This shift is not detectable with the Exu^{D39/41N,ΔC} or Exu^{R339S,ΔC} Exuperantia (Fig. 2.9 two middle panels). In the negative control the RNA is degraded (Fig. 2.9 right), so no firm conclusion can be drawn from this experiment, it has to be repeated. Interestingly, this buffer is the only one containing calcium ions, which could mean that the catalytic activity of Exuperantia might be dependent on calcium ions; it is known that DEDD exonucleases need metal ions to be active [71, 84], in most cases this metal ion is Mg²⁺.

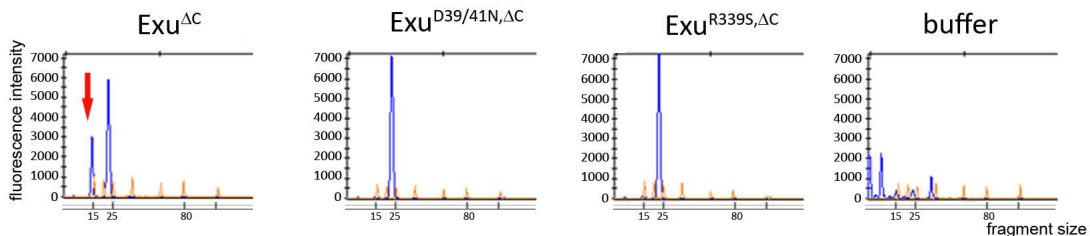


Figure 2.9 Fragment analysis using capillary electrophoresis with NusA:Exuperantia.

NusA:Exu^{ΔC} construct wild-type, with Asp^{39/41}Asn (D^{39/41}N) and Arg³³⁹Ser (R³³⁹S) mutation with selected buffer. The red arrow indicates the RNA peak of smaller size, which arises after treatment with wild-type Exuperantia (left) but not when treated with Exuperantia carrying point mutation in catalytic residues (D^{39/41}N, 2nd from left) or a point mutation in SAM-like domain (R³³⁹S, 3rd from left). No RNA is detectable in the buffer control (right).

2.4. Generation and analysis of new *exuperantia* alleles

2.4.1. EMS mutagenesis and screen for new *exuperantia* alleles

Since 1990 several alleles of *exuperantia* have been described [56]. So far, three missense mutations were identified (Table 1.1). *exu*⁴ harbors an early stop-codon (Gln⁵³Stop) and is assumed to be a protein null, *exu*^{QR9} and *exu*^{PJ4} highly conserved amino acids in the DEDD domain and the SAM-like domain, respectively, are affected. They all cause amorphic phenotypes [56]. In order to identify more functional residues a screen for additional *exuperantia* alleles was performed. Ethyl methanesulfonate (EMS) was used as mutation causing compound, as it produces mainly point mutations. *white*⁻ males were mutagenized in groups of 100. Subsequently, they were divided into three groups and crossed to 40-50 virgin females of the genotype: *w*⁻/*w*⁻; *If*/*CyO*, *hs::hid*. The females carry *white*⁻ mutation and a dominant eye marker mutation, *If*, on the 2nd chromosome, which was balanced by *CyO*, *hs::hid*, causing larvae to die after heat-shock treatment. As depicted in Figure 2.10 this balancer-chromosome can be used later to select for larvae carrying the potentially mutagenized chromosome (+*). Virgin females of the F₁ generation were crossed individually to males heterozygous for an *exu*-null allele. By applying a heat shock, larvae carrying the *CyO*, *hs::hid* balancer-chromosome were eliminated. Consequently, only flies carrying the 2nd chromosome with potential mutations will emerge. The mutagenized chromosome (+*) is now either balanced with *CyO*, *bw*. These flies can eventually be used to establish a stock, or it is hemizygous over the *exu*-null allele (*exu*^{VL}). These egg-lay of the hemizygous female

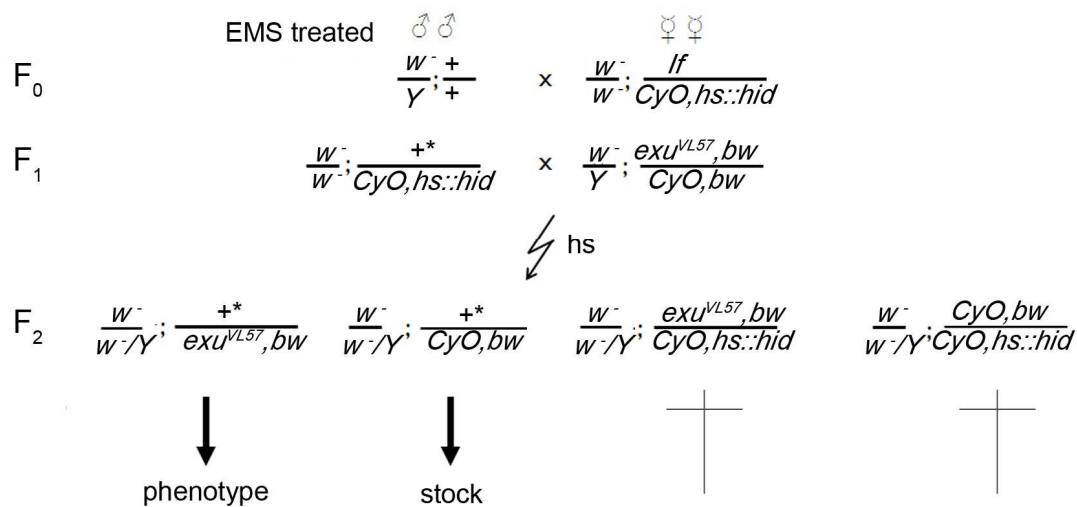


Figure 2.10 Allele screen for *exuperantia*.

F0 EMS treated wild-type males were crossed to females carrying a dominant eye marker (*If*) over a *CyO* balancer with a heat shock inducible (*hs*) *head involution defective* (*hid*) transgene ($w^-/w^-; If/CyO, hs::hid$). **F1** The collected virgins, which possibly carry a newly induced mutation are balanced with *CyO, hs::hid* and were crossed to males carrying an *exu*-null allele (exu^{VL}) balanced with *CyO, bw*. **F2** Heat shock treatment during larval stages leads to the elimination of flies carrying the *CyO, hs::hid* balancer. The other flies carry the mutated chromosome over exu^{VL} or over *CyO, bw* and can be used to screen for phenotypes in the egg lays or to establish balanced stocks for candidate mutants.

flies were screened for anterior cuticle defects. Two potential new *exuperantia* alleles were isolated, which showed cuticle malformation comparable to *exu*-mutants (Fig. 2.11). In total more than 4000 genomes were screened.

To confirm the generation of two new mutations in *exuperantia*, I sequenced the genomic region in these flies and was able to verify two novel alleles, exu^{i3} and exu^{g18} . In exu^{i3} allele the start codon is mutated from ATG to TTG. The exu^{g18} allele was identified as a change of valine³²⁷ into glutamic acid, which lies within the SAM-like domain and is in close proximity to the residue altered in the exu^{PJ42} allele (Arg³³⁹Ser).

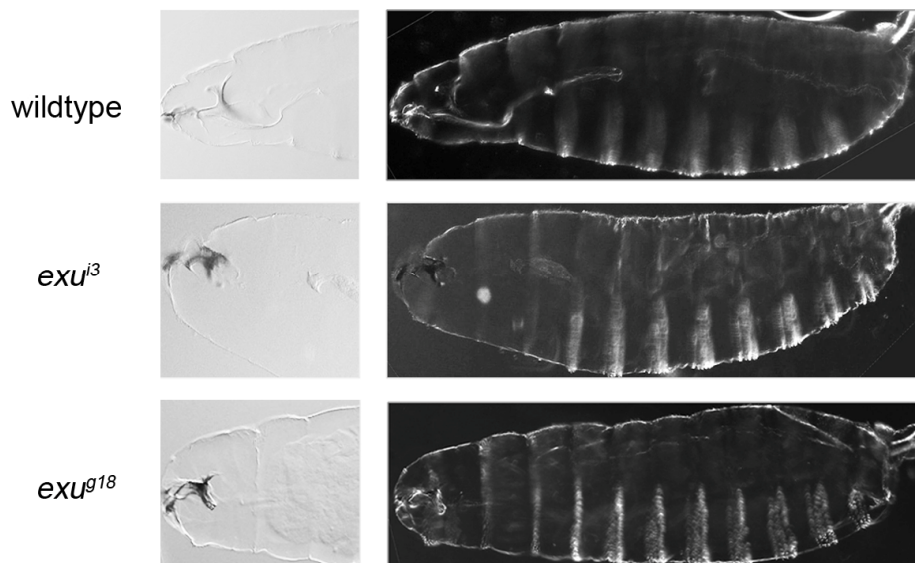


Figure 2.11 Cuticles of embryos carrying the newly identified alleles.
 In comparison to the wild-type cuticle (upper row) the two newly identified *exu* alleles (*exu^{j3}* and *exu^{g18}*) show a strongly reduced head skeleton.

2.4.2. Phenotypic analysis of *exuperantia* alleles

With these two new alleles four point mutations of *exuperantia* are now available. To confirm that the proteins carrying the point mutations are stable, I performed Western blots (Fig. 2.12). Ovary extracts from females, hemizygous for *exu^{QR}*, *exu^{PJ42}* and *exu^{g18}* show a band comparable to wild-type, indicating that the mutant proteins are expressed and stable. In ovary extract from females hemizygous for *exu^{XL}*, which is known to be an *exu* RNA-null allele, and *exu^{j3}* no Exuperantia is detectable. This confirms that the identified start codon mutation in *exu^{j3}* leads to a protein null phenotype. However, no systematic analysis of the *exu* alleles had been done, so far. To do so, I generated hemizygous (*exu* alleles over deficiency) and trans-heterozygous flies.

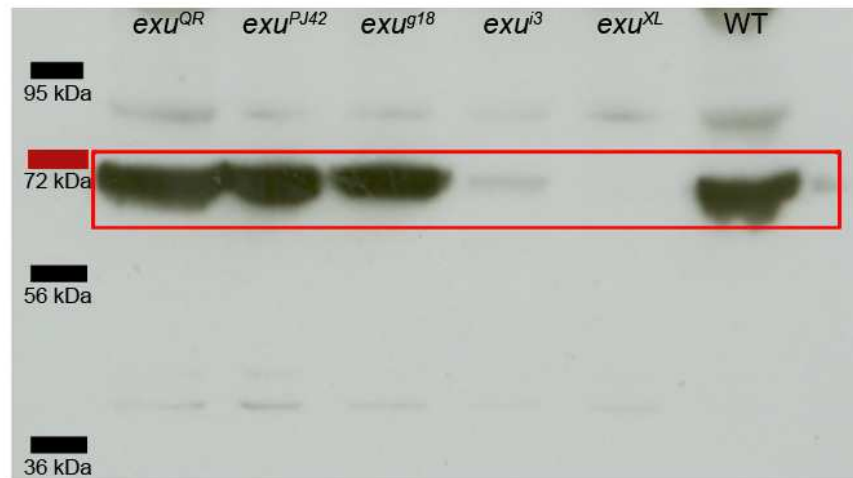


Figure 2.12 Western Blot using a polyclonal rabbit-anti-Exuperantia.

Protein extracts of ovaries from hemizygous flies carrying the indicated *exu* allele. WT is protein extract of wild-type flies. The red box indicates the specific Exuperantia bands.

To analyze the strength of the phenotype of the different *exuperantia* alleles in a quantitative way I analyzed the expression-pattern of the pair-rule gene *even-skipped* (*eve*). As previously described, the expression of the patterning genes (gap genes, pair-rule genes) depends on the establishment of Bicoid protein gradient in the embryo.

The position of the first Eve stripe is an indicator for the establishment of the anterior-posterior axis and for the function of Exuperantia in the localization of *bicoid* mRNA. In all different *exu* allelic combinations I measured the distance of the first Eve stripe to the anterior tip of the embryo. In *exu*-null mutants the first Eve stripe appears at approximately 21% of egg length (anterior: 0%; posterior: 100%) in contrast to 32% in wild-type flies (Fig. 2.13). All trans-heterozygous flies show a phenotype indistinguishable from *exu* null mutants, indicating that they all fail to the same extent to localize *bicoid* mRNA and thereby to generate the anterior Bicoid morphogen gradient in the embryo.

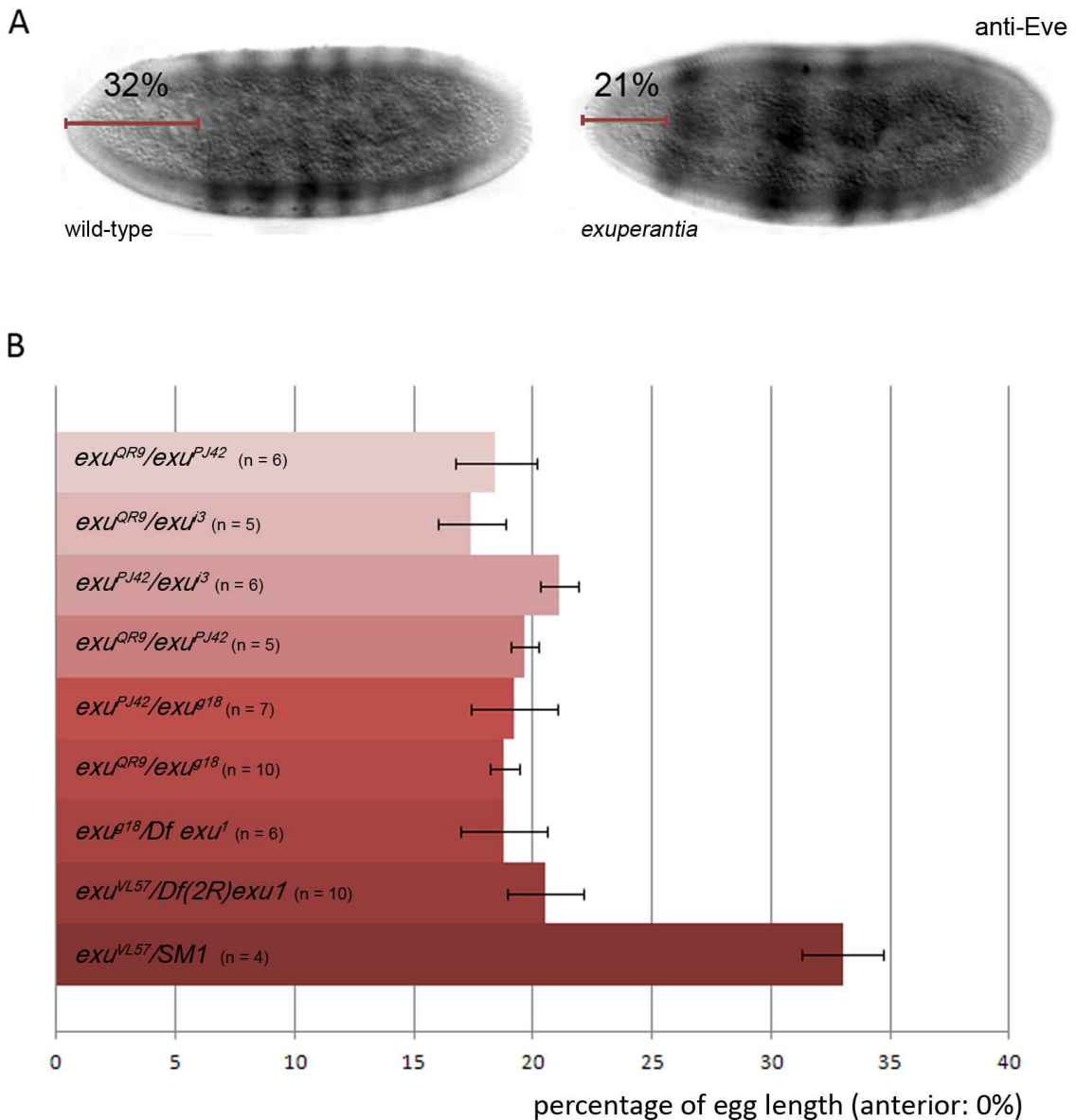


Figure 2.13 Eve staining and quantification of trans-heterozygous embryos.

A Eve staining in embryos laid by wild-type and *exu*-mutant females. The bar indicates the distance from the anterior tip of the embryo to the first Eve stripe. In embryos from wild-type mothers the first Eve stripe arises around 32% of egg length, in contrast to embryos from *exu*-mutant flies where the first Eve stripe is shifted towards the anterior and arises at 21% egg length (anterior: 0%; posterior: 100%). **B** Quantification of the position of the first Eve stripe in embryos from different trans-heterozygous flies (genotype indicated). Error bars show standard deviation.

2.4.3. Functional analysis of *exuperantia* alleles

To test if the observed phenotype could be due to reduced amount of *bicoid* mRNA I used quantitative real-time PCR. I quantified the levels of *bicoid* and *oskar* mRNAs in ovaries, freshly laid eggs (0-30 min), and embryos (0-2 hrs after egg lay) (Fig. 2.14 A-C). *actin* mRNA was used as internal standard to allow the comparison between the different samples. The resulting ratios were compared with wild-type values. While in embryos the fold changes for both transcripts, *oskar* and *bicoid*, vacillate around 1 (Fig. 2.14 B and C), it seems that in ovaries of all trans-heterozygous flies the amount of *bicoid* mRNA is reduced to about half (Fig. 2.14 A). However, several indications suggest that the apparent reduction in the levels of *bicoid* mRNA is not due to the mutations in *exuperantia* but rather caused by the experimental setup. It is only detectable in ovaries and not in embryos. And, most importantly, in further experiments described below (Fig. 2.19) no reduction of *bicoid* mRNA levels in ovaries from *exuperantia* mutant flies was found. This indicates a high variability between experiments, which could be caused by genetic background effects or general limitations of the method.

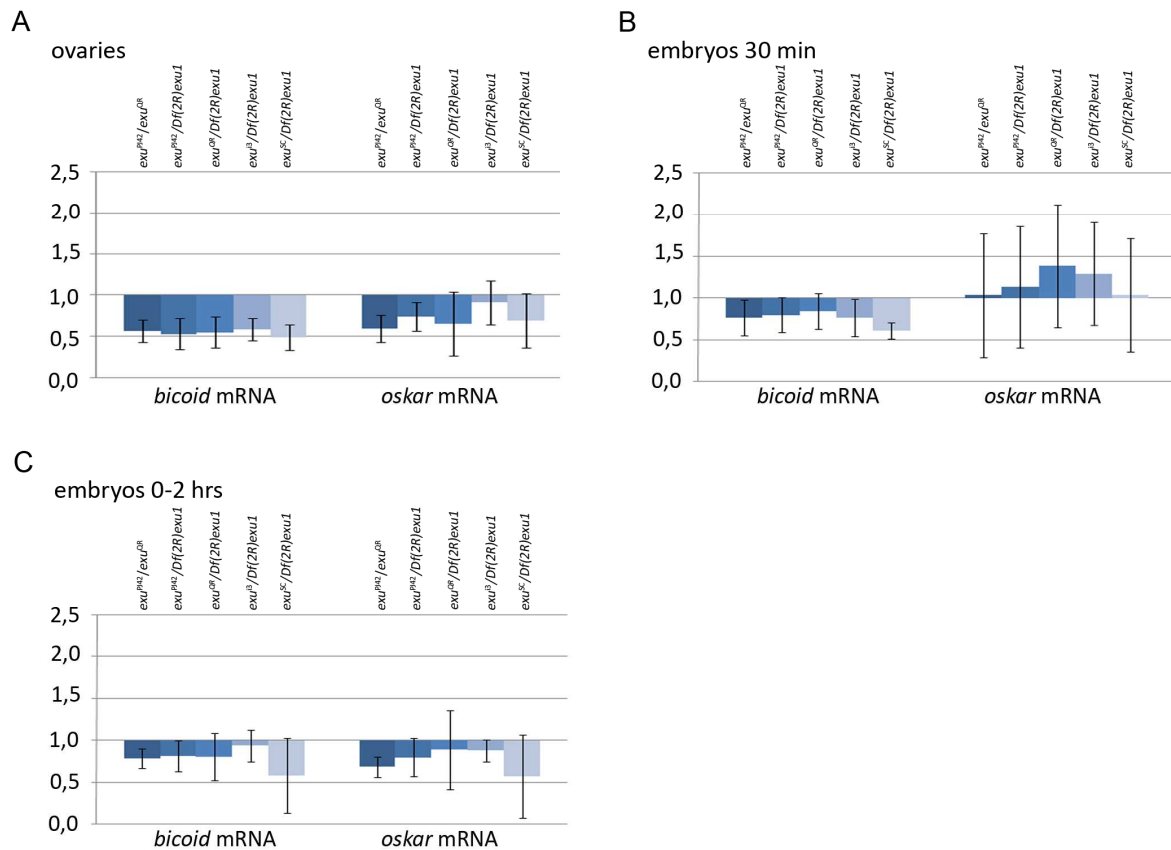


Figure 2.14 quantitative real-time PCR of ovaries and embryos from trans-heterozygous flies.

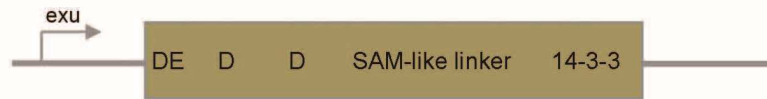
A-C show the fold change of relative *bicoid* mRNA (left) and *oskar* mRNA (right) levels in three developmental stages compared to wild-type. The germ-line specific *actin* mRNA was used to normalize the values. The genotype of the mother is indicated above the column. **A** ovaries, **B** freshly laid embryos (max. 30 min) and **C** embryos 0-2 hours. Error bars indicate the standard deviation. Each experiment was repeated three times with three technical replicates.

2.4.4. Generation and analysis of *exuperantia* transgenes

Based on the identification of two domains in Exuperantia, DEDD domain and SAM-like domain, I designed several transgenes with the aim to analyze these domains independently and in combination (Fig. 2.15). Additionally, I introduced point mutations to examine the potential catalytic activity of the exonuclease domain. It was known from previous work that fusion to GFP does not interfere with Exuperantia's function. The

fusion protein localizes similar to the endogenous Exuperantia protein and is competent to rescue the *exu*-mutant phenotype, regardless of the position of GFP at the N- or C-terminus [63]. A transgene based on the genomic region was generated, which places Venus, a variant of YFP (yellow fluorescent protein) and a StrepTag II, 3' to the coding sequence of *exuperantia*, resulting in a C-terminal Exuperantia Venus-StrepTag fusion protein. The genomic fragment I used was based on the previously described fusion protein construct [63]. This genomic fragment contains the *exuperantia* promoter including the regulatory elements to drive expression of the transgene. Besides the full-length Exuperantia I also generated a truncated version in which the C-Terminus containing the putative 14-3-3 binding motifs was deleted (Exu^{ΔC}:Venus). In both constructs I also introduced the “catalytically dead” mutations (see above). The change of two aspartatic residues (Asp^{39/41}) into asparagine (D^{39/41}N) is predicted to leave the target binding functionality intact but to abolish the catalytic activity, as it was shown for RNaseT [71]. The “catalytically dead” mutations were also introduced into a non-tagged full length Exuperantia as a control transgene.

exuperantia:



generated constructs:

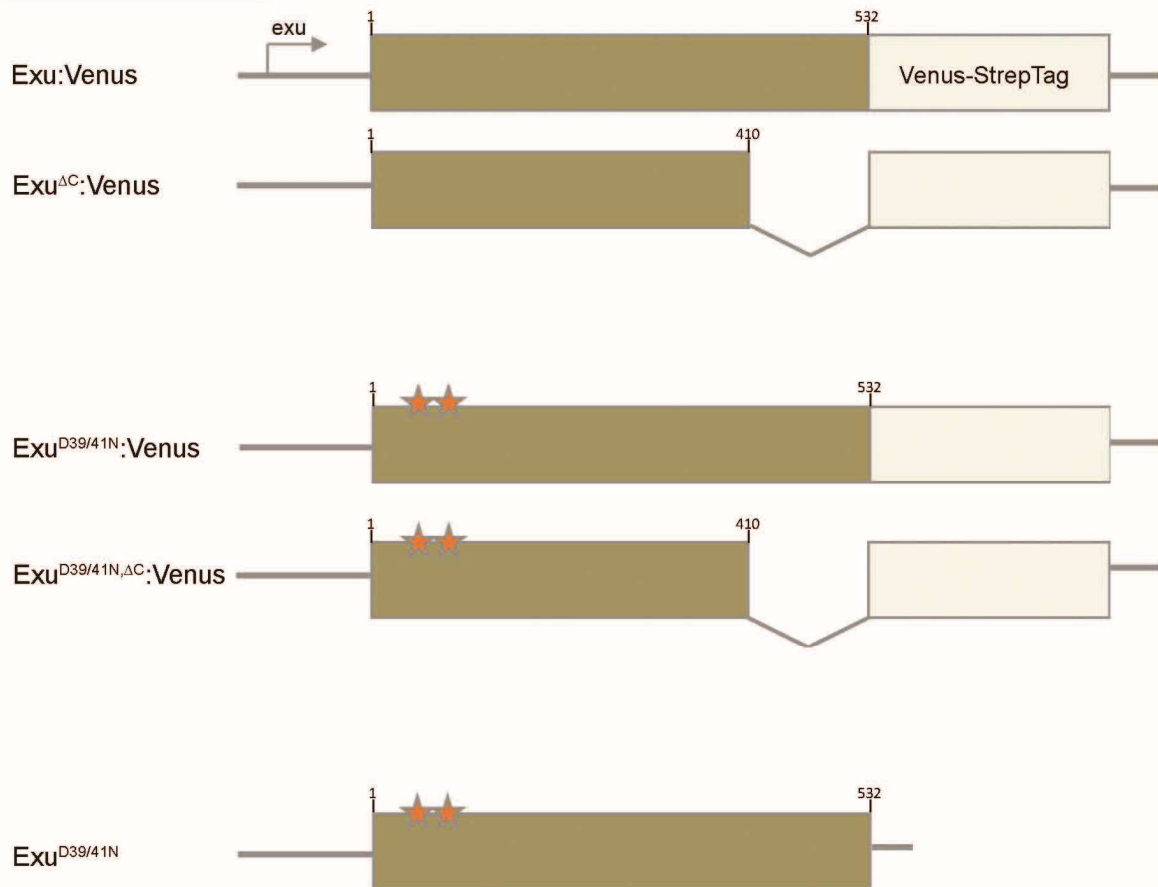


Figure 2.15 Rescue and localization constructs of Exuperantia.

A 5.6 kbp genomic fragment of *exuperantia* was modified to encode an Exuperantia protein which is C-terminally fused to a Venus-StrepTag. The genomic fragment was additionally modified to lead to a C-terminally truncated protein (as indicated). The stars indicate the mutations of two of the four potentially catalytic residues in the DEDD exonuclease domain.

2.4.5. Generation of *exuperantia* transgenic flies

Transgenic flies for all constructs were generated using standard P-element mediated transgenesis with the *mini-white*⁺ gene as a marker (Fig. 2.15). As host for the transgenes, *white*¹¹¹⁸ mutant flies were used. Successful integration of the construct into the genome of the flies is detectable by a partial rescue of the *white*¹¹¹⁸ phenotype, due to the *mini-white*⁺ gene on the integrated construct. Flies with orange eyes carry the *mini-white*⁺ gene and therefore the *exu* transgene as well. The integration of the different transgenes was additionally verified by sequencing using construct specific primers. No dominant negative effect of the constructs was detectable in wild-type background.

2.4.6. Analysis of the rescue potential of the transgenes

All transgenes were crossed into an *exu*-mutant (*exu*ⁱ³/*Df*(2*R*)*exu*1) background to assess their rescue potential. As phenotypic read-out I used the expression pattern of *even-skipped* as a measure for embryonic patterning (Fig. 2.16). The full length Exuperantia protein C-terminally fused to Venus (Exu:Venus) rescues the mutant phenotype and leads to a re-positioning of the first Eve stripe from around 21% egg length (0% most anterior to 100% most posterior) in the mutant background to around 32%, comparable to wild-type. The same results were obtained for the truncated version of Exuperantia (Exu^{ΔC}:Venus), indicating that the C-terminus is not necessary for Exuperantia's function. Transgenes carrying the “catalytically dead” mutations fail to rescue the *exu*-mutant phenotype. These data suggest that the catalytic residues are essential for Exuperantia's function in *bicoid* mRNA localization. Since the C-terminally truncated version, missing the putative 14-3-3 binding sites, is able to rescue the phenotype I will call it furtheron “minimal construct”, indicating that within this fragment of Exuperantia all essential elements for *bicoid* mRNA localization are included.

Surprisingly, unlike the Venus-tagged versions, untagged full length but "catalytically dead" Exuperantia ($Exu^{D39/41N}$) rescues the *exu-mutant* phenotype (Fig. 2.16). This is an obvious discrepancy compared to the consistent picture derived from the analysis of the Venus-StrepTag fusion proteins.

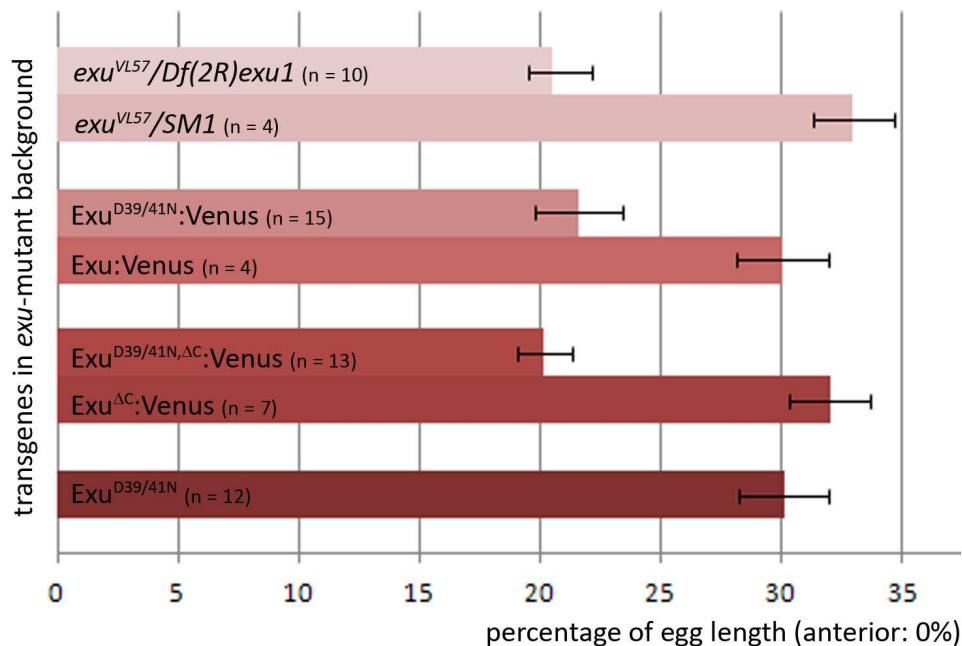


Figure 2.16 Quantification of the position of the first Eve stripe in embryos laid by flies carrying different Exuperantia transgenes.

The transgenes are indicated. Error bars show standard deviation.

2.4.7. Localization of Exuperantia fusion protein in mutant background

I analyzed the localization of the transgene-encoded Exuperantia fusion proteins in otherwise *exu*-mutant egg chambers (*exuⁱ³/Df(2R)exu1,cn,bw,sp*). Prior studies using GFP-tagged Exuperantia [63], as well as our own analysis of the published transgene (Fig. 2.17 A, B) and immunohistochemical [61] analysis, have shown that Exuperantia localizes within the oocyte anteriorly during early stages and throughout all stage of oogenesis at the posterior pole [59]. In the nurse cells Exuperantia exists in a soluble form (diffuse cytoplasmic signal), and in a particle-bound form. These particles have

been described before and have been termed sponge bodies [62]. They are believed to contain *bicoid* mRNA amongst a number of other mRNA species. The current view in the field is that *bicoid* mRNPs get modified by an as yet unknown but Exuperantia dependent process, while being localized in these sponge bodies [62, 74]. Both full length proteins of our series, independently of the catalytic mutations (Exu:Venus,

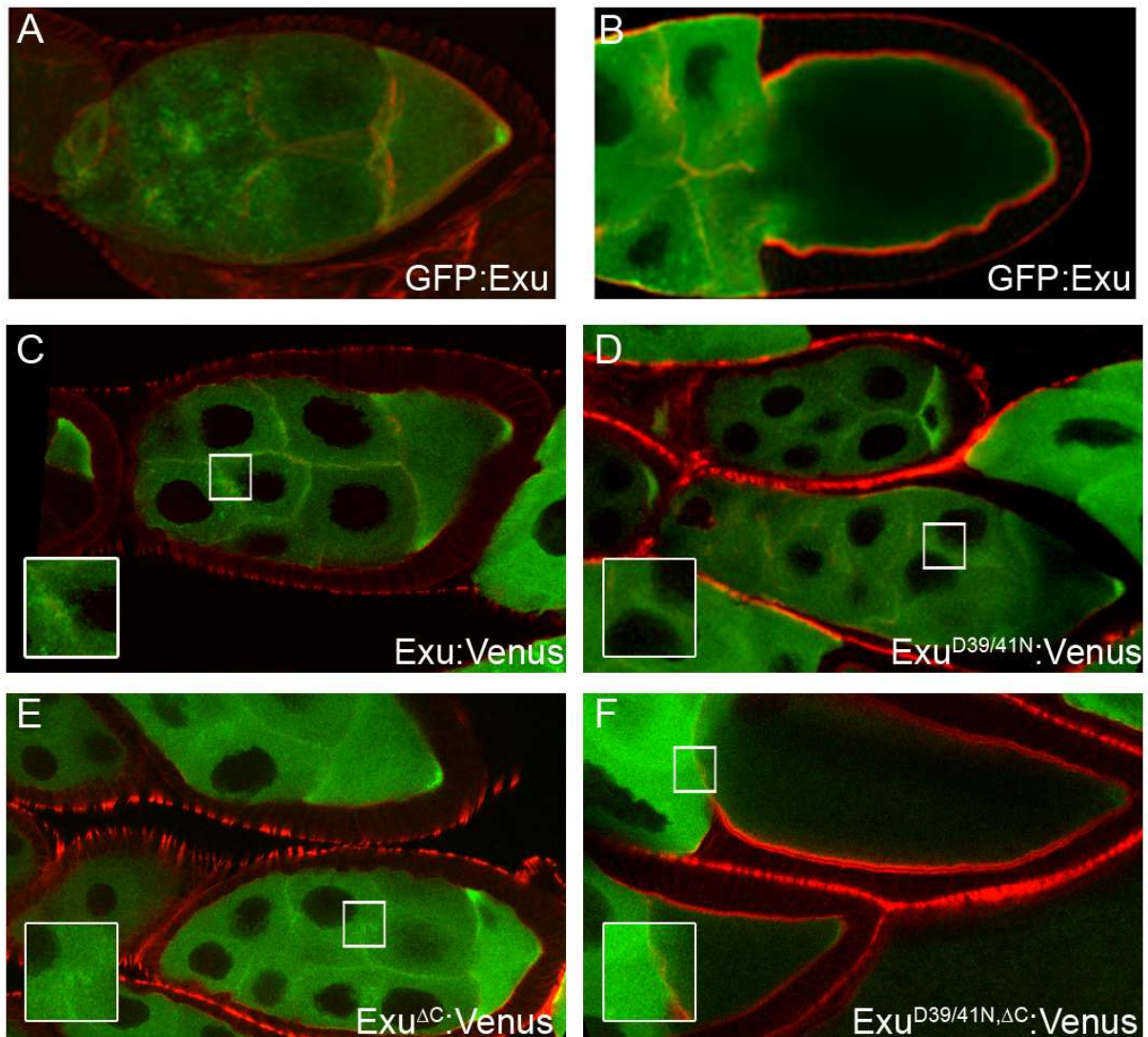


Figure 2.17 Localization of Venus-tagged Exuperantia in *exu*-mutant background.

A,B Localization of the previously published GFP-Exuperantia fusion protein [63]. **C-F** Exuperantia C-terminally fused to Venus; **C** full-length Exuperantia; **D** Exuperantia full-length with mutations in potential catalytic residues of DEDD domain; **E** C-terminally truncated; **F** mutations in potential catalytic residues of DEDD domain and C-terminally truncated.

Exu^{D39/41N}:Venus), localize similar to the original GFP:Exuperantia protein in oocytes and nurse cells (Fig. 2.17 A-D). Both show the early localization at stage 9 at the anterior margin of the oocyte and localization at the posterior pole until later stages. In the nurse cells, both proteins show a cytoplasmic distribution with particulate accumulations (Fig. 2.17 C,D inset) which could represent the earlier described sponge bodies. Exu^{ΔC}:Venus localizes similar to the full length proteins (Fig. 2.17 E inset). In contrast to this, the truncated and catalytically dead protein (Exu^{D39/41N,ΔC}:Venus), only occurs in the soluble form and fails to be recruited into sponge body like particles (2.17 F inset).

This observation strongly suggests that, in the context of the “minimal construct” the catalytic residues of the DEDD exonuclease domain are required for sponge body localization in the nurse cells.

2.4.8. Co-localization of Exuperantia with *bicoid* mRNA

To examine the localization of the different Venus-tagged Exuperantia proteins together with the distribution of *bicoid* mRNA, I used a *bicoid*-MS2 MS2-coat-mCherry reporter system (see Fig. 1.1). Three of the proteins co-localize with *bicoid* mRNA during early stages in the oocyte and during all stages in the nurse cells (Fig. 2.18 A-E,G). Only Exu^{D39/41N,ΔC}:Venus (truncated & "catalytically dead" Exuperantia) does not co-localize with the *bicoid* mRNA during any stages of oogenesis (Fig. 2.18 G,H). It is not recruited into RNPs, which are properly formed, as expected. This indicates that there is no co-recruitment by oligomerization with wild-type Exuperantia. The three proteins, which co-localize with *bicoid* mRNA, also localize normally in an *exu*-mutant background (Fig. 2.17 C-E). Comparing the results of the transgenes, indicates a possible redundancy affecting protein localization between the DEDD domain and the C-terminus containing the potential 14-3-3 binding motifs. The localization of Exuperantia protein is only affected when the DEDD domain is mutant and the C-terminus is truncated (compare Exu^{D39/41N,ΔC}:Venus and Exu^{ΔC}:Venus and Exu^{D39/41N,ΔC}:Venus and Exu^{D39/41N}:Venus in

Fig 2.17 and Fig. 2.18). It also shows an independence of localization and function of Exuperantia in *bicoid* mRNA localization, since Exu^{D39/41N}:Venus shows wild-type localization but no wild-type function.

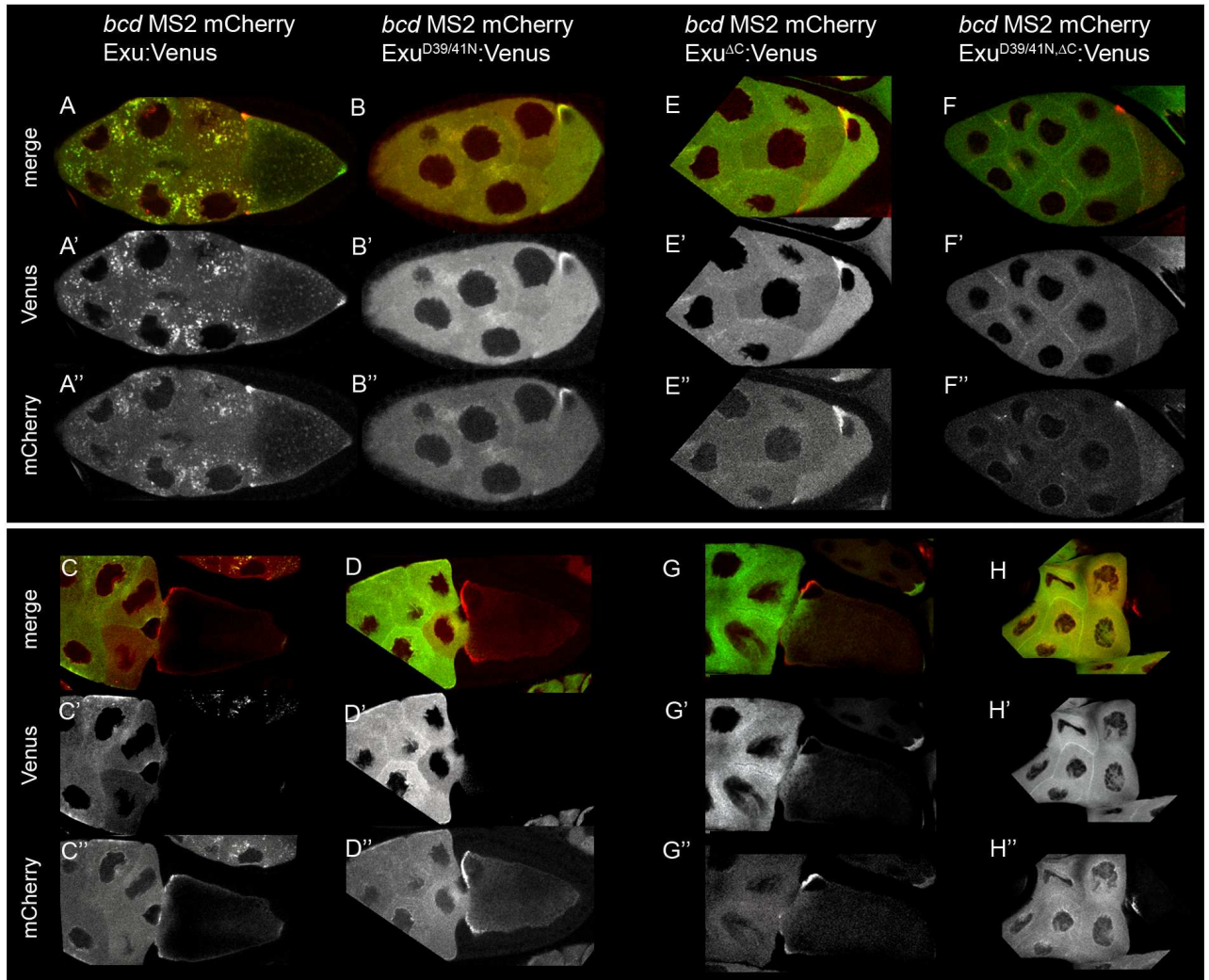


Figure 2.18 Co-localization of *bicoid* MS2-reporter and Exuperantia proteins. Localization was observed in wild-type flies carrying the indicated transgenes. **A, B, E, F** early stages of oogenesis (stage 9) **C,D,G,H** late stages of oogenesis (stage 10B). Channels are shown separately (**A'-H'** and **A''-H''**) and merged (**A-H**). ,

2.4.9. Analysis of exonuclease activity

The rescue assays show the importance of the catalytic residues Asp³⁹ and Asp⁴¹ for the function of Exuperantia. I used again quantitative real-time PCR to assay the levels of *bicoid* and *oskar* mRNAs in ovaries, freshly laid eggs and older embryos from flies carrying the different transgenes in an *exu*-mutant background (Fig. 2.19). The RNA ratios were determined as described above (see 2.4.3.) In ovaries, the values of *bicoid* and *osk* mRNAs vary around 1 and no significant difference is detectable between ovaries from *exu*-mutant flies (*exu*ⁱ³/*Df*(2*R*)*exu*1) and flies carrying additionally one of the transgenes (Fig 2.19 A). A similar result was obtained for the *bicoid* mRNA levels in embryos, regardless of the developmental stage (Fig 2.19 B,C). *oskar* mRNA levels seem to be slightly lower in embryos of all genotypes. But taking into account the high variability between the data, shown in the error bars, and that there is no significant difference between the transgenes with a potential active and a non-active exonuclease domain, these differences are probably not related to the different genotypes but to the technical variance of the assay.

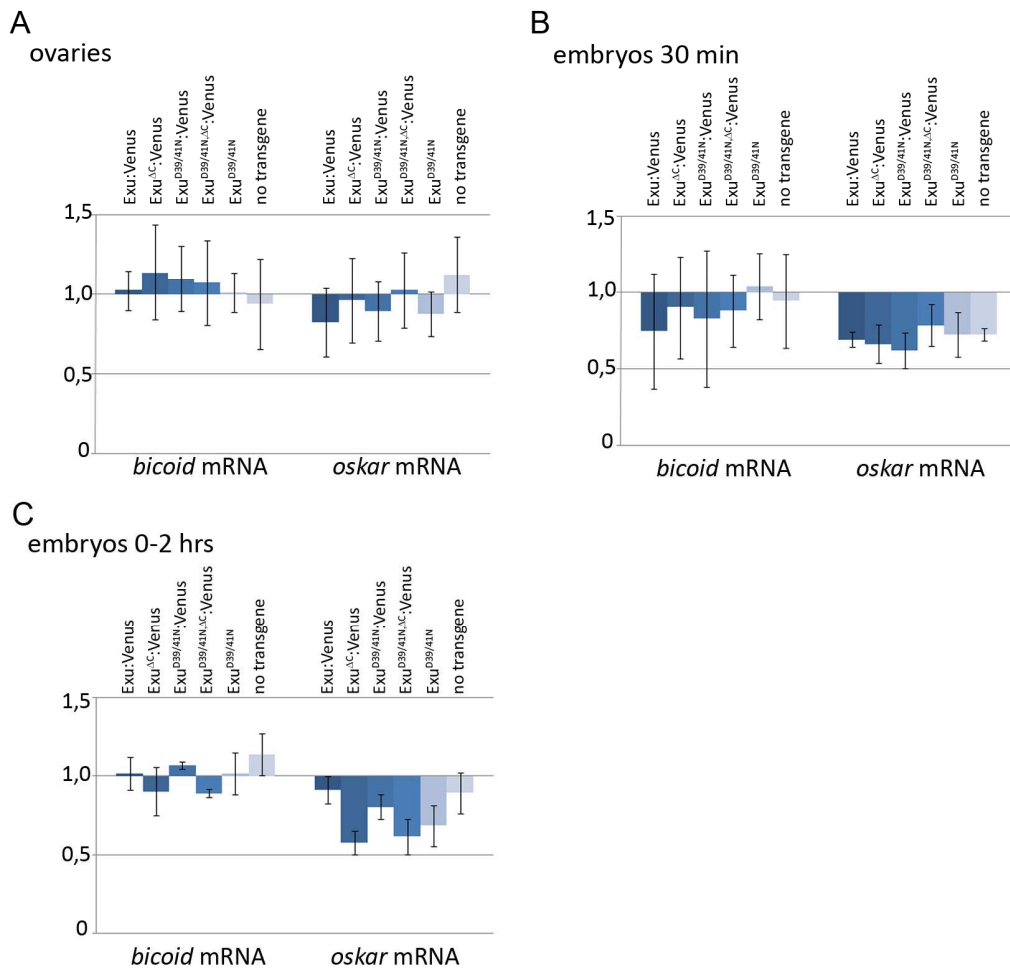


Figure 2.19 Quantitative real-time PCR results for *bicoid* and *oskar* mRNA of ovaries and embryos of *exu*-mutant flies carrying different transgenes.

A-C Shown are the differences of relative *bicoid* mRNA (left) and *oskar* mRNA (right) levels in three different developmental stages compared to wild-type. The germ-line specific *actin* mRNA was used to normalize the values. Transgenes carried by the otherwise *exu*-mutant flies are indicated. **A** ovaries, **B** freshly laid embryos (max. 30 min) and **C** embryos 0-2 hours. Error bars indicate the standard deviation. Each experiment was repeated three times with three technical replicates.

2.4.10. Summary of the transgene analysis

A summary of the results from above is depicted in table 2.1. Both full-length Exuperantia proteins, either wild-type or containing mutations of the catalytic residues (Exu:Venus, Exu^{D39/41N}:Venus) localize normally in an *exu-mutant* background and both co-localize with the *bicoid* mRNA reporter in a wild-type background. Despite wild-type localization pattern the catalytically dead full-length protein (Exu^{D39/41N}:Venus) does not rescue the *exu-mutant* phenotype.

The protein encoded by the “minimal construct” (Exu^{ΔC}:Venus) shows a wild-type localization pattern in an *exu-mutant* background and co-localizes with the *bicoid*-reporter in the wild-type background; it also rescues the *exu-mutant* phenotype. The localization as well as the ability to rescue are lost when the protein is catalytically dead (Exu^{D39/41N,ΔC}:Venus).

These results indicate that the function of Exuperantia highly depends on its catalytic residues. However, this is in disparity to the rescuing ability of the untagged full-length, catalytically dead Exuperantia Exu^{D39/41N}.



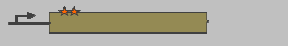


name	construct	localization	co-localization	rescue
Exu:Venus		yes	yes	yes
Exu ^{D39/41N} :Venus		yes	yes	no
Exu ^{D39/41N}		-	-	yes
Exu ^{ΔC} :Venus		yes	yes	yes
Exu ^{D39/41N,ΔC} :Venus		no	no	no

Table 2.1 Summary of transgenic rescue constructs

3. Discussion

At the time this project was started, very little was known about Exuperantia, one of the key players in *bicoid* mRNA localization. It was known that Exuperantia has a function during spermatogenesis [56] and that it is essential for *bicoid* mRNA localization during all stages of oogenesis [53, 56, 59, 61, 64]. The role of Exuperantia in spermatogenesis remains to be elucidated. Its function in RNA localization during oogenesis had been studied in more detail. However, the molecular details are still unclear. It is known that Exuperantia co-localizes with *oskar* mRNA [61] throughout oogenesis; and *oskar* mRNA was found in an RNase sensitive protein-RNA complex that could be co-immunoprecipitated with Exuperantia protein [65]. Albeit *exu*-mutants do not show a mis-localization of *oskar* mRNA, the experiments hint at an interaction of *oskar* mRNA and Exuperantia protein. On the other hand, Exu protein co-localizes with *bicoid* mRNA only transiently in the nurse cells and in early oocytes, but the mutant phenotype clearly shows the importance of *exuperantia* for *bicoid* mRNA localization during all stages of oogenesis.

There are now four alleles which indicate important amino acid residues in Exuperantia protein: *exu*^{QR9} (Gly⁴⁴Gln), *exu*^{D39/41N} (Asp^{39/41}Asn), *exu*^{g18} (Val³²⁷Glu) and *exu*^{PJ42} (Arg³³⁹Ser) (Fig. 3.1 red asterix). All of them result in amorphic phenotypes (Fig. 2.13 and 2.16). No hypomorphic alleles were found. The C-terminus with the putative 14-3-3 binding motifs is not essential for Exuperantia function in *bicoid* mRNA localization. This is clearly demonstrated by the function of truncated Exu^{AC}:Venus, which shows comparable rescue capability to full-length Exuperantia (Exu:Venus, Fig. 2.16). The weak *bicoid* mRNA localization defects, which have been reported for mutants where the serine residues in the phosphorylation sites are changed into alanines [5], could not be confirmed. This leaves the question open, whether the truncation of the protein leads to a weaker phenotype than the described point mutations or whether genetic background effects could be responsible for the observed differences.

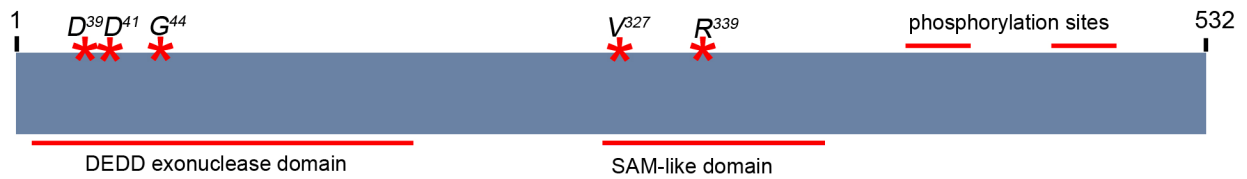


Figure 3.1 Schematic overview of Exuperantia.

Indicated are the identified domains in Exuperantia, DEDD domain and SAM-like domain, the C-terminal phosphorylation sites, and residues shown to be functionally important in Exuperantia.

The EMS-induced allele *exu^{QR9}*, and *exu^{D39/41N}*, which is carried on a transgene, show the importance of the N-terminal DEDD domain. This domain was originally identified using the HHpred program from the MPI-toolkit [75], where a homology between the N-terminal part of Exuperantia and DEDD 3' - 5' DnaQ-like exonucleases (SCOP family c.55.3.5) was found (Fig. 2.1 A). This finding is based on the predicted similarity of secondary structure elements, the conservation of the well-described Exo motifs (I-III) [84] as well as the conservation of four catalytic residues Asp³⁹, Asp⁴¹, Glu¹⁵⁰ and Asp²⁵⁸ in Exuperantia. The homology between DEDD exonucleases and Exuperantia had been reported earlier [66]. Here too, a hidden Markov model (HMM) had been used, in this case to identify RNaseD-like exonucleases. In the published alignment domains from two *Drosophila* proteins are included: the N-terminal part of Exuperantia and the central part of Egalitarian. In the case of Egalitarian the function of the exonuclease-like domain has been examined further [67]. It was shown that the catalytic residues (Asp⁵⁶¹, Glu⁵⁶³, Asp⁶²¹, and Asp⁷⁰⁸ in Egalitarian) are not essential for the function of Egalitarian, suggesting that it is probably not an enzymatically active exonuclease. These observations lead to the conclusion that this domain might simply be involved in RNA binding [76].

In contrast to Egalitarian, the function of the N-terminal exonuclease-like domain of Exuperantia was never tested. The identification of the domain by HHpred strengthens the previous finding and is a strong argument in favor of a thorough analysis. Some facts from the analysis of the amino acid sequence point towards the possibility that Exuperantia could have retained exonuclease activity. First, there is a high similarity in the secondary structure and the Exo motifs are conserved. Second, two of the catalytic

residues are interchanged by compensatory mutations; the original sequence (D-E-D-D) is changed to D-D-E-D in Exuperantia and, third, the position of the third catalytic residue is shifted within the α -helix. These changes are predicted to leave the catalytic center intact and could therefore mean that the enzymatic activity is conserved. To test if the catalytic residues are important for Exuperantia's function *in vivo*, transgenes were generated in which two of the catalytic residues (aspartic acid at position 39 and 41) were changed into asparagine (Fig. 2.15). Transgenes carrying these mutations would be expected to be "catalytically dead", since the corresponding mutations in RNase T abolish enzymatic activity but do not affect target binding [71]. The site specific mutations were introduced into full length (Exu^{D39/41N}:Venus) and truncated (Exu^{D39/41N,ΔC}:Venus) Exuperantia. Both Venus-tagged "catalytically dead" transgenes are not able to rescue the *exu*-mutant phenotype (Fig. 2.16), unlike the corresponding wild-type transgenes (Exu:Venus, Exu^{ΔC}:Venus). These results show that the catalytic residues are important for Exuperantia's function *in vivo*. Unlike Egalitarian, Exuperantia could have enzymatic activity.

Surprisingly, the control transgene, encoding full-length Exuperantia without Venus-tag but with the "catalytically dead" mutations, is able to rescue the *exu*-mutant phenotype (Fig. 2.16). This result was obtained with two independently generated transgenic fly stocks. The identity of the transgenes was confirmed by sequencing, ruling out a contamination of one of the fly stocks, for example with a wild-type transgene. All data are put together in Table 2.1. These results appear difficult to reconcile at first, but one possibility to explain them could lie in a possible redundancy between the N-terminal DEDD-domain and the C-terminus of Exuperantia containing the potential 14-3-3 binding sites. One could postulate that the C-terminal fusion to Venus interferes with the putative 14-3-3 binding sites, thus making the N-terminal DEDD domain essential. A series of transgenes encoding untagged or N-terminally tagged Exuperantia could elucidate this issue. If the hypothesis is true, then the N-terminally tagged full-length protein should be able to rescue the mutant phenotype even when the catalytic residues are mutated, because in this situation no C-terminal tag would interfere with the putative 14-3-3 binding sites. In addition one would expect that untagged, but truncated

Exuperantia ($Exu^{\Delta C}$) is still functional to rescue the mutant phenotype but with the mutations ($Exu^{D39/41N,\Delta C}$) would lose this functionality.

The EMS-induced alleles exu^{g18} and exu^{PJ42} change amino acid residues in the newly identified SAM-like domain. The amorphic phenotype of the mutants shows the importance of this part of the protein. SAM domains are mostly associated with homo- and heteromeric protein-protein interactions and are characterized by the presence of a five-stranded α -helical bundle [77]. In a manually generated alignment of this domain from Exuperantia with SAM domains from various other proteins the conservation of several positively charged residues becomes apparent (asterisk in Figure 2.2 A; red: conservation in all aligned proteins, black: positively charged residues in Exuperantia). Two of the SAM domains in the alignment are known to bind RNAs, VTS1 from *S. cerevisiae* (PDB-ID 2D3D [78]) and Smaug from *D. melanogaster* (PDB-ID 1OXJ [79]). Their RNA-binding capacity depends on these positively charged residues (red residues in Smaug in Fig. 2.2 A). They were shown by mutagenesis to be important for RNA binding. It is important to note that several of these residues are conserved in the SAM-like domain of Exuperantia (Fig. 2.2 A, red asterisk). In exu^{g18} , the first amino acid residue of α -helix1 is changed from valine to glutamic acid ($Val^{327}Glu$, highlighted in red in Fig. 3.2), which introduces a negative charge and is likely to disrupt RNA binding. In the previously known allele exu^{PJ42} , Arg^{339} is changed into a serine residue (highlighted in red in Fig. 3.2). This point mutation is in the equivalent position of a positively charged residue in Smaug (Lys^{612}) shown to be necessary for RNA binding [79].

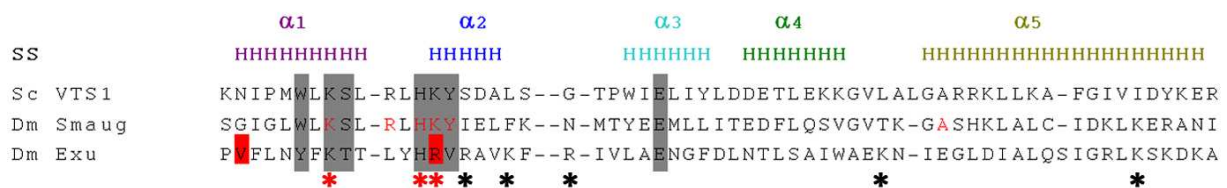


Figure 3.2 Alignment of two known RNA binding SAM domains and Exuperantia.

Shown are the characteristic 5 α -helices of SAM domains. VTS1 from *S. cerevisiae* and Smaug from *D. melanogaster* are known to bind RNAs mainly through conserved positively charged residues (red residues). Residues which were shown to abolish RNA binding when mutated in Smaug are highlighted with grey boxes. The already known (exu^{PJ42}) and the newly identified (exu^{g18}) functional residue in Exuperantia are highlighted in red. ss - secondary structure

The presence of several positively charged residues within the SAM-like domain and the conservation of some residues, which have already been shown in other SAM domains to be important for RNA binding, as well as the amorphic phenotype of the two point mutants, suggest an RNA binding capacity of Exuperantia via the SAM-like middle part.

The identified point mutations in Exuperantia indicate that nucleic acid binding and catalytic activity could be important for its function *in vivo*. To test a possible exonuclease activity *in vitro*, a biochemical assay was developed, which is based on fragment analysis using capillary electrophoresis. In the assay I used three different NusA-tagged proteins: a truncated wild-type version of Exuperantia containing the DEDD domain and the SAM like domain, the “catalytically dead” version and a version mimicking the probably RNA binding defective *exu*^{PJ42} allele (Arg³³⁹Ser). After testing several different buffer compositions, without positive results, one buffer was identified, where specific exonucleolytic RNA degradation was detectable. Here, the substrate oligonucleotide is degraded, when incubated with wild-type Exuperantia protein, but no degradation is detectable when incubated with the “catalytically dead” or *exu*^{PJ42}-mimicking protein. This could indicate that the modified, recombinant proteins lost their catalytic activity (*Exu*^{D39/41N, ΔC}) or their target binding potential (*Exu*^{R339S, ΔC}). Unfortunately, in this experiment, in the negative control, where no recombinant protein was used, the RNA substrate was no longer detectable after the incubation period. This could be due to a contamination with RNase. These preliminary experiments are indicative for an exonuclease activity. The activity of exonucleases is highly dependent on metal ions, which are bound within the catalytic center. The buffer, which showed promising results, is the only one containing calcium ions, which would indicate a calcium dependence of Exuperantia's activity. Most known DEDD exonucleases have two Mg²⁺ ions in their active centers, complexed mainly by the side-chains of the four acidic catalytic residues. The overall geometry of the catalytic center is preserved in Exuperantia, however, the compensatory mutations and the shift of residue E¹⁵⁰ may allow the substitution of Mg²⁺ by more voluminous ions, like Ca²⁺. Furthermore, the loss of activity in the two mutant versions of Exuperantia, indicates a cooperation of exonuclease domain and SAM-like domain, meaning that the SAM-like domain

promotes target binding and the enzymatic activity lies in the N-terminal domain. It is known for 3' exonucleases that their target specificity is often promoted not by the catalytic domain itself, but by either RNA binding domains or protein-protein interactions with other target specific partners [73].

The fact that Exuperantia acts in the nurse cells on the *bicoid* mRNA, to affect its later localization within the oocyte [74] is compatible with an enzymatic function of Exuperantia. *bicoid* mRNA could be a direct target of Exuperantia, alternatively, Exuperantia could modify another RNA involved in the *bicoid* mRNA localization process. An interesting hypothesis would be that microRNAs (miRNAs) are involved in the folding of the *bicoid* localization element (BLE). Exuperantia might be needed to modify such a miRNA in a way that allows binding to the *bicoid* 3'UTR. In this case, a loss of the miRNA pathway would have the same phenotype as a loss of Exuperantia function. However, in *dicer* mutants (Q¹¹⁷Stop) *bicoid* mRNA localization is unaffected, as indicated by the wild-type localization of GFP-Staufen, a marker for *bicoid* localization during late stages of oogenesis [85] (data not shown). Alternatively, binding of a specific microRNA to the *bicoid* 3'UTR might interfere with the folding of the BLE. In this case, the *exu-mutant* phenotype should be rescued by mutations in the microRNA pathway.

To see if Exuperantia acts directly on *bicoid* I analyzed the 3'UTR of *bicoid* mRNA in *exu*-mutant flies (Fig. 2.3). No difference in the length, the amount of the different fragments or the sequence of the *bicoid* 3'UTR could be detected in these flies with respect to wild-type. This argues against *bicoid* mRNA being a direct target of a possible exonuclease activity. I also tested if the overall mRNA levels of *bicoid* and *oskar* are changed in different *exuperantia* trans-heterozygous flies compared to wild-type flies (Fig. 2.14), since Exuperantia might affect the stability of these mRNAs. No difference was found in the mRNA levels between ovaries and embryos from wild-type and *exu*-mutant flies.

Apart from *bicoid* mRNA and microRNAs other small RNAs, long non-coding RNAs or mRNAs could be possible targets for Exuperantia. In *exu*-mutants the target RNAs are not degraded and will therefore be present in the ovaries and could be detected by RNAseq. Alternatively, the targets could be cross-linked to Exuperantia and purified by

immunoprecipitation (CLIP). For this purpose, the full-length Venus-tagged “catalytically dead” Exuperantia protein is ideally suited. Several commercially available anti-GFP antibodies can be used to immunoprecipitate Venus-tagged proteins; and more importantly, the “catalytically dead” Exuperantia protein should still bind its target without degrading it, allowing identification by RNAseq (CLIPseq).

Both Venus-tagged full-length proteins, wild-type and “catalytically dead”, localize normally in the nurse cells and the oocyte. Within the oocyte they co-localize at the posterior pole with *oskar* mRNA and during early stages (up to stage 9) also at the anterior pole where *bicoid* mRNA and remnants of *oskar* mRNA are found. The ability to rescue the mutant phenotype is not strictly correlated with the localization of the protein. The truncated wild-type Venus-tagged protein shows wild-type localization and rescues the *exu*-mutant phenotype, in contrast to the “catalytically dead” truncated version. This protein does not rescue the *exu*-mutant phenotype and also shows no wild-type localization in oocyte and nurse cells. This shows that the localization of the full-length “catalytically dead” Venus-tagged protein is dependent on the C-terminus containing the putative 14-3-3 binding motifs. As discussed before, these motifs are not relevant for Exuperantia’s function in *bicoid* mRNA localization. By comparing the Venus tagged proteins it becomes clear that the catalytic residues in the N-terminal DEDD domain of Exuperantia are essential for the protein's function, strongly arguing for an enzymatic activity of Exuperantia. The fact that there are no hypomorphic *exuperantia* alleles known might reflect its catalytic properties. As oogenesis takes several days, even reduced activity of Exuperantia might still be sufficient to process enough of its substrate, thus allowing *bicoid* mRNA to localize. On the other hand, detection of weaker alleles might only be possible using a more direct read-out for *bicoid* mRNA localization than cuticle patterning. Axis formation in the embryo is a well buffered system. In embryos containing only half the amount of *bicoid* mRNA the resulting shallow Bicoid protein gradient will be compensated for during later development.

Exuperantia being an enzyme, and not solely acting as an RNA-binding protein, could nicely explain the earlier results that its function is only required in the nurse cells for later localization of *bicoid* mRNA in the oocyte. It also explains why there is only limited co-localization of Exuperantia protein with *bicoid* mRNA.

4. Material and Methods

4.1. *Drosophila* rearing

Fly cultures and genetic crosses were done according to standard procedures.

4.2. EMS mutagenesis and allele screen

(adapted from [86])

To induce random point-mutations Ethyl methanesulfonate (EMS) was used. It is highly mutagenic, carcinogenic and teratogenic. Therefore it is strongly recommended to work with care; one key element, besides wearing appropriate protection, is to work under a closed chemical hood and to have a sufficient amount of the decontamination solution (10% w/v sodium-thiosulfate in 1 M sodium hydroxide solution) at hand; the decontamination solution should be available in a tank to decontaminate equipment and in a spray flacon.

Collect enough virgin females of the appropriate genotype ($w^{\bar{}}/w^{\bar{}}$; *If/Cyo,hs::hid*) and keep them at 18°C until needed. Collect freshly eclosed males and keep them on food for three days. Prepare a sufficient number of empty big bottles by placing filter papers on the bottom of each vial and add 100 males per bottle. Starve the flies for eight hours. In the evening prepare a solution of 30mM EMS in 1% sucrose, shake or vortex until EMS is dispersed into little drops. Using a 10 ml disposable syringe dispense 2-3 ml of the EMS solution per bottle. This should be just enough to saturate the filter papers without making it too wet so that the flies stick to it. Discard used syringes and Falcon tubes in prepared container with decontamination solution. Leave the males in the bottles with the EMS solution over night. In the next morning carefully transfer them into fresh bottles containing food, where they can clean themselves and let them recover for at least 30 min. During the recovery distribute the females into bottles containing extra yeast (40-50 females per vial). Divide the surviving males from each vial into three groups and add each group to a vial of virgins. Use dedicated EMS-CO₂ pad or ether to anesthetize flies at this point. After 4 days remove the males from the crosses and

transfer the females into a new yeasted vial. This can be repeated several more times. In the next generation the F1 virgin flies were collected and crossed with males carrying an *exu* allele ($w/Y; exu^{VL}/CyO, bw$). By applying heat shocks (put vials at day 2 and day 3 for 1 hour in a water bath at 37°C) the larvae carrying the *CyO,hs::hid* balancer were killed, and only F2 flies will emerge that carry the mutagenized chromosome with the potential new allele (+*) over *exu*^{VL} or *CyO, bw* balancer (Fig. 3.1). The egg lays from females of the genotype +*/*exu*^{VL} *bw* were screened for larval patterning defects, which would indicate the generation of a new *exu* allele. The flies carrying the balancer chromosome were then used to establish stocks.

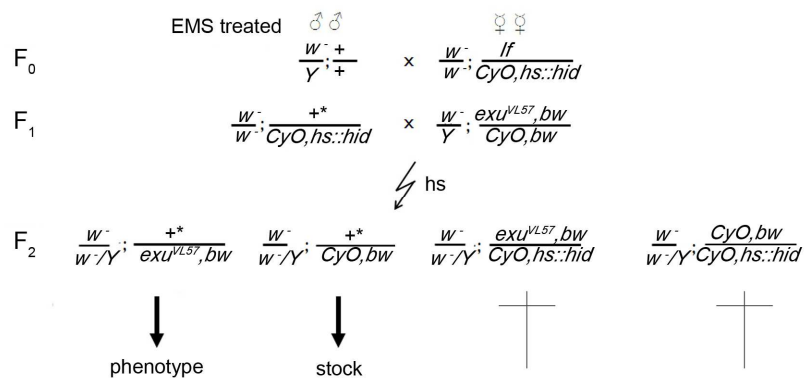


Figure 4.1 Crossing scheme.

F₀ EMS treated wild type males were crossed to females carrying a dominant eye marker (*If*) balanced with *CyO, P{hs-hid}4* ($w^-/w^-; If/CyO, hs::hid$) F₁ virgin females, which possibly carry a newly induced mutation and the *CyO,hs::hid* balancer chromosome were crossed to males containing a partial deletion in *exu* genomic region (*exu*^{VL}) balanced with *CyO,bw*. F₂ Applying heat shocks to larvae and thereby inducing expression of the lethal *hid* transgene permits the elimination of all flies carrying the *CyO,hs::hid* balancer. The surviving flies carry the mutated chromosome over *exu*^{VL} (allows to screen for phenotype in the egg lays) or have the same chromosome balanced with *CyO,bw*, which allows to establish a stock.

4.3. Western blot

The samples, whole flies or ovaries from flies, were homogenized in PBS with added proteinase inhibitors (Roche # 11697498001). Loading buffer was added to the samples and they were boiled for 2 minutes. Samples were cleared by centrifugation at maximum speed in a table-top centrifuge for 5 minutes and the supernatant was loaded on 12% polyacrylamide mini-gels (6x8 cm) containing 0.1% SDS (SDS PAGE). Gels were run submerged in running buffer at 200V for approx. 1 hour. While running the gel nitrocellulose membranes, big enough to cover the gels, were equilibrated in water. After the gel run is finished a "blot sandwich" was assembled in the following order by using available chambers: Moistened sponge, two blotting buffer soaked filter papers, gel, equilibrated membrane, two blotting buffer soaked filter papers and a sponge. Proteins were transferred onto the nitrocellulose membranes submerged in 1xWestern buffer in a cooled blotting-chamber with a constant current of 200 mA for 1 hour. After transfer the membranes were briefly washed with PBS and then blocked by incubating with 5% milk powder in PBST. Primary antibody of choice (rabbit-anti-Exuperantia, 1:1.000) was added over night. The next day the membranes were washed with PBST three times for 20 minutes each. A peroxidase-coupled secondary antibody appropriate for the host of the primary antibody was used (goat-anti-rabbit-POD, 1:10.000). Use the ECL detection kit (GE healthcare RPN2132) to develop the blot.

4.4. *in situ* hybridization

Fix embryos in a 4% formaldehyde/heptane mixture in a 1:1 ratio for 25 min at room temperature, while keeping in motion. Remove the aqueous phase and add same volume methanol, shake well for 1 minute to remove vitelline membranes. Wash several times with methanol and, if needed, store in methanol at -20°C.

When staining ovaries dissect females in PBST and fix them afterwards with 4% formaldehyde in PBST for 25 minutes at room temperature, wash several times with PBST. Dehydrate ovaries with methanol and leave in methanol for at least several hours or store in methanol at -20°C. Rehydrate ovaries or embryos by washing with

PBST several times. Incubate at 95°C for 5 minutes and shake every now and then. Incubate for 1 hour at 70 °C in hybridization solution. Change hybridization solution and add RNA probe, incubate over night at 70°C. Wash first with hybridization solution at 70°C for 20 minutes afterwards wash with hybridization solution/PBST in a 1:1 ratio for 20 minutes at 70°C. Rinse with PBST and wash for 1 hour at room temperature.

When using a fluorescently labeled probe directly mount in Vecta shield, for Dig labeled probes incubate with alkaline phosphatase linked anti-DIG antibody (Roche # 11093274910, 1:2000) in PBST for 2 hours at room temperature. Rinse three times with PBST and wash for one hour. To develop the staining remove residual phosphate buffer by washing with staining buffer and stain by adding 3,5 µl BCIP (50mg/ml) and 4,5 µl NBT (50mg/ml) to 1ml staining buffer.

4.5. Cuticle preparation

Collect embryos on apple juice-agar plates. Allow to age for 24-36 hr at 25 °C. Remove yeast paste, add 60% bleach solution to the plate and let stand for 2 minutes to dechorionate the embryos. Pour through a small mesh and rinse with plenty of luke warm water. Collect embryos and bring into 1ml of PBS/heptane solution (1/1). Embryos with intact vitelline membranes will stay at the interphase, while hatched larvae will settle to the bottom of the tube. Use a pipette to suck up the aqueous phase and the hatched larvae from the bottom of the tube, keep the vitellinized larvae from interphase and the upper heptane phase. Add equal volume of methanol. Close cap of the reaction tube and shake vigorously for 15 seconds to de-vitellinize. The majority of embryos will now settle to the bottom of the tube. Remove the upper phase without removing any embryos. Now all of the embryos should settle. Remove liquid and wash several times with methanol. Use some methanol to transfer the embryos to a glass slide. Use the methanol to distribute the embryos evenly. Let the methanol air dry briefly and then add some drops of Hoyer's/lactate. Cover carefully with a cover slip avoiding bubbles. Incubate the slide at 65°C overnight.

4.6. Antibody staining

Fix embryos in a 4% formaldehyde/heptane mixture in a 1:1 ratio for 25 min at room temperature, while keeping in motion. Remove the aqueous phase and add same volume methanol, shake well for 1 minute to de-vitellinize embryos. Wash several times with methanol and, if needed, store in methanol at -20°C. Rehydrate with PBST for at least one hour while changing buffer several times.

When staining ovaries dissect females in PBST and then fix with 4% formaldehyde in PBST for 25 minutes at room temperature, afterwards wash several times with PBST. Use 20% BSA in PBST as blocking solution, rotate samples while incubating for one hour at room temperature. Remove the blocking solution and add 10% BSA in PBST with your first antibody of interest. Rotate your sample either for two hours at room temperature or over night at 4°C. Remove the antibody solution carefully. Wash your sample with PBST at least three times for twenty minutes. Add an appropriate secondary antibody, which is fluorescently labeled or linked to alkaline phosphatase. If an enzymatically tagged antibody is used remove the residual phosphate buffer by washing with staining buffer and stain by adding 3,5 µl BCIP (50mg/ml) and 4,5 µl NBT (50mg/ml) to 1ml staining buffer (see *in situ* hybridization).

4.7. quantitative RT-PCR

mRNA was isolated from ovaries or embryos with the Dynabeads mRNA DIRECT™ Kit (Invitrogen, # 61011) according to the protocol provided by the supplier.

To obtain cDNA this mRNA was used as template for the reverse transcription using AMV reverse transcriptase Kit (Invitrogen, # 12328019) following the manufacturer's protocol. RT-PCR was performed according to standard procedures using iQ SYBR Green Supermix (Bio-Rad 170-8882).

4.8. Generation of transgenic flies

4.8.1. construct generation

The DNA-constructs used for transgenesis all carry a *mini-white*⁺ gene, which allows easy identification of successful transgenesis.

For the first transgenes the pCaSpeR4-vector was used. Transgenesis using pCaSpeR is based on P-element mediated random integration. For the site directed integration an attB-based transgenesis system was used [87].

A 5,6kbp genomic region of *exuperantia* was used. This fragment had been used for the generation of rescue-transgenes in the past [63]. To amplify the genomic region by PCR from wild-type flies the following primer-pair was used:

forward: GGTACCCCTTATCAGTAAGCAGCATAGGCG
reverse: ACTAGTGTTGAAGTAGCCGAAATCGGG

The PCR fragment was cloned into pCR[®]II-TOPO[®] TA (Invitrogen # K460040) vector, sequenced and then cloned into pCaSpeR4 via Acc65I and SpeI.

This genomic *exuperantia* fragment in pCaSpeR4 was used for further modifications. To add the C- or N-terminal Venus fusion I used overlapping PCR (Fig. 3.2). I designed primers, which amplify Venus (Fig 3.2 green) and are overlapping with the coding region of *exu* (*exu* CDS) or the 3' UTR sequence (Fig. 3.2 primer pair A). I also designed primers to amplify a fragment from the coding sequence of *exu* overlapping at the 3' end with Venus (Fig. 3.2 primer pair B) and a primer pair, which amplifies the 3'UTR of *exu* so that it overlaps at the 5'-end with the Venus sequence (Fig. 3.2 primer pair C).

I used these three fragments with partially overlapping sequences as template, the forward primer of pair B and the reverse primer of pair C to combine everything in a second round of PCR. The same method was used to generate the C-terminal truncations and N-terminal Venus fusions (for primer sequences see Appendix D).

The N-terminal fusion constructs were additionally cloned into the attB site containing vector pUAS attB, for site directed transgenesis. To change the vector the in-Fusion

PCR technique (Clontech #639616) was used. Primer design and procedure were done according to the protocol. To amplify the constructs I used a primer pair, which amplifies the full constructs and is applicable to all different variants

forward: TCACTGGAAGTAGGAATTCGGTACCCCTTATCAGTA
reverse: CGACACTAGTGGA TCTGTTGAAGTAGCCGAAATCGG

To linearize the attB vector I used BamHI and NheI.

4.8.2. site directed mutagenesis

To introduce the Asp^{39/41}Asn mutations two fragments were amplified with primers that carry the mis-sense mutations of interest:

pair 1 forward: TAAGTGCTAAGCCGTCTTCG
reverse: GTGGT**GTTGATATTCACGCC**
pair 2 forward: GGCGT**GAATATCAACACCAC**
reverse: CAGGCCGTA**CTTCTTCAACGACTCC**

The reverse primer of pair 1 and the forward primer of pair 2 contain the mis-sense mutations (highlighted in blue). Using the corresponding primer pairs two fragments were amplified. These two fragments were subsequently joined together by a second round of PCR with forward primer 1 and reverse primer 2. Using unique restriction sites (BlnI and SanDI) the mutated fragment was brought back into the genomic *exuperantia* constructs.

4.8.3. transgenesis

The DNA for micro-injection to generate transgenic flies was used at a concentration of 0,5 µg/µl. For the P-element mediated transgenesis a ratio of 1:4 of helper plasmid (Δ2-3 turbo) and pCaSpeR-plasmid (24 µg pCaSpeR-plasmid and 6µg of Δ2-3 turbo) was

used. The DNA was precipitated with ethanol and ammonium acetate and dissolved in water.

For P-element mediated transgenesis *w*¹¹¹⁸ flies were used; targeted insertions on the 1st chromosome were generated in the stock: M{vas-int.Dm}ZH-102D, M{3xP3-RFP.attP}ZH-2A (Bloomington stock number 24480). A cage of well-fed and fairly young flies was prepared a few days in advance and apple juice plates containing yeast paste were changed regularly. At the day of injection the plate was changed every 30 minutes in the morning and the injection was started after the flies laid reliably, usually in the early afternoon. Embryos were collected in 30 min intervals, the yeast paste was removed from the plate to dechorionate the embryos with Bleach (Klorix)/tap water in a 1:1 ratio for approx. 2 minutes. The embryos were poured through a little basket/net and washed well with tap water (lukewarm). To align and orient the embryos on a piece of apple juice plate a fine brush or a thin needle was used. The washing and lining up of the embryos should take no longer than 10 minutes, to ensure that embryos don't develop too far. To fix the embryos on a cover slip heptan-eluted glue from sticky tape (Tesafilm) was brought on a cover slip and this cover slip was gently touched onto the aligned embryos to pick them up. All embryos have to have their posterior ends directed towards the edge of the cover slip to enable injection. The embryos were dried in a chamber containing silica gel between 6 and 16 minutes (normally around 8 min). Afterwards, to avoid further dehydration, they were covered with Voltalef 10S oil. The embryos were injected under a microscope at 18°C using an Eppendorf FemtoJet micro-injection set up. After injection they were kept on apple agar plates at 18°C. It is very important to make sure that the embryos are well covered with oil. After one and a half days the hatched larvae were collected. The emerged flies were subsequently crossed to *white*¹¹¹⁸ flies. In the next generation flies with an integrated transgene will have yellow to orange eyes.

4.9. Protein expression

4.9.1. generation of constructs

The coding sequence of Exuperantia was amplified from cDNA of wild-type flies and brought into respective expression vectors by either single cutting enzymes, whereby the restriction sites were integrated into the primer sequence, or using the infusion system (Clontech #639616), whereby the vector specific homologous sequences were added to the primers (Appendix E).

For the Arg³³⁹Ser mutation identified in the *exu*^{PJ42} allele, the locus was amplified out of *exu*^{PJ42}/*Df(2R)exu1* fly extract:

forward: AAGTCTGAGATCGCTGCCCTCAAG

reverse: GAATGTCCGACGGCCATATC

The fragment was brought into the Exuperantia expression vector replacing the wild-type region using single cutting enzymes.

The “catalytically dead” mutation Asp^{39/41}Asn was generated using single step mutagenesis (see 4.9.1.1.)

4.9.2. single step mutagenesis

For the site-specific generation of the “catalytically dead” mutations a plasmid containing wild-type Exuperantia was used as a template in a PCR with two overlapping primers carrying the mutations (highlighted in blue)

forward: GGCGTGAATATCAACACCAC

reverse: GTGGTGTTGATATTCACGCC

The Expand long template PCR system was used (Roche #11681842001) and the following reaction was set up.

1µl plasmid DNA 100-300ng
2,5µl mutant sense primer (10µl)
2,5µl mutant antisense primer (10µl)
1µl dNTPs (12,5µM)
5µl polymerase buffer (10x)
37µl water
1µl polymerase 2,5U/µl

The PCR was done with the following settings:

2 min 95°C
30 cycles à
15 sec 95°C
1 min 68°C
2min/kbp 72°C

To test for a successful amplification of the plasmid run 10 µl on a gel. Add 1µl of DpnI to the residual PCR reaction and let digest 1 hr at 37°C to get rid of template DNA. Transform competent cells with 1µl of digested PCR reaction.

4.9.3. general protein expression

Exuperantia expression vectors were transformed into different competent cells of the BL21(DE3) strain (BL21(DE3), BL21(DE3)RIPL, BL21(DE3)LysS, C41). Several colonies were used to set up starter cultures in 5ml 2xTY medium, containing the appropriate antibiotic. Cells were grown at 37 °C for seven hours.

2ml of the starter cultures were used to inoculate 1 liter of selective medium. Before induction with 1mM IPTG 2ml of the culture was withdrawn and saved as uninduced

control. To check for protein over expression extract of induced and uninduced cultures were separated on a 12% polyacrylamide gel and stained with Coomassie. When expression of the protein was detected, the cells were harvested by centrifugation at 3.000g for 20 minutes. Different methods were used to open cells to test for solubility of the protein.

For sonication cells were resuspended in lysis buffer (25ml for 1 l of culture) and kept on ice. The cells were sonicated at 65% duty cycle (Branson, Sonifier 250; output control at level 3) for thirty seconds and then chilled on ice. This was repeated three times. The treated cells were transferred into a centrifugation tube and cell fragments and insoluble proteins were spun down at 26.000g at 4°C for 25min. To find out which fraction contained the protein of interest, both, soluble and insoluble fractions were compared by SDS PAGE and Coomassie staining. The soluble protein in the supernatant was filtered through a 0.45µm syringe filter before proceeding with the purification.

To open the cells with a french press the tubing of the press was rinsed with water and equilibrated with lysis buffer. The cells were resuspended in lysis buffer (25ml for 1 l of culture) and brought through the french press with approximately 1000 bar (but not more) twice. The flow through was collected. Tubes were cleaned with 20% Ethanol and water. Make sure that the tubes don't run dry. The flow through was filtered through a 0.45µm syringe filter before proceeding with the purification.

4.9.4. His-tagged recombinant Exuperantia

For Ni-affinity-purification columns were used, which have to be packed. The Ni-NTA agarose (Qiagen # 30230) was equilibrated in 5 volumes of Ni-buffer. The filtered cell lysate was incubated with the prepared Ni-NTA beads, while rotating for 20 minutes at room temperature. The mixture was loaded to the columns. The cap was removed and the flow through was collected to test for proper binding of the His-tagged proteins. The columns were washed with Ni-buffer and the wash fractions were collected. To assay the protein concentration of the flow through 5x Roti-Quant Bradford assay (BioRad #K015.2) was used, by adding 10 µl of the fraction to 90µl Bradford solution. The column was washed until no protein was detected by the Bradford assay.. To elute the

proteins from the columns elution buffer was used and the eluate was collected until Bradford did not turn blue anymore. To regenerate the Ni-NTA column it was washed with 1M imidazol. After imidazol it was washed carefully with water before 25% Ethanol was added. The cap and lid of the column was closed and it was stored under 25% Ethanol.

4.9.5. TEV protease cleavage

The cleavage of the 6xHis-tag using the TEV protease was combined with the dialysis to remove imidazol from the elution buffer. First, 4l of Ni-buffer without imidazol was prepared and dialysis tube with a molecular weight cut off of 10kDa (Thermo Scientific #68100) was soaked in water. The TEV protease was added to the eluted protein, the mixture was brought into the dialysis tube and dialyzed over night while stirring. The cleaved protein-tag was removed by affinity purification with Ni-NTA columns. The columns were first equilibrated with Ni-buffer and then the dialyzed protein mixture was centrifuged to remove precipitated protein. The supernatant was loaded on Ni-columns to bind the now proteolytically cleaved 6xHis-tag. The flow through contains the protein of interest and was collected, the concentration of the protein was determined using the Bradford assay. The flow through was concentrated using Amicon centrifuge tubes (Millipore # UFC901024) and glycerol was added (final concentration 10%) before freezing. The columns were regenerated with 1M imidazol and washed with water before 25% ethanol was added. Store column in 25% ethanol.

4.9.6. GST-tagged recombinant Exuperantia

6 liter cultures were grown to $OD_{600}=0,6$, induced with 1mM IPTG and then grown over night at 20°C. Cells were harvested by centrifugation for 20 min at 4°C at 3000g. The bacterial pellet was resuspended in PBS and the solution was distributed to 4-5 50ml Falcon tubes and centrifuged again. One Protease Inhibitor tablet (Roche # 04693159001) was dissolved in 50 ml PBS and this was used to resuspend the pellet.

The pellet was frozen at -80°C in this solution. The cells were thawed and 1 pinch of lysozyme powder, 200 μL DNase I (1U/ μl) and 120 μL MgCl_2 was added. To lyse the cells they were incubated for one hour at 4°C while rotating. The cell fragments were centrifuged at high speed (26.000g) for 1 hour at 4°C and the supernatant was collected and filtered through a $5\mu\text{m}$ filter. The protino glutathione agarose beads (Macherey Nagel, # 745500.100) were equilibrated with three volumes of water and twice with preparation buffer. After equilibration they were incubated with the filtered lysate for 1 hour at 4°C while rotating slowly. The beads were washed three times with preparation buffer, to monitor samples of washing and beads supernatant were kept. After washing the beads were resuspended in 5ml of preparation buffer and additionally 250 μl TEV protease (enzyme kindly provided by Fulvia Bono) was added to each tube. The mixture was incubated over night while rotating at 4°C . After TEV cleavage the protein of interest should be in the supernatant. The supernatant was collected in a new tube and washing buffer from the beads was added for a maximum of 50 ml. The protein was purified further using HiS column.

4.9.7. HiS-column (ion exchange)

For protein purification using the HiS column, the column was equilibrated with 30 ml water and 30ml with HiS buffer A with a flow rate of 5 ml/min and MaxPressure: 0.5 MPa. The protein was loaded onto the column with a flow rate of 3 ml/min for about 50 ml. The protein concentration in this purification was determined using UV_{280} -light. Before the protein was loaded, the column was washed until no protein was detectable anymore and a UV base line was reached. The gradient for purification started with 100% HiS buffer A and reached over 200ml 100% the HiS buffer B with an increased salt concentration. Every minute a 5ml fraction was collected. The fractions were run on an SDS page and the proteins were detected with Coomassie staining. Fractions carrying the protein of interest were combined and subsequently concentrated to 1ml using Vivaspin centrifuge tubes (VWR # 512-3754). The concentrated protein was then used in gel filtration.

4.9.8. Gel filtration

For the protein purification using gel filtration, the column was equilibrated with 30ml of gel filtration buffer. After equilibration the protein was loaded over the loop to the column. By adding 25ml of gel filtration at a flow rate of 0.5 ml/min with MaxPressure of 1.1 MPa the protein was eluted from the column and fractions of 0.5 ml were collected. The fractions were tested on a SDS page for presence of the protein of interest by Coomassie staining. The fractions containing the proteins were collected, combined and concentrate using Amicon centrifuge tubes (Millipore # UFC901024). 10% glycerol was added before freezing the protein.

4.10. Fragment analysis

For the fragment analysis either singlestranded or doublestranded RNA was used. RNA-oligonucleotides with a fluorescent label at the 5'-end were ordered from biomers.net (for sequence and RNA information see Appendix F).

To anneal complementary RNA oligonucleotides, the following reaction was set up:

1µl	10x LA Taq Puffer
2µl	25mM MgCl ₂
0,1µl	27nt RNA labeled (1mM)
0,1µl	27nt RNA
6,8µl	water

To ensure the comparability, singlestranded RNA-oligonucleotides were treated identically. The annealing was performed in a thermocycler using the following program:

10 sec	90°C
1 hr	down to 25°C (1% ramp)

Doublestranded RNA was prepared freshly for each experiment. The reaction containing the doublestranded RNA-oligonucleotides was diluted 1:100 with water. The purified proteins (wild-type and mutated) were diluted to the same concentration. Proteins and RNA-oligonucleotides were incubated as follows:

10µl reaction

- 5 µl exonuclease test buffer (2x)
- 0,5µl RNA (single- or doublestranded)
- 0,5µl protein (1,5mg/ml)
- 4µl RNase free water

As negative control the storage buffer with 10% glycerol was used. 1 µl RNase 1 was added to the storage buffer as positive control. The reactions were incubated over night at room temperature. Prepare formamide for fragment analyzer by preparing a master mix containing for each reaction 9 µl Hi-Di formamide (Applied Biosystem # 4440753) and 0,5 µl GeneScan 120 LIZ size standard (Applied Biosystem #4324287). Heat master mix at 65°C for five minutes and keep on ice until needed. Dilute the reaction 1:10 and add 1µl of it to 9µl Hi-Di master mix in a 96 well plate. Close properly, shake well and spin reaction down at the bottom. Analyze the fragment size using gel electrophoresis in an ABI 3730xl DNA analyzer.

4.11. PCR and sequencing

PCR and sequencing was done according to manufactural protocols. Sequencing reactions were set up using BigDye Terminator v3.1 Cycle sequencing Kit (Applied Biosystem #4336921) according to the protocol and read in ABI 3730xl DNA analyzer. Sequence analysis and comparison was performed using Lasergene. Primer sequences used for sequencing see Appendix G.

4.12. alphabetical list of buffer

bleach solution

60% Klorix (household bleach solution)
40% tap water

elution buffer

50mM TrisHCl pH 8,0
150mM NaCl
300mM Imidazol pH 8,0
1:3000 β -Mercaptoethanol

exonuclease test buffer (2x)

40mM TrisHCl pH 8,0
20mM $MgCl_2$
100mM KCl
10mM DTT after [71]

gel filtration buffer

20 mM TrisHCl pH 7.5
300 mM NaCl
1 mM DTT
filter (0,22 μ m)

HiS buffer A

20 mM TrisHCl pH 7.5
300 mM NaCl
10% Glycerol
1 mM DTT
filter (0,22 μ m)

HiS buffer B

20 mM TrisHCl pH 7.5
1300 mM NaCl
10% Glycerol
1 mM DTT
filter (0.22 μ m)

Hoyer's/lactate

30 g gum arabic in 50 ml distilled water
stir overnight
200 g chloral hydrate, while stirring add in small
quantities
20 g glycerol
centrifuge at least 3hr at 12000 g to
clear
1:1 lactate

hybridization solution

5ml deionised formamid
2ml 5x SSC pH 6,8 at 20°C
to 10 ml water
add 10µl ssDNA (10mg/ml)
20µl tRNA (20mg/ml)
5 µl Heparin (50mg/ml)

loading buffer

1,2g sodium dodecyl sulfate
6mg bromophenol blue
1,2ml Tris 0.5M pH 6.8
2,1ml water
4,7ml glycerol
heat it up and stir it until dissolved
0,93g DTT

lysis buffer

50mM TrisHCl pH 8,0
150mM NaCl
10mM Imidazol pH 8,0
0,1% Triton-X-100
1:3000 β-Mercaptoethanol
1 tablet protease inhibitor (for 50ml)
yellow tip lysozyme crystal
1:10000 DNaseI

Ni-buffer

50mM TrisHCl pH 8,0
150mM NaCl
10mM Imidazol pH 8,0
1:3000 β -Mercaptoethanol
1 tablet protease inhibitor (for 50ml)

phosphate buffered saline (PBS)

2,67mM Potassium Chloride
1,47mM Potassium Phosphate monobasic
137.93mM Sodium Chloride
8,1mM Sodium Phosphate dibasic
add water

preparation buffer

20 mM TrisHCl pH 7.5
300mM NaCl
10% Glycerol
1 mM DTT
filter (0,22 μ m)

running buffer (10x)

300g Tris
1400g Glycin
100g SDS
add water to 1l
dilute to 1x with water

SDS page

separating gel (12%)

3,1ml water
3ml 40% Acryl amid (29:1)
3,75ml 1MTris pH 8,8
100 μ l 10% SDS
100 μ l 10% APS
4 μ l 10% TEMED

stacking gel

3.6ml water
630µl 40% Acryl amid (29:1)
630µl 1M Tris pH 6,8
50µl 10% SDS
10µl 10% APS
5µl 10% TEMED

staining buffer

100mM TrisHCl pH 9,4
150mM NaCl
50mM MgCl₂
0,2% Tween 20

western buffer (10x)

75,75g Glycin
360g TrisBase
add water to 2500ml, pH 8,3

western buffer (1x)

100ml 10x western buffer
150ml Methanol
750ml water

5. Appendix

Appendix A

selected sequences modeled by HMM by Moser et al. [66]

PubMed ID	species	FASTA sequence
Mge_Y366 (Y366_MYCGE)	<i>M. genitalium</i>	>gj 1351558 sp P47606.1 Y366_MYCGE RecName: Full=Uncharacterized protein MG366 MITKSFLLKNFDRSKELIPLSYNDVFSAVNQFLKSYTDVNDIDIIIEENLI EDPVFELDVLELLNEDPMLLLDSKNPRVQEAKIANKAKKNIKDYFNL PIFFDTSLDKNVSVYQKAELTEKKIQEIITSKKSAIIFKPIFEIEDCLIQP DAIIVHEKGLCEFVVIKATTNTRKYFLEIYDFVLFKKIGYKLLNYF CTVKYELQNKNNVSFFLNTEIKTSKNSFSLSSKEKDYFKNKPFNHPE KIAYIHKKKSNVNGFLVLIKLIDNLIKNNIVDLNKISDFVTKEIDSKSVRN IQPLIKNAAKIQINFWDQIQDIKKYQELKINQIVFNYSNFDSFWSNYL LRNLIKLVFAHKYNEIFKLSGKLANWSQLTYAYKENKSITINQLLHELN QKKSANFNSTNKISFFLEAWNSEKGFAGNKFKNNTWNKLNKLNKLV YDFFETISSIRIINNSLPFSQIVTQC SLIVDKNEIDDKRKLNCENLIFDP LFISVNDFKKVIDSLYQNNCSYDFVFNKSFENRLLMATLINEQIY KEKVKAIVDNLFDLADIFTIENNCLAFKQLNGFSSIKKVLTIIDESFLKA SKSIGYQNLKIQKGDVAQEVALSRFLNCLNKNEWNQVAFELKKYCE NDVRAMISIVLFIQDLIKKNDLFTFYSEN
Mpn_ORF664 (g1673969)	<i>M. pneumoniae</i>	>gj 1673969 gb AAB95946.1 conserved hypothetical protein [Mycoplasma pneumoniae M129] MLTKAFFLKNFDRSKELIPLSYADVFGAASQLLKKHHKQVDTEIDVQ EDLIEDPVFEIDILELLNEAPELLFDSKNPRVKEAQIIIEKAKKDIASYFH LDNILD TDNLGLKATVTEKIQFTEKQIEAAVQNKKAIIIFKPVFTVNQC LIQPDVVVHANGLCFVVIKATTNTRKFFILEIYDFLLFEKLGKYKLV NYFCIVNYELKNKHNVVSFFLNTEIKTAKNSSTSKTKEEQVLYGHLP NDPKKIAYIHSKKS GG VNGFLLV KLVDNIIRSGVTNLEQISFVRELN APSIRSLKQIIESEVAKVQLDFWNIIDDVKQH QELQDNQITFNYSDAFN SFWNNYLLRNLIKLVFAYKYSEIFRLSGKLAKWDEVEAYKENKSVKI DGFLYELNQGKMKKTKNPATSQFNKIHFFLRAWNDKKGIAVGNKFK SVWQKLKEKKVYDFDFETISSAVRVIDKSLPFTQIVTQC SLIVDDNTES DKSKLVCQNLIFDPLTIGIEDFKTVVDALYQKQCDQYSFVYVYKSF NRLLEMATFINEAPYQQRVQAIENLFDLADIFGLENDCLAFKQLDGF SSIKKVLPMIDQRFLDASRTVSYQSLKVQKGDVAQELTLARFLNCLD EQQWAQTALELKQYCENDVRAMIAIELFIKDFITNQL
SPC_LR0569 (slr0569)	<i>Synechocystis</i>	>gj 1001244 dbj BAA10485.1 slr0569 [Synechocystis sp. PCC 6803] MESATMSFPISKTYFLAGLHCPKRLWLSICRPEDASPM SLAAEQRIK QGKAIGVAARESFKNGILVDGNLKHCLKSWELTVVAGQGQVECLF EPAFLYDDILVRCVLRRLPSGNWEIIEVKSATKLKDEHIADLTLQHY VLEGLGLTVEKTSLMVVNPMARNWSVQDRFCYQDVTAAVVRWR GQLPQKLAEFRTLLTEPTAPQVPIGSHCDRYPYRCPFKDHCWQNVPP ISIFDIPLLKQDKLQNL MNSNIWNLE DIPAEFPLTQKQRTFIDRMTAAK PQIQDQLLRQLLGGIQPNQPL YFFDVETHSSAIPRFAGLHPYERCIFQ YSCHRLNPDGSLHEHFEYLHTEDSDPRLPLLI SLIHIGDRGSVVVYVY SFEKGV LQQLAAAYPNYGAKINQIIDRLWDLQVIFKRAYFHPGFRGS YSLKKVLPVMAPQFCHDDLVIKSGNEAPLVWEALLECSAPDKRAEM AQLREYCGLDTLGMVKIYEV LQQELKD
Bbu_P93 (BBTROP93)	<i>B. burgdorferi</i>	>gj 436324 emb CAA49311.1 p93 [Borrelia burgdorferi] MKKMLLIFSFFLVFLNGFPLNAREVDKEK LKDFVNMDLEFVNYKGPY

DSTNTYEQIVGIGEFARPLINSNSNSSSYYGKYFVNRIFDDQDKKASV
DIFSIGSKSELDLSILNLRILTG YLMKSFYERSSAELIAKAITIYNAVY
RGDLDYKFEFYIEASLKLSTKENAGLSRVYSQWAGKTQIFPLKKNIL
SGNVESDIDIDSLVTDKVVAAALLSENEGVNFARDITDIQGETHKADQ
DKIDIELDNFHESDSNITETIENLRDQLEKATDEEHKKEIESQVDAKKK
QKEELD KKAIDLKAAQKLDFAEDNLDIQRDTVREKLQENINETNKE
KNL PKPGDVSSPKVDKQLQIKESLEDLQEQLKEASDENQKREIEKQI
EIKKND EELFKNKD HKALDLKQELNSKASSKEKIEGEEEDKELDSKK
NLEPVSEADKVDKISKSNNNEVSKLSPLDEPSYSDIDSKEGVNDKDV
DLQKTKPQVESQPTSLNEDLIDV SIDSSNPVFEVIDPITNLGTLQLID
LNTGVRLKESAQQGIQRYGIYEREKDLVVIKIDSGKAKLQILDKLENLK
VISESNFEINKNSSLVDSRMILVVVKDDSNAWRLAKFSPKNLDEFIL
SENKILPFTSFAVRKNFIYLQDELKSLVTLDVNTLTKVKV

Sce_YLR106c (S64942) *S. cerevisiae* >gi|1256854|gb|AAB67548.1| Ylr106cp [Saccharomyces cerevisiae]
aa 2593-3360
...FLNINLEFTDVLQLSRGHSITLLWDIFRKNYPPTTSNSWLAFEKLINLS
EKFDKVRLLQFSESYNSIKDLMDVFRLLNDDVLNKNLSEFNLLLSKLE
DGINELELISNKFLNKRKH YFADEFDNLI
RYTFSVDTAELIKELAPASSLATQKLTKLITNKYNYPPIFDVLWTEKNA
KLTSFTSTIFSSQFLEDVVRKSNLKSFSGNQIKQSISDAELLSSTIK
CSPNLLKSQMEYYKNMLLSWLRKVIDIHVGGDCLKLTKELCSLIEEK
TASETRVTF AEYIFPALDLAESSKSLEELGEAWITFGTGLLLLFPVDS
PYDPAIH DYVLYDLFLKTKTFSQNLMSWRNVRKVVISGDEEIFTEKLI
NTISDDAPQSPRVYRTGMSIDSLFDEWMAFLSSTMSSRQIKELVSS
YKCNSDQSDRRLEMLQNSAHFLNRLESGYSKFADLNDILAGYIYSI
NFGFDLLKQKSKDRASFQISPLWSMDPINISCAENVLSAYHEL SRF
KKGDMEDTSIEKVLMYFLTLFKFHKRDTNLEIFEAAALYTLYSRWSVR
RFRQEQEENEKSNMFKFNDNSDDY EADFRKLPDYEDTALVTNEK
DISSPENLDDIYFKLADTYISVFDKDH DANFSSSELKSGAIITILSEDLK
NTRIEELKSGSL SAVINTLDAETQSFKNTEVFGNIDFYHDFSIPFQKA
GDIIETVLSV LKLLKQWPEHATL KELYRVSQEFLNYPIKTPLARQLQ
KIEQIYTYLAWEKEYASS...

BPPH2_DPO (DPOL_BPPH2) Bacteriophage Phi-29 >gi|118849|sp|P03680.1|DPOL_BPPH2 RecName: Full=DNA
polymerase; AltName: Full=Early protein GP2
MKHMPRKMYSCDFETTTKVEDCRVWAYGYMNI EDHSEYKIGNSLD
EFMAWVLKVQADLYFHNLKFDGAFIINWLERNGFKWSADGLPNTYN
TIISRMGQWY MIDICLGYK GKRKIHTVIYDSLKLPFPVKKIADKDFLT
VLKGDIDYHKERPVG YKITPEEYAYIKNDIQIIAEALLIQFKQGLDRMT
AGSDSLKGFKDIITTKFKKVFPTLSLGLDKEVRYAYRGGFTWLNDR
FKEKEIGEGMVFDVNSLYPAQMYSRLLPYGEP IVFEGKYVWDEDYP
LHIQHIRCEFELKEGYIPTIQIKRSRFYK GNEYLKS SSGEIADLWLSNV
DLELMKEHYDLYNVEYISGLKFKATTGLFKDFIDKWYI KTTSEGAIK
QLAKLMLNSLYGKFASNPDV TGKVPY LKENGALGFR LGEEETKDPV
YTPMGVITAWARYTTITAAQAC YDRIIYCDTDSIHLTGTEIPDVIKDIV
DPKLLGYWAH ESTFKRAKYLRQKTYIQDIYMKEVDGKLV EGGSPDDY
TDIKFSVKCAGMTDKIKKEVTFENFKVGF SRKMKPKPVQVPGGVVLV
DDTFTIK

Ski_ORF2 (S15961) *S. klyveri* >gi|74627258|sp|Q09038|Q09038_SACKL Similarity to DNA
polymerase (ski_ORF2)
MNKELEFLKNEVSYTETEDLDFLKSEVFKIHPYTRSIEKLEKNSTENSI
RSTIEYNQY GQEIYSKLSSNQIELEEAKQLMHKKFIQLRNKNRVPLKR
KRKKKLKFDHDVETLIIHKKYKIDLNL CNMDETQTFTHKDISIIPTRKSI
LKHIHVDRKYNYYCFVTLTLTGPTIFGGVTSKVPILNVQGIPNNDYDE
RMTKALNDIIERIPDYEEKESNIVCTRILITITQATWKSIDNWYPKTTRK
FKKFKDFTLFLASNRNENCLKQCVEKLGGKWNYNKKLEDMLPQKKII
TYIPALMDIQYVNSMEDLITDYNEEYISLDCKNIARLLKWNHGHIGVITK
LDPTRKIGKIQQKQRLEVEDTNT EEIFFDIESFTNEKNFQIPYLICWSK
TNGSIHKRIGKNCINDFVQYIINL KKNVILYAWFGSGYDYQHVLPHYK
KKCIKDKYI IKNMITYSELYFKH SKIILKDPFLFILSLDKAAKAFNVIN

KGSFPHSLIKDWPDLQKIYPHWIKTQRKIIIEFKHDNKLNIKINTTLEED
NITNNSTIIEKAIIEYCSIDVIAMKQVWQFKKLVKENLQISISEKTFTLS
QLSMKIMEASLDRNIELYVPTSEEYQFIRNSIYGGRVAAKNGTYNEEI
VYADVSLYPSAMKLEHSYGKPSKVFSINFNKHGIYDVTLIHKSNSK
PNHYLEFVPRRIDKLIWSWFKEHRGTYHTYDLLIAIQEGFEIICHSGI
EYPNKG YIFNNFIDKLYTLKDIHTNCKCKEQPCPIRMVAKIALNGGGY
GKFVQKPIDKEVYIVKRDVVAGECENLSQNGEIGICGRIVKPKFF
NLDGEDYDKMIERDDDDPIYSTQCGVSILSASRYRLYNLCKKFEGLI
YSDTDSIFVRKNTIDWELFKNTCGKNL GELDSTIDKTKNAIHYMLIGG
PKMYAFQYKNNKNNIITKLHCKGVPTFMLSIDQFEYLLHKKDRKLAY
HFEIIRRLVTVTTDKIHKDIKQT

**Kla_DPO
(DPO1_KLULA)**

K. lactis

>gj|1352308|sp|P09804.2|DPO1_KLULA RecName: Full=DNA
polymerase
MNYIINLKMDYKDKALNDLRNVYADFDSLPLDFRQILIKDRATLLQKE
DVEKKILERQEDAKKYAEYLKQSEIPERISLPNIKRHKGVVISFEETSE
DMVLEPRPFIFDGLNIRCFRRETIFSLKNKILNMVKESSSFKNVSRQS
VSFMYFKIFNKGKVIASSTKSVNIYEDKIDERLEDLCNNFDDVLLKIIDV
TYGYESL FVSETYSYVIFYAKSIYFPQPRCVNNWGNIPNLTFFDSFK
LFTANKNNVSCIKQCSRFLWQKDFNTLEEMIEYKNGNICIVTPQLHIN
DVRDIKSFNDIRLYSESPIKTF SVIDNTITYLFYFKEHLGVIFNITKSRH
DRRVTKFSPLSKFSDVKNITVCFDIESYFDPEKESQVNIPIFCCASII
YNKVIGNIVDFEGRDCVAQMIEYVVDICGELNISSVELIAHNGGGYDF
HYLSSMYNPAAIKNILIRNNSFISFNFAHDGVKFSVKDSYSFLLCCLA
NASKAFLNEETFKKTD FPHDLKTADDLYKVYKEWSSVNTINHVVE
KEKLLITSEHIVNFTKNDKSKTLIEWSKDYCRNDVLLVSKVWLEFKNA
VEDIFNCELVDQTM TLAGLSYKLFQANMPFDVELRHPNKEDYFNMR
EALIGGRCISVNGIYKDVLC LDVKSLYPASMAFYDQPYG SFKRVSSR
PKDELGIYYVRVTPNRNKS NFFPIRSHNKITYNNFEESTYIAWYTNV
DIDIGLSEGHNIEYIPFDSYGNIGYSWSKKGKIFEKYIKDVL YKLKIKYE
KQNNKVKRNVIKIIMNSLW GKFAQKWVNF EYFIKSEDDIDFESEEAY
KIWDTDFMLIKKIKESTYSSKPIQNGVFTLSWARYHMKSIWDAGAKE
GAECIYSDTDSIFVHKEHFKNNAKFMLNGLKVP IIGSEVGGQLELECEF
DKLLCAGKKQYMGFYTYFQDGKPCIKKRFKIPSNYIPELYAHL
SGADKEAKIQFLKFRREWG SVKGYIENKTVKAT

**CP1_DPO
(DPOL_BPCP1)**

Citrus greening
disease-
associated bacteri-
um phage CP-1

>gj|20137778|sp|Q37989.1|DPOL_BPCP1 RecName: Full=DNA
polymerase (CP1_DPO)
MTCYYAGDFETTNEEETE VWLSCFAKVIDYDKLDTFKVNTSLEDFL
KSLYLDL DKTYTETGEDEFIIFHNLKFDG SFLSFFLNNDIECTYFIND
MGVWYSITL EFPDFTL TFRDSLKILNFSIATMAGLFKMPIAKGTTPLLK
HKPEVIKPEWIDYIHVDVAILARGIFAMYEEENFTKYTSASEALTEFKR
IFRKS KRKFRDFFPILDEKVDDFCRKHIVGAGRLPTLKHGRRTL NQLI
DIYDINSMPATMLQNALPIGIPKRYKGPKEIKEDHYYIYHIKADFDL
KRGYLP TIQIKKLDALRIGVRTSDYVTT SKNEIDL YLTNFDLDFLK
HYDATIMYVETLEFQTESDLFDDYITTYRYKKENAQSPA EKQKAKIML
NSLYGKFGAKIISVKKL LAYLDDKILRFKNDDEEEVQPVYAPVALFVT
SIARHF IISNAQENYDNFLYADTDSLHLFHSDSLVLDIDPSEFGKWAH
EGRAVKAKYLR SKLYIEELIQEDGTTHL DVKGAGMTPEIKEKITFENF
VIGATFEGKRASKQIKGGT LIYETTFKIRETDYLV

**Zma-m_DPO
(DPOM_MAIZE)**

Z. mays

>gj|118887|sp|P10582.1|DPOM_MAIZE RecName: Full=DNA
polymerase; AltName: Full=S-1 DNA ORF 3
MQPARRHTKKKNMNYMRYESLTREQFERFLKDVHVKCYRGEPRYVI
PYEGHLIAVQDFE EYPKAGAVTMLASAFMELLINRVYPSIQGSAKFT
LQYRLNIDGNPINITLSKAIKLYADGTRIANEFILKEIINVLNKYAENYQ
SCDVEAISVRAYSEG SIDLNQASIPTKDESLNYLKGALIKYSDINNLEI
PKMGRRSKRRYQSYIPVDKTEMKNKTLFFVADLETLLLKRRD TDVD
KTHVPYAGGYMMVDM EKWVNADHITTFYAHDYSKVCQDFHDMSEK
MLTEMINRIVKDVQRRGSSMVVYFHNL SQFDGIMILSFLT KSYKNCHI

EPIMRNDCIYSIKLYKVSKNKDKRLVLTfMDSYLLLKVKLADLADSFC
 PELGGKGSFDHQNVTVDKLPSIREDSLTYLKQDILITAAMQRAKAI
 WEEYGIDILKVLTISALALKIFRRVYKDDDDNWIIYIPDDNEAQFIREG
 YYGGHTDVYKPYGENLYYDYNLSLYPSSMLDDMPIGKTRVWVSDLG
 SKKSKIVLNDMFGFIRAFIICPKHIKKPLLPYKDDGTIIIFPTGRFLGVY
 FSEELKYAVSLGYKVYPICGYIFDRKESPFKRFVYDIYSKRLDAKAKG
 EKALDFIYKITMNSLYGRFGISPESTTTTQIVSTEESSRKLALYNDGFVQ
 SYELSSDKCLVTCKNVRSLDLLKSSDRPTYAAVQISAAVTGYARIR
 MHPFISRDDCYTDTDSVVVERELPEEEVSPTALGKFKHEHFVEYGI
 FLAPKSYMLKASSVDQPIIKFKGAGKDEADEEWFINQLADPRAKKVIS
 YVRKFSRNFRELLVQEKMKYTMGLESKKREYVFDKNGVWVDTKP
 CHIGDFDVKSINPTS YWIIMNLLLEENEDLRNEFSNSEIMIANWEIKADA
 AKKRKASKLRGKPLRGGDTPSHIEE

**Dme_EXU
 (EXU_DROME)**

D. melanogaster

>gi|7302340|gb|AAF57429.1| exuperantia, isoform A [*Drosophila melanogaster*]
 MVADNIDAGVAIAVADQSSSPVGDKVELPAGNYILVGVDDIDTTGRRL
 MDEIVQLAAYTPTDHFEEQYIMPYMNLNPAARQRHQVRVISIGFYRML
 KSMQTYKIIKSKSEIAALKDFLNWLEQLKTAKGSSDGIYLIYHEERKF
 IPYMILESLKKYGLLERFTASVKSFANSINLAKASIGDANIKNYSRLKLS
 KILSTTKEEDAACSASTSGSGSGLGSGSSMVSIVSISPRDSTVTNG
 DDKQSSKNAVQGGKRELFDFGNASVRAKLAFDVALQLSNSDGGKPEPK
 SSEALENMFNAIRPFAKL VVSDVLELDIQIENLERQNSFRPVFLNYFK
 TTLYHRVRAVKFRIVLAENGFDLNTLSAIWAIEKNIEGLDIALQSIGRLK
 SKDKAELELLEDSYFDPKKTTPVVKVGNSSNNNNYRRRNRGGR
 QSVKDARPSSSPASSTEF GAGGDKSRSVSSLPDSTTKTPSPNKPR
 MHRKRNSRQSLGATPNGLKVAEEISSSGVSELNNSAPPVAVTISPVVA
 QPSPTPVAITASN

**Dme_EGL
 (DMU86404)**

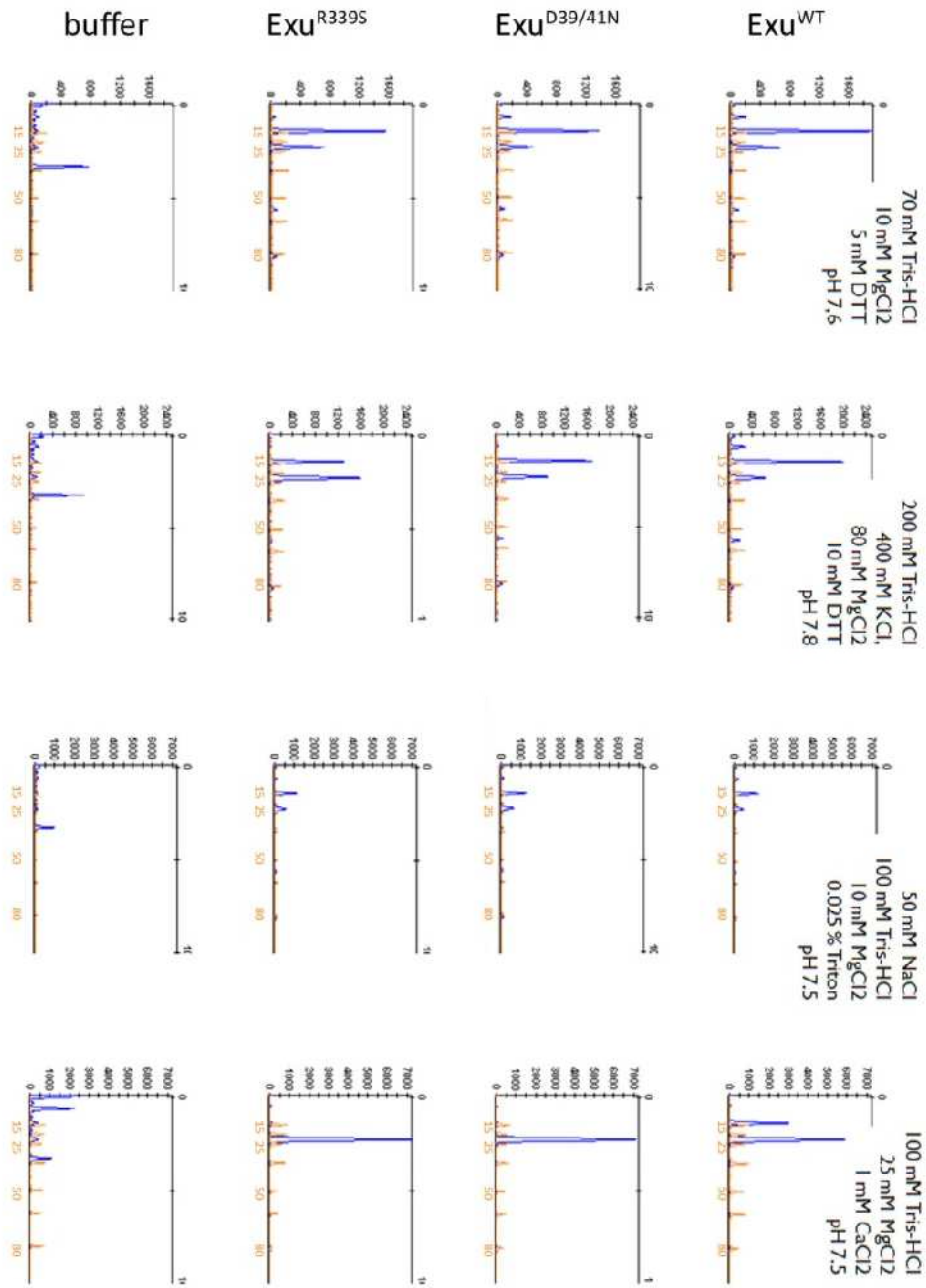
D. melanogaster

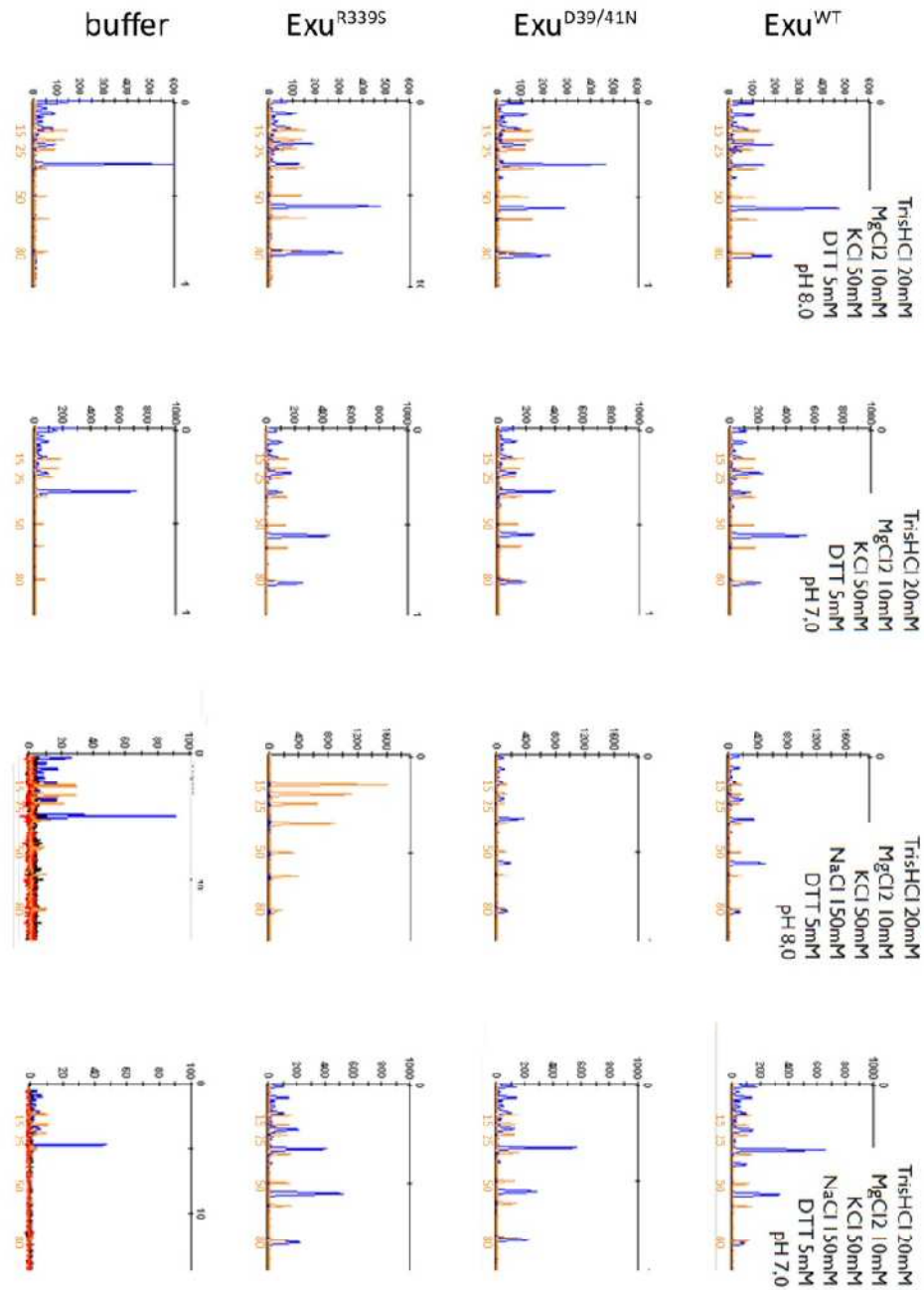
>gi|220902361|gb|AAF47054.4| egalitarian [*Drosophila melanogaster*]
 MESMEYEMARNMTLLFFLERLLDKGEPRTVHDLSCQFGNKEFTKE
 MRQIAGGSQSGKFLAQYPAIFLVDGDYVQVNAVQHNNADDGGC
 GKRDIYIQEAKDYFKNKMLQYGAEEVPRVRSLLGHRSQASPQVRHI
 SGQHIKEFTDFLMKHTDTFKVTDDYVMLVGCENMTDLPARDLHLP
 QSNIDTRGTQQMLDFFAQCIQEVKGPLLVLDQLFHLLTTNFPQDQWLR
 MFKTPGDLSSFLKLFADCFHIQANLVTLQKPKLSDTHIQQAQAQTR
 EQFNALNNNSASIRKQEPPTGGGGVGGVSSVQQLQSPALRTNG
 HTNNNNGSNGSNNNNNNNNSIACPNFKLNAPVSNVMGGQSQGFQ
 QPKSEPSSGFDSYVPMSELKLENLCENNYPSANTCYGPINNSSQQT
 QQVQTQQQQPQHATQNPAEQRLNSVNQTLKQRINTLVIRTLAENL
 EKDKQSLANQQGGPISPHASPVHSIANSSSNQAGSAANNANSNSN
 ANPNNANHSPSHSYFVGDTWKIKVLQNTTVIANVKQSVFVTDIILKYA
 AKNESIVVSLDCEGINLGLKGEITLIEIGTTRGEAFLFDVQSCPAMVTD
 GGLKTVLEHDQVIKVIHDCRNDAAANLYLQFGILLRNVDFTQAAHAILQ
 YQESGKQVYKAKYISLNSLCEQYNAPCNPIKDQLKQIYRRDQKFWA
 KRPLTREMMLYAAGDVLVLIHDQLFGNLRARQIKPENRALFSELCTEQI
 LMQIKPNEVKIRKKQRKVSTEVSDLKQKLAQTSKSIVLSNREIRLLRY
 MDL TEDEKERLKGYYKVAKKLEKMEAGNPSKDQSDSEDEQEPNE
 NDAFPSLDSVPSDNSLSGTFSPRFSSEPPSLTESMQMLEEILQNK
 MDRIARIDKLEAILTTATSLPCEQIIASNSMQEQLGSSIIATTENLQIIRE
 KSKNIKNCNCQGERSVTPIMRTTDRVVKLVDAESQTLSTGDVVITKI
 FFQDEHERAKEAALLSNSPAKRVSP

Appendix A: selected sequences modelled by a RNaseD exonuclease with HMM
 (ORF - open reading frame)

Appendix B

Fragment analysis with different buffer recipes





Appendix B Fragment analysis with several buffer. The composition of the used buffer is indicated above every column. The columns are vertical and include from left to right buffer, Exu^{R339S}, Exu^{D39/41N} and Exu^{WT} as indicated above. The recombinant Exuperantia used in this assay is the C-terminally truncated Exu^{ΔC}, which is the “minimal construct” to rescue the *exu*-mutant phenotype. Fluorescently labeled 27nt RNA oligos (blue peak) were incubated with the indicated protein. The shift of the RNA peak is set in relation to a DNA size standard (GeneScan 120 LIZ - orange peak). Sized are indicated in orange underneath.

Appendix C

Appendix C1

fold change and standard deviation of indicated *exu*-transheterozygous flies

genotype	stage	transcript	fold change (WT=1)	standard deviation
<i>exu^{PJ42}/exu^{QR9}</i>	ovary	<i>bicoid</i>	0,567302	0,135097
		<i>oskar</i>	0,590545	0,163583
	embryo (30 min AEL)	<i>bicoid</i>	0,762304	0,286259
		<i>oskar</i>	1,034924	0,51644
	embryo (0-2 hrs AEL)	<i>bicoid</i>	0,781542	0,117217
		<i>oskar</i>	0,687036	0,12152
<i>exu^{PJ42}/Dfexu1</i>	ovary	<i>bicoid</i>	0,527824	0,191657
		<i>oskar</i>	0,7378	0,177018
	embryo (30 min AEL)	<i>bicoid</i>	0,79781	0,210503
		<i>oskar</i>	1,13251	0,726012
	embryo (0-2 hrs AEL)	<i>bicoid</i>	0,814244	0,186052
		<i>oskar</i>	0,798147	0,230636
<i>exu^{QR9}/Dfexu1</i>	ovary	<i>bicoid</i>	0,548243	0,187176
		<i>oskar</i>	0,651974	0,388952
	embryo (30 min AEL)	<i>bicoid</i>	0,843219	0,214204
		<i>oskar</i>	1,386561	0,739883
	embryo (0-2 hrs AEL)	<i>bicoid</i>	0,803006	0,280287
		<i>oskar</i>	0,89029	0,47059
<i>exuⁱ³/Dfexu1</i>	ovary	<i>bicoid</i>	0,582736	0,131141
		<i>oskar</i>	0,910075	0,265369
	embryo (30 min AEL)	<i>bicoid</i>	0,762751	0,220793
		<i>oskar</i>	1,289519	0,615632
	embryo (0-2 hrs AEL)	<i>bicoid</i>	0,936552	0,189535
		<i>oskar</i>	0,880849	0,130439
<i>exu^{SC}/Dfexu1</i>	ovary	<i>bicoid</i>	0,484539	0,153554
		<i>oskar</i>	0,68661	0,328923
	embryo (30 min AEL)	<i>bicoid</i>	0,607344	0,095418
		<i>oskar</i>	1,037653	0,681321
	embryo (0-2 hrs AEL)	<i>bicoid</i>	0,580574	0,448327
		<i>oskar</i>	0,573297	0,491298

Appendix C2

fold change and standard deviation of *exu*-mutant flies carrying indicated transgenes

construct	stage	transcript	fold change (WT=1)	standard deviation
Exu:Venus	ovary	<i>bicoid</i>	1,026208	0,126738
		<i>oskar</i>	0,823731	0,214909
	embryo (30 min AEL)	<i>bicoid</i>	0,75077	0,377605
		<i>oskar</i>	0,694484	0,051772
	embryo (0-2 hrs AEL)	<i>bicoid</i>	1,01698	0,103131
		<i>oskar</i>	0,912467	0,089642
Exu ^{D39/41N} :Venus	ovary	<i>bicoid</i>	1,100468	0,206602
		<i>oskar</i>	0,896618	0,185861
	embryo (30 min AEL)	<i>bicoid</i>	0,83247	0,446611
		<i>oskar</i>	0,622801	0,117839
	embryo (0-2 hrs AEL)	<i>bicoid</i>	1,069	0,025068
		<i>oskar</i>	0,804238	0,078328
Exu ^{ΔC} :Venus	ovary	<i>bicoid</i>	1,141403	0,298039
		<i>oskar</i>	0,966792	0,26855
	embryo (30 min AEL)	<i>bicoid</i>	0,905591	0,33988
		<i>oskar</i>	0,6653	0,126605
	embryo (0-2 hrs AEL)	<i>bicoid</i>	0,902567	0,154516
		<i>oskar</i>	0,57655	0,075091
Exu ^{D39/41N,ΔC} :Venus	ovary	<i>bicoid</i>	1,074042	0,23835
		<i>oskar</i>	1,028202	0,26841
	embryo (30 min AEL)	<i>bicoid</i>	0,882845	0,23902
		<i>oskar</i>	0,786934	0,13598
	embryo (0-2 hrs AEL)	<i>bicoid</i>	0,890782	0,02548
		<i>oskar</i>	0,614629	0,114686
Exu ^{D39/41N}	ovary	<i>bicoid</i>	1,013744	0,126733
		<i>oskar</i>	0,878498	0,140351
	embryo (30 min AEL)	<i>bicoid</i>	1,043388	0,219299
		<i>oskar</i>	0,724328	0,145370
	embryo (0-2 hrs AEL)	<i>bicoid</i>	1,01666	0,091675
		<i>oskar</i>	0,683707	0,113914
none	ovary	<i>bicoid</i>	0,940652	0,283885
		<i>oskar</i>	1,130094	0,237744
	embryo (30 min AEL)	<i>bicoid</i>	0,946793	0,308317
		<i>oskar</i>	0,7251	0,041251
	embryo (0-2 hrs AEL)	<i>bicoid</i>	1,139726	0,132716
		<i>oskar</i>	0,894678	0,130483

Appendix C3

primer sequence for qPCR fragments of *bicoid*, *oskar* and *actin42A*

<i>transcript</i>	<i>name</i>	<i>sequence</i>
<i>bicoid</i>	<i>bicoid</i> fw	AAGTCCGAGTCTCGTGTGGCATC
	<i>bicoid</i> rev	TCATGTCGTCGCTACTGCCATC
<i>oskar</i>	<i>oskar</i> fw	TCCCGATATAGATAGTGAGGTGCG
	<i>oskar</i> rev	GCTCGCTTTCAGGTTGAAGATCC
<i>actin42A</i>	<i>actin42A</i> fw	TGTGTGCAGCGGATAACTAGAAAC
	<i>actin42A</i> rev	GAGTCCTTTTGTCCCATTCTACC

Appendix C quantitative RT-PCR. **C1** values for ovaries and embryos from *exu* transheterozygous flies **C2** values for ovaries and embryos from *exu*-mutant flies (*exu^{j3}/Df(2R)exu1*) carrying different transgenes. Listed are differences in mRNA levels of *bicoid* and *oskar* standardized to germ-line specific *actin* mRNA level. That difference is expressed in fold change, whereby the wild-type situation is set as 1. AEL = after egg lay **C3** primer sequences used for amplification.

Appendix D

primer sequences to generate fusion proteins

	name	sequence	amplicon:	
C-terminal fusion				
general	<i>venus-exu-3'</i> F	GGAGCCATCCCCAGTTCGAAAAGTAAAATCCAGTTCTGGTGGATCCGTAA	3'UTR	
	<i>exu-3'</i> R	TTCTTTAGCTTCAATGTGAAAGTTTTCTACAT		
full	<i>exuCDS-venus</i> F	CATCACGGCCTCCAAGGTGACCATGGTGAGCAAGGGCGAGGAG	<i>venus</i>	
	<i>venus-exu3'</i> R	TTACGGATCCACCAGAACTGGATTTTACTTTTCGAACTGGGGATGGCTCC		
	<i>exuCDS -venus</i> R	CTCCTCGCCCTTGCTCACCATGGTCACCTTGGAGGCCGTGATG		CDS
	<i>exuCDS</i> F	CGTATGCACCGTAAGCGCAA		
□C	<i>exuCDS^{□C}-venus</i> F	GCCGGTTGTCAAGGGTGTGACCATGGTGAGCAAGGGCGAGGAG	venus	
	<i>venus-exu3'</i> R	TTACGGATCCACCAGAACTGGATTTTACTTTTCGAACTGGGGATGGCTCC		
	<i>exuCDS^{ΔC}-venus</i> R	CTCCTCGCCCTTGCTCACCATGGTCACACCCTTGACAACCGGC	CDS ^{ΔC}	
	<i>exuCDS</i> F	CGTATGCACCGTAAGCGCAA		
N-terminal venus fusion				
general	<i>exu5'UTR</i> F	TAAGTGCTAAGCCGTCTTCG	5'UTR	
	<i>exu5'UTR-venus</i> R	GGGTGGCTCCACCCATTTTCTTATATGATCTGCGGAAAGCAA		
	<i>exu5'UTR-venus</i> F	TTGCTTTCCGCAGATCATATAAGAAAATGGGGTGGAGCCACCC		<i>venus</i>
	<i>venus-exuCDS</i> R	GCATCGATGTTATCGGCAACCATCTTGTACAGCTCGTCCATGCC		
full	<i>venus-exuCDS</i> F	GGCATGGACGAGCTGTACAAGATGGTTGCCGATAACATCGATGC	CDS	
	<i>exu CDS</i> R	GCTTTCCGAGACTGTAGTTCTT		
□C	<i>venus-exuCDS</i> F	GGCATGGACGAGCTGTACAAGATGGTTGCCGATAACATCGATGC	CDS ^{ΔC}	
	<i>venus-exuCDS^{ΔC}</i> R	CGGATCCACCAGAACTGGATTTTAACCCTTGACAACCGGCTT		
	<i>exuCDS^{□C}-exu3'</i> F	AAGCCGGTTGTCAAGGGTTAAAATCCAGTTCTGGTGGATCCG		3'UTR
□S, □C	<i>exu3'UTR</i> R	TAATAATTTGCGAGTACGCAAAG	CDS ^{ΔS□ΔC}	
	<i>venus-exuCDS</i> F	GGCATGGACGAGCTGTACAAGATGGTTGCCGATAACATCGATGC		
	<i>venus-exuCDS^{ΔS□ΔC}</i> R	CCATACGTCCGTTTGCCAAGTAAAATCCAGTTCTGGTGGATCC		
	<i>exuCDS^{ΔS□ΔC}-exu3'</i> F	GGATCCACCAGAACTGGATTTTACTTGGCAAACGGACGTATGG		3'UTR
	<i>exu3'</i> R	TAATAATTTGCGAGTACGCAAAG		
N-terminal ST fusion				
general	<i>exu5'UTR</i> F	TAAGTGCTAAGCCGTCTTCG	<i>exu 5'UTR</i>	
	<i>exu5'UTR-ST</i> R	ATGGGGTGGAGCCACCCGCAGTTTCGAAAAAATGGTTGCCGATAACATCGATG		
	<i>exu5'UTR-ST</i> F	TTTTTCGAACTGCGGGTGGCTCCACCCATTTTCTTATATGATCTGCGGAAAGCAATC		StrepTag
	<i>venus-exuCDS</i> R	GCATCGATGTTATCGGCAACCATCTTGTACAGCTCGTCCATGCC		

Appendix E

primer sequence for expression of recombinant Exuperantia

<i>name</i>	<i>sequence</i>
enzyme cloning into pOPHis and pOPGST	
CDS-NdeI-fw	CATATGATGGTTGCCGATAACATCGATGCCG
CDS-BamHI-rev	GGATCCTTAGTTGGAGGCCGTGATGGCC
CDS ^{ΔC} -BamHI-rev	GGATCCTTAACCCTTGACAACCGGCTTCAC
enzyme cloning into pETM41	
DEDD-NcoI-fw	TTATGCCATGGTTGCCGATAACATCGA
DEDD-A BamHI-rev	AACGGGGATCCTTAACGTATGGCATTAAACAT
DEDD-B BamHI-rev	TTTGGGGATCCTTATTCCGGCTTGCCG
DEDD-C BamHI-rev	TTGCTGGATCCTTAAGATTGCTTATCGTCACCATT
DEDD-D BamHI-rev	ACGGTGGATCCTTAACGTCCCTGGGG
DEDD-E BamHI-rev	TCTTCGGATCCTTACTCCTTGGTCGTGGACA
In fusion cloning into petMCN-GST-TEV	
CDS-IF-fw	TTACTTCCAGGGCCATATGATGGTTGCCGATAACATCGATGC
CDS-IF-rev	TAGACTATTAGGATCCTTAGTTGGAGGCCGTGATGG
CDS ^{ΔSΔC} - IF-fw	TTACTTCCAGGGCCATATGAAAAGCTCGGAGGCATTGGA
CDS ^{ΔSΔC} - IF-rev	TAGACTATTAGGATCCTTAATCGAAATAGCTGTCCAGAAGC
CDS ^{ΔSΔC} - IF-rev	TAGACTATTAGGATCCTTATTCCGGCTTGCCGTC
In fusion cloning into pet28aNusA	
CDS-IF-fw	AGCAAATGGGTCGCGATGGTTGCCGATAACATCGATGC
CDS ^{ΔC} - IF-rev	GACGGAGCTCGAATTTTAATCGAAATAGCTGTCCAGAAGC

Appendix F

biomers.net datasheet for 5' fluorescently labeled RNA oligos



Oligonukleotiddatenblatt


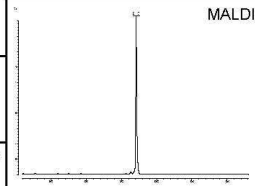
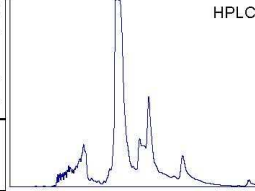

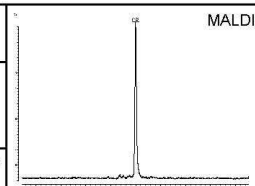
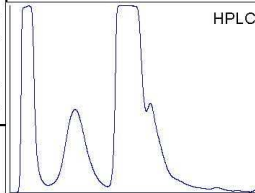

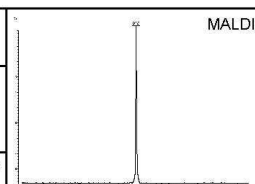
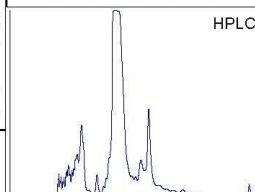
Ines Wolff
MPL für Entwicklungsbiologie

72076 Tübingen
Deutschland

Auftragsnummer: 00114495
Kundennummer: 10827
(Bitte bei Rückfragen angeben)

Freitag, 11. März 2011


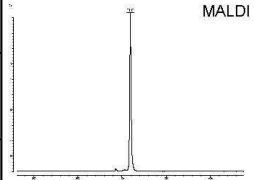
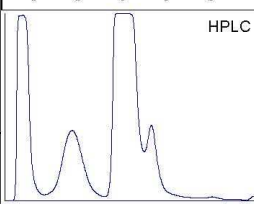
Nur für Forschungszwecke!

27_nt_labeled 00114495_1 RNA		 800153		
5'-ggu uug uuu gug ugg gug ugu gug ugg -3'				
Scale RM27 Menge 10,3 OD 36,5 nmol 342,6 µg Vol.f.100pmol/µl 365 µl Konz. - pmol/µl Gelöst in - µl	Länge 27 Tm 65 °C GC-Gehalt 51,00% A: 0,0 C: 0,0 G: 14,0 U: 13,0 Ext.Koeff.: 283400 MW Soll 9391 g/mol MW Ist 9417 g/mol	Reinigung HPLC Getrocknet 5'-Mod.: 6-Fam (RNA) 3'-Mod.: - Interne Mod.: -		
27_nt_unlabeled 00114495_2 RNA		 800154		
5'-cca aac aaa cac acc cac aca cac acc -3'				
Scale RM27 Menge 17,3 OD 56,6 nmol 480,5 µg Vol.f.100pmol/µl 566 µl Konz. - pmol/µl Gelöst in - µl	Länge 27 Tm 65 °C GC-Gehalt 51,00% A: 13,0 C: 14,0 G: 0,0 U: 0,0 Ext.Koeff.: 305200 MW Soll 8491 g/mol MW Ist 8499 g/mol	Reinigung HPLC Getrocknet 5'-Mod.: - 3'-Mod.: - Interne Mod.: -		
26_nt_labeled 00114495_3 RNA		 800155		
5'-ggu uug uuu gug ugg gug ugu gug ug-3'				
Scale RM27 Menge 21,3 OD 78,5 nmol 710,4 µg Vol.f.100pmol/µl 785 µl Konz. - pmol/µl Gelöst in - µl	Länge 26 Tm 62 °C GC-Gehalt 50,00% A: 0,0 C: 0,0 G: 13,0 U: 13,0 Ext.Koeff.: 271700 MW Soll 9046 g/mol MW Ist 9067 g/mol	Reinigung HPLC Getrocknet 5'-Mod.: 6-Fam (RNA) 3'-Mod.: - Interne Mod.: -		

biomers.net GmbH
Söflinger Str. 100
D-89077 Ulm / Germany
Tel.: +49 (0)731 70396 0
Fax: +49 (0)731 70396 11

info@biomers.net
www.biomers.net
Handelsregister Ulm
HRB 4656
Steuernr.88001/42768
Ust.Id DE 813608611

Geschäftsführer:
Dr. Matthias Resmini
Barbara Zimmermann
Chandra Mohan Sarkar

26_nt_unlabeled 00114495_4 RNA		 800156			
5'-cca aac aaa cac acc cac aca cac ac-3'					
Scale	RM27	Länge	26	Reinigung	HPLC
Menge	11,9 OD	Tm	62 °C	Getrocknet	
	40,0 nmol	GC-Gehalt	50,00%	5'-Mod.:	
	327,2 µg	A: 13,0 C: 13,0 G: 0,0 U: 0,0		3'-Mod.:	
Vol.f.100pmol/µl	400 µl	Ext.Koeff.:	297700	Interne Mod.:	
Konz.	- pmol/µl	MW Soll	8186 g/mol		
Gelöst in	- µl	MW Ist	8188 g/mol		
					

Nur für Forschungszwecke!

biomers.net GmbH
Söfflinger Str. 100
D-89077 Ulm / Germany
Tel.: +49 (0)731 70396 0
Fax: +49 (0)731 70396 11

info@biomers.net
www.biomers.net
Handelsregister Ulm
HRB 4656
Steuernr.88001/42768
Ust.Id DE 813608611

Geschäftsführer:
Dr. Matthias Resmini
Barbara Zimmermann
Chandra Mohan Sarkar

Appendix G

primer for sequencing of *exuperantia*

<i>name</i>	<i>sequence</i>
<i>exu fw</i>	CCTGCAGCTAACCGAATTCAAG
<i>exu rev</i>	GAATGTCCGACGGCCATATC
<i>exu-seq-I</i>	TAGTGACTCAGCTAATTTTCG
<i>exu-seq-II</i>	GGCGGGTCCCAGCTCGGACG
<i>exu-seq-III</i>	TCCGGTGTTCTGAACTACT
<i>exu-seq-V</i>	ACGTTATCTACAAAGCAAAT
<i>exu-seq-VI</i>	ACGACTCCAGGATCATGTAG
<i>exu-seq-V</i>	CTACATGATCCTGGAGTCGT
<i>exu-seq-VII</i>	CGTCCGAGCTGGGACCCGCC
<i>exu-seq-VIII</i>	GTTGATTGTAAATATGAAAC
<i>exu-seq-IX</i>	GTTTCATATTTACAATCAAC
<i>exu-seq-X</i>	ACAATATAGTTTTCAAACGT
<i>exu-seq-XI</i>	GGTTTTCGATGGGCTCTTT
<i>exu-seq-XII</i>	CTGATTATTGTTTTTCTGCC

6. References

1. Becalska, A.N. & Gavis, E.R. Lighting up mRNA localization in *Drosophila* oogenesis. *Development* **136**, 2493-503 (2009).
2. Lecuyer, E. et al. Global analysis of mRNA localization reveals a prominent role in organizing cellular architecture and function. *Cell* **131**, 174-87 (2007).
3. Jung, H., Yoon, B.C. & Holt, C.E. Axonal mRNA localization and local protein synthesis in nervous system assembly, maintenance and repair. *Nat Rev Neurosci* **13**, 308-24.
4. Kugler, J.M. & Lasko, P. Localization, anchoring and translational control of oskar, gurken, bicoid and nanos mRNA during *Drosophila* oogenesis. *Fly (Austin)* **3**, 15-28 (2009).
5. Holt, C.E. & Bullock, S.L. Subcellular mRNA localization in animal cells and why it matters. *Science* **326**, 1212-6 (2009).
6. St Johnston, D. Moving messages: the intracellular localization of mRNAs. *Nat Rev Mol Cell Biol* **6**, 363-75 (2005).
7. Brenner, H.R., Witzemann, V. & Sakmann, B. Imprinting of acetylcholine receptor messenger RNA accumulation in mammalian neuromuscular synapses. *Nature* **344**, 544-7 (1990).
8. Simon, A.M., Hoppe, P. & Burden, S.J. Spatial restriction of AChR gene expression to subsynaptic nuclei. *Development* **114**, 545-53 (1992).
9. Ding, D., Parkhurst, S.M., Halsell, S.R. & Lipshitz, H.D. Dynamic Hsp83 RNA localization during *Drosophila* oogenesis and embryogenesis. *Mol Cell Biol* **13**, 3773-81 (1993).
10. Bashirullah, A. et al. Joint action of two RNA degradation pathways controls the timing of maternal transcript elimination at the midblastula transition in *Drosophila melanogaster*. *Embo J* **18**, 2610-20 (1999).
11. Bergsten, S.E. & Gavis, E.R. Role for mRNA localization in translational activation but not spatial restriction of nanos RNA. *Development* **126**, 659-69 (1999).
12. Wolke, U., Weidinger, G., Kopranner, M. & Raz, E. Multiple levels of posttranscriptional control lead to germ line-specific gene expression in the zebrafish. *Curr Biol* **12**, 289-94 (2002).
13. Forrest, K.M. & Gavis, E.R. Live imaging of endogenous RNA reveals a diffusion and entrapment mechanism for nanos mRNA localization in *Drosophila*. *Curr Biol* **13**, 1159-68 (2003).
14. Ephrussi, A., Dickinson, L.K. & Lehmann, R. Oskar organizes the germ plasm and directs localization of the posterior determinant nanos. *Cell* **66**, 37-50 (1991).
15. Ephrussi, A. & Lehmann, R. Induction of germ cell formation by oskar. *Nature* **358**, 387-92 (1992).
16. Wang, C., Dickinson, L.K. & Lehmann, R. Genetics of nanos localization in *Drosophila*. *Dev Dyn* **199**, 103-15 (1994).
17. Nakamura, A., Amikura, R., Mukai, M., Kobayashi, S. & Lasko, P.F. Requirement for a noncoding RNA in *Drosophila* polar granules for germ cell establishment. *Science* **274**, 2075-9 (1996).
18. Jeong, J.H. et al. The transport of Stauf2-containing ribonucleoprotein complexes involves kinesin motor protein and is modulated by mitogen-activated protein kinase pathway. *J Neurochem* **102**, 2073-84 (2007).
19. Brendza, R.P., Serbus, L.R., Duffy, J.B. & Saxton, W.M. A function for kinesin I in the posterior transport of oskar mRNA and Stauf protein. *Science* **289**, 2120-2 (2000).
20. MacDougall, N., Clark, A., MacDougall, E. & Davis, I. *Drosophila* gurken (TGF α) mRNA localizes as particles that move within the oocyte in two dynein-dependent steps. *Dev Cell* **4**, 307-19 (2003).
21. Januschke, J. et al. Polar transport in the *Drosophila* oocyte requires Dynein and Kinesin I cooperation. *Curr Biol* **12**, 1971-81 (2002).

22. Takizawa, P.A. & Vale, R.D. The myosin motor, Myo4p, binds Ash1 mRNA via the adapter protein, She3p. *Proc Natl Acad Sci U S A* **97**, 5273-8 (2000).
23. Weil, T.T., Forrest, K.M. & Gavis, E.R. Localization of bicoid mRNA in late oocytes is maintained by continual active transport. *Dev Cell* **11**, 251-62 (2006).
24. Bullock, S.L. & Ish-Horowicz, D. Conserved signals and machinery for RNA transport in *Drosophila* oogenesis and embryogenesis. *Nature* **414**, 611-6 (2001).
25. Bullock, S.L. et al. Differential cytoplasmic mRNA localisation adjusts pair-rule transcription factor activity to cytoarchitecture in dipteran evolution. *Development* **131**, 4251-61 (2004).
26. Driever, W. & Nusslein-Volhard, C. A gradient of bicoid protein in *Drosophila* embryos. *Cell* **54**, 83-93 (1988).
27. St Johnston, D., Driever, W., Berleth, T., Richstein, S. & Nusslein-Volhard, C. Multiple steps in the localization of bicoid RNA to the anterior pole of the *Drosophila* oocyte. *Development* **107 Suppl**, 13-9 (1989).
28. Tomancak, P., Guichet, A., Zavorszky, P. & Ephrussi, A. Oocyte polarity depends on regulation of gurken by Vasa. *Development* **125**, 1723-32 (1998).
29. Kim-Ha, J., Smith, J.L. & Macdonald, P.M. oskar mRNA is localized to the posterior pole of the *Drosophila* oocyte. *Cell* **66**, 23-35 (1991).
30. Wilkie, G.S. & Davis, I. *Drosophila* wingless and pair-rule transcripts localize apically by dynein-mediated transport of RNA particles. *Cell* **105**, 209-19 (2001).
31. Driever, W. & Nusslein-Volhard, C. The bicoid protein determines position in the *Drosophila* embryo in a concentration-dependent manner. *Cell* **54**, 95-104 (1988).
32. Driever, W., Siegel, V. & Nusslein-Volhard, C. Autonomous determination of anterior structures in the early *Drosophila* embryo by the bicoid morphogen. *Development* **109**, 811-20 (1990).
33. St Johnston, D. & Nusslein-Volhard, C. The origin of pattern and polarity in the *Drosophila* embryo. *Cell* **68**, 201-19 (1992).
34. Frohnhofer, H.G., Lehmann, R. & Nusslein-Volhard, C. Manipulating the anteroposterior pattern of the *Drosophila* embryo. *J Embryol Exp Morphol* **97 Suppl**, 169-79 (1986).
35. Schupbach, T. & Wieschaus, E. Germline autonomy of maternal-effect mutations altering the embryonic body pattern of *Drosophila*. *Dev Biol* **113**, 443-8 (1986).
36. Stephenson, E.C. & Mahowald, A.P. Isolation of *Drosophila* clones encoding maternally restricted RNAs. *Dev Biol* **124**, 1-8 (1987).
37. Driever, W., Thoma, G. & Nusslein-Volhard, C. Determination of spatial domains of zygotic gene expression in the *Drosophila* embryo by the affinity of binding sites for the bicoid morphogen. *Nature* **340**, 363-7 (1989).
38. Struhl, G., Struhl, K. & Macdonald, P.M. The gradient morphogen bicoid is a concentration-dependent transcriptional activator. *Cell* **57**, 1259-73 (1989).
39. Huynh, J.R. & St Johnston, D. The origin of asymmetry: early polarisation of the *Drosophila* germline cyst and oocyte. *Curr Biol* **14**, R438-49 (2004).
40. Lin, H. & Spradling, A.C. Fusome asymmetry and oocyte determination in *Drosophila*. *Dev Genet* **16**, 6-12 (1995).
41. Roth, S. & Lynch, J.A. Symmetry breaking during *Drosophila* oogenesis. *Cold Spring Harb Perspect Biol* **1**, a001891 (2009).
42. Bastock, R. & St Johnston, D. *Drosophila* oogenesis. *Curr Biol* **18**, R1082-7 (2008).
43. Goldstein, B. & Macara, I.G. The PAR proteins: fundamental players in animal cell polarization. *Dev Cell* **13**, 609-22 (2007).
44. Munro, E.M. PAR proteins and the cytoskeleton: a marriage of equals. *Curr Opin Cell Biol* **18**, 86-94 (2006).

45. Riechmann, V. & Ephrussi, A. Axis formation during *Drosophila* oogenesis. *Curr Opin Genet Dev* **11**, 374-83 (2001).
46. Benton, R., Palacios, I.M. & St Johnston, D. *Drosophila* 14-3-3/PAR-5 is an essential mediator of PAR-1 function in axis formation. *Dev Cell* **3**, 659-71 (2002).
47. Benton, R. & St Johnston, D. *Drosophila* PAR-1 and 14-3-3 inhibit Bazooka/PAR-3 to establish complementary cortical domains in polarized cells. *Cell* **115**, 691-704 (2003).
48. Theurkauf, W.E., Smiley, S., Wong, M.L. & Alberts, B.M. Reorganization of the cytoskeleton during *Drosophila* oogenesis: implications for axis specification and intercellular transport. *Development* **115**, 923-36 (1992).
49. Steinhauer, J. & Kalderon, D. Microtubule polarity and axis formation in the *Drosophila* oocyte. *Dev Dyn* **235**, 1455-68 (2006).
50. Krauss, J., Lopez de Quinto, S., Nusslein-Volhard, C. & Ephrussi, A. Myosin-V regulates oskar mRNA localization in the *Drosophila* oocyte. *Curr Biol* **19**, 1058-63 (2009).
51. Theurkauf, W.E., Alberts, B.M., Jan, Y.N. & Jongens, T.A. A central role for microtubules in the differentiation of *Drosophila* oocytes. *Development* **118**, 1169-80 (1993).
52. Irion, U., Adams, J., Chang, C.W. & St Johnston, D. Miranda couples oskar mRNA/Staufen complexes to the bicoid mRNA localization pathway. *Dev Biol* (2006).
53. Kalifa, Y., Armenti, S.T. & Gavis, E.R. Glorund interactions in the regulation of gurken and oskar mRNAs. *Dev Biol* **326**, 68-74 (2009).
54. St Johnston, D., Beuchle, D. & Nusslein-Volhard, C. Staufen, a gene required to localize maternal RNAs in the *Drosophila* egg. *Cell* **66**, 51-63 (1991).
55. Ghosh, S., Marchand, V., Gaspar, I. & Ephrussi, A. Control of RNP motility and localization by a splicing-dependent structure in oskar mRNA. *Nat Struct Mol Biol* **19**, 441-9.
56. Trucco, A., Gaspar, I. & Ephrussi, A. Assembly of endogenous oskar mRNA particles for motor-dependent transport in the *Drosophila* oocyte. *Cell* **139**, 983-98 (2009).
57. Hachet, O. & Ephrussi, A. Splicing of oskar RNA in the nucleus is coupled to its cytoplasmic localization. *Nature* **428**, 959-63 (2004).
58. Hazelrigg, T. et al. The exuperantia gene is required for *Drosophila* spermatogenesis as well as anteroposterior polarity of the developing oocyte, and encodes overlapping sex-specific transcripts. *Genetics* **126**, 607-17 (1990).
59. Hegde, J. & Stephenson, E.C. Distribution of swallow protein in egg chambers and embryos of *Drosophila melanogaster*. *Development* **119**, 457-70 (1993).
60. Schnorrer, F., Bohmann, K. & Nusslein-Volhard, C. The molecular motor dynein is involved in targeting swallow and bicoid RNA to the anterior pole of *Drosophila* oocytes. *Nat Cell Biol* **2**, 185-90 (2000).
61. Stephenson, E.C. Localization of swallow-Green Fluorescent Protein in *Drosophila* oogenesis and implications for the role of swallow in RNA localization. *Genesis* **39**, 280-7 (2004).
62. Irion, U. & St Johnston, D. bicoid RNA localization requires specific binding of an endosomal sorting complex. *Nature* **445**, 554-8 (2007).
63. Ferrandon, D., Elphick, L., Nusslein-Volhard, C. & St Johnston, D. Staufen protein associates with the 3'UTR of bicoid mRNA to form particles that move in a microtubule-dependent manner. *Cell* **79**, 1221-32 (1994).
64. Ferrandon, D., Koch, I., Westhof, E. & Nusslein-Volhard, C. RNA-RNA interaction is required for the formation of specific bicoid mRNA 3' UTR-STAU-FEN ribonucleoprotein particles. *Embo J* **16**, 1751-8 (1997).
65. Schnorrer, F., Luschnig, S., Koch, I. & Nusslein-Volhard, C. Gamma-tubulin37C and gamma-tubulin ring complex protein 75 are essential for bicoid RNA localization during *drosophila* oogenesis. *Dev Cell* **3**, 685-96 (2002).

66. Arn, E.A., Cha, B.J., Theurkauf, W.E. & Macdonald, P.M. Recognition of a bicoid mRNA localization signal by a protein complex containing Swallow, Nod, and RNA binding proteins. *Dev Cell* **4**, 41-51 (2003).
67. Macdonald, P.M., Luk, S.K. & Kilpatrick, M. Protein encoded by the exuperantia gene is concentrated at sites of bicoid mRNA accumulation in Drosophila nurse cells but not in oocytes or embryos. *Genes Dev* **5**, 2455-66 (1991).
68. Berleth, T. et al. The role of localization of bicoid RNA in organizing the anterior pattern of the Drosophila embryo. *Embo J* **7**, 1749-56 (1988).
69. Ephrussi, A. & St Johnston, D. Seeing is believing: the bicoid morphogen gradient matures. *Cell* **116**, 143-52 (2004).
70. Schupbach, T. & Wieschaus, E. Female sterile mutations on the second chromosome of Drosophila melanogaster. I. Maternal effect mutations. *Genetics* **121**, 101-17 (1989).
71. Hazelrigg, T. & Tu, C. Sex-specific processing of the Drosophila exuperantia transcript is regulated in male germ cells by the tra-2 gene. *Proc Natl Acad Sci U S A* **91**, 10752-6 (1994).
72. Marcey, D., Watkins, W.S. & Hazelrigg, T. The temporal and spatial distribution pattern of maternal exuperantia protein: evidence for a role in establishment but not maintenance of bicoid mRNA localization. *Embo J* **10**, 4259-66 (1991).
73. Crowley, T.E. & Hazelrigg, T. A male-specific 3'-UTR regulates the steady-state level of the exuperantia mRNA during spermatogenesis in Drosophila. *Mol Gen Genet* **248**, 370-4 (1995).
74. Wilsch-Brauninger, M., Schwarz, H. & Nusslein-Volhard, C. A sponge-like structure involved in the association and transport of maternal products during Drosophila oogenesis. *J Cell Biol* **139**, 817-29 (1997).
75. Wang, S. & Hazelrigg, T. Implications for bcd mRNA localization from spatial distribution of exu protein in Drosophila oogenesis. *Nature* **369**, 400-03 (1994).
76. Riechmann, V. & Ephrussi, A. Par-1 regulates bicoid mRNA localisation by phosphorylating Exuperantia. *Development* **131**, 5897-907 (2004).
77. Wilhelm, J.E. et al. Isolation of a ribonucleoprotein complex involved in mRNA localization in Drosophila oocytes. *J Cell Biol* **148**, 427-40 (2000).
78. Moser, M.J., Holley, W.R., Chatterjee, A. & Mian, I.S. The proofreading domain of Escherichia coli DNA polymerase I and other DNA and/or RNA exonuclease domains. *Nucleic Acids Res* **25**, 5110-8 (1997).
79. Navarro, C., Puthalakath, H., Adams, J.M., Strasser, A. & Lehmann, R. Egalitarian binds dynein light chain to establish oocyte polarity and maintain oocyte fate. *Nat Cell Biol* **6**, 427-35 (2004).
80. Zuo, Y. & Deutscher, M.P. Exoribonuclease superfamilies: structural analysis and phylogenetic distribution. *Nucleic Acids Res* **29**, 1017-26 (2001).
81. Steitz, T.A. & Steitz, J.A. A general two-metal-ion mechanism for catalytic RNA. *Proc Natl Acad Sci U S A* **90**, 6498-502 (1993).
82. Bernad, A., Blanco, L., Lazaro, J.M., Martin, G. & Salas, M. A conserved 3'----5' exonuclease active site in prokaryotic and eukaryotic DNA polymerases. *Cell* **59**, 219-28 (1989).
83. Zuo, Y. & Deutscher, M.P. Mechanism of action of RNase T. I. Identification of residues required for catalysis, substrate binding, and dimerization. *J Biol Chem* **277**, 50155-9 (2002).
84. Derbyshire, V. et al. Genetic and crystallographic studies of the 3',5'-exonucleolytic site of DNA polymerase I. *Science* **240**, 199-201 (1988).
85. Ibrahim, H., Wilusz, J. & Wilusz, C.J. RNA recognition by 3'-to-5' exonucleases: the substrate perspective. *Biochim Biophys Acta* **1779**, 256-65 (2008).
86. Cha, B.J., Koppetsch, B.S. & Theurkauf, W.E. In vivo analysis of Drosophila bicoid mRNA localization reveals a novel microtubule-dependent axis specification pathway. *Cell* **106**, 35-46 (2001).

87. Soding, J., Biegert, A. & Lupas, A.N. The HHpred interactive server for protein homology detection and structure prediction. *Nucleic Acids Res* **33**, W244-8 (2005).
88. Dienstbier, M., Boehl, F., Li, X. & Bullock, S.L. Egalitarian is a selective RNA-binding protein linking mRNA localization signals to the dynein motor. *Genes Dev* **23**, 1546-58 (2009).
89. Qiao, F. & Bowie, J.U. The many faces of SAM. *Sci STKE* **2005**, re7 (2005).
90. Aviv, T. et al. The NMR and X-ray structures of the *Saccharomyces cerevisiae* Vts1 SAM domain define a surface for the recognition of RNA hairpins. *J Mol Biol* **356**, 274-9 (2006).
91. Green, J.B., Gardner, C.D., Wharton, R.P. & Aggarwal, A.K. RNA recognition via the SAM domain of Smaug. *Mol Cell* **11**, 1537-48 (2003).
92. Aviv, T. et al. The RNA-binding SAM domain of Smaug defines a new family of post-transcriptional regulators. *Nat Struct Biol* **10**, 614-21 (2003).
93. Trundova, M. & Celer, V. Expression of porcine circovirus 2 ORF2 gene requires codon optimized *E. coli* cells. *Virus Genes* **34**, 199-204 (2007).
94. Dumon-Seignovert, L., Cariot, G. & Vuillard, L. The toxicity of recombinant proteins in *Escherichia coli*: a comparison of overexpression in BL21(DE3), C41(DE3), and C43(DE3). *Protein Expr Purif* **37**, 203-6 (2004).
95. Esposito, D. & Chatterjee, D.K. Enhancement of soluble protein expression through the use of fusion tags. *Curr Opin Biotechnol* **17**, 353-8 (2006).
96. Zuo, Y. & Deutscher, M.P. Mechanism of action of RNase T. II. A structural and functional model of the enzyme. *J Biol Chem* **277**, 50160-4 (2002).
97. Martin, S.G., Leclerc, V., Smith-Litiere, K. & St Johnston, D. The identification of novel genes required for *Drosophila* anteroposterior axis formation in a germline clone screen using GFP-Staufen. *Development* **130**, 4201-15 (2003).
98. Bökel, C. EMS Screens. Vol. 420 119-138 (2007).
99. Bischof, J., Maeda, R.K., Hediger, M., Karch, F. & Basler, K. An optimized transgenesis system for *Drosophila* using germ-line-specific phiC31 integrases. *Proc Natl Acad Sci U S A* **104**, 3312-7 (2007).